AD-A250 410

AFOSR-TP-
AFOSR-TR- ` ` 2 ` 0 ` 8 ` 8

②

ROLE OF INTERFACES AND INTERPHASES IN THE EVOLUTION MECHANICS OF MATERIAL SYSTEMS

K. REIFSNIDER, W. STINCHCOMB, D. DILLARD,
R. SWAIN, K. JAYARAMAN, Y. CHANG
J. LESKO, M. ELAHI, Z. GAO, A. RAZVAN

Materials Response Group

Virginia Tech

92-12953

REPORT DOCUMENTATION PAGE

Form Approved
OMB No. 0704-0188

1a. REPORT SECURITY CLASSIFICATION Unclassified	1b. RESTRICTIVE MARKINGS
2a. SECURITY CLASSIFICATION AUTHORITY	3. DISTRIBUTION/AVAILABILITY OF REPORT
2b. DECLASSIFICATION/DOWNGRADING SCHEDULE	Approved for public release, distribution unlimited
4. PERFORMING ORGANIZATION REPORT NUMBER(S)	5. MONITORING ORGANIZATION REPORT NUMBER(S)

6a. NAME OF PERFORMING ORGANIZATION Virginia Polytechnic Inst. and State University	6b. OFFICE SYMBOL (If applicable)	7a. NAME OF MONITORING ORGANIZATION Air Force Office of Scientific Research
6c. ADDRESS (City, State, and ZIP Code) Engineering Science and Mechanics Dept. Patton Hall Blacksburg, VA 24061-0219		7b. ADDRESS (City, State, and ZIP Code) Aerospace Sciences Div., AFOSR/NA Building 410, Bolling AFB Washington, DC 20332-6448
8a. NAME OF FUNDING/SPONSORING ORGANIZATION AFOSR	8b. OFFICE SYMBOL (If applicable) NA	9. PROCUREMENT INSTRUMENT IDENTIFICATION NUMBER AFOSR 89-0014

8c. ADDRESS (City, State, and ZIP Code) Aerospace Sciences Div., AFOSR/NA Building 410, Bolling AFB Washington, DC 20332-6448	10. SOURCE OF FUNDING NUMBERS			
	PROGRAM ELEMENT NO. 61102F	PROJECT NO. 2302	TASK NO. B3	WORK UNIT ACCESSION NO.

11. TITLE (Include Security Classification)
Role of Interfaces and Interphases in the Evolution Mechanics of Material Systems (U)

12. PERSONAL AUTHOR(S)
K. Reifsnider, W. Stinchcomb, D. Dillard, R. Swain, K. Jayaraman

13a. TYPE OF REPORT Final	13b. TIME COVERED FROM 12/1/90 TO 12/1/91	14. DATE OF REPORT (Year, Month, Day) 26 March 1992	15. PAGE COUNT

16. SUPPLEMENTARY NOTATION

COSATI CODES			18. SUBJECT TERMS (Continue on reverse if necessary and identify by block number)
FIELD	GROUP	SUB-GROUP	

19. ABSTRACT (Continue on reverse if necessary and identify by block number)

This final report summarizes the activities conducted under this grant during the three-year program. An extensive search and interpretation of the literature was conducted. Several methods of characterizing the interface was identified and tested. Progress was made in the identification of the effect of the interface on the cyclic response of composite laminates. A major advance has been made in the analysis of interphases at the fiber-matrix level. A new "Interface Mechanics Laboratory" has been established with assistance from Virginia Tech and Virginia Institute for Material Systems.

20. DISTRIBUTION/AVAILABILITY OF ABSTRACT ☐ UNCLASSIFIED/UNLIMITED ☒ SAME AS RPT ☐ DTIC USERS	21. ABSTRACT SECURITY CLASSIFICATION U
22a. NAME OF RESPONSIBLE INDIVIDUAL	22b. TELEPHONE (Include Area Code)	22c. OFFICE SYMBOL

DD Form 1473, JUN 86 Previous editions are obsolete. SECURITY CLASSIFICATION OF THIS PAGE

Table of Contents

1. Evolution Mechanics of Material Systems

The Role of Interfaces and Interphases

Final Report 1988-1991

Summary

The general objective of this investigation was to apply the discipline of mechanics to the prediction and description of the long-term behavior of composite materials by developing experimental information, conceptual understanding, and analytical representations of the evolution of the properties of constituent materials and interfaces in composite material systems as a function of (generalized) time during the application of time-variable mechanical, thermal, and chemical loadings. The general approach to this objective was to develop mechanistic representations of the "state of the material" under those conditions, and to join those descriptions with micromechanical descriptions of the "state of stress" in "critical elements" to support an estimate of remaining strength, and, thereby, to predict remaining life. We have named this enterprise "evolution mechanics."

The current program focused on a particular aspect of this general objective, the study of the "Role of Interfaces and Interphases in the Evolution Mechanics of Material Systems." The objective of the program was to achieve accurate and realistic representations of the geometry, arrangement, properties, and property distributions (as a function of space) associated with the region between fibers and matrix material in continuous and short fiber reinforced composite materials, to develop engineering methods of characterizing the interphasal strength and properties in such composites, to use the analysis to interpret that data in terms of stiffness and strength, and to use a "critical element method" to extend these findings to the prediction of the changes in stiffness and strength (evolution) as well as the life of such materials under typical engineering conditions in a manner which reflects the influence of interphases.

This Final Report summarizes the activities conducted under this grant during the three year program. Highlights of the program results to date include the following:

1. An extensive search and interpretation of the literature was conducted.

2. Some 16 different material systems were investigated. This is critical matter since it is essential to have experimental data from material systems which have widely different characteristics in order to test any philosophy or analysis in a rigorous fashion. This achievement overcomes the single most difficult and persistent obstacle to the progress of the experimental program.

A comprehensive program of characterization and investigation of the effect of interface treatment on the fatigue response of open-hole coupons under fully reversed loading was conducted. Damage development was monitored during the tests; damage and failure modes were determined. Stacking sequence was varied. Results were correlated with several parameters such as measurements of interfacial strength, and transverse strain to failure.

3. Several methods of characterizing the interface were identified and tested. A remarkable new engineering method for such characterization has been developed which shows great promise, especially in the interpretation of the data in terms of engineering response such as compression strength. We regard the development of this experimental method to be a breakthrough; it is already being sought by laboratories and industrial firms throughout the U.S. and abroad.

4. Progress was made in the identification of the effect of the interface on the cyclic response of composite laminates. In particular, a method was developed which uses the dynamic response, especially the phase lag and spectral details of the specimen response to cyclic excitation, to characterize the material in a way that is sensitive to damping and shear behavior, known to be influenced by interfacial effects.

5. A major advance has been made in the analysis of interphases at the fiber-matrix level. Our experimental program provided the surprising information that the microstructural morphology of the interphase region between the fiber and the matrix is often not constant, and, therefore, the properties in that region often vary with spatial position. This probelm has been ignored in the mechanics literature. A closed form formulation ard series solution has been found for several problems which include the continuous variation of material properties known to occur (as a function of distance from the fiber) in the matrix surrounding a fiber for many material systems, especially thermoplastic systems. This is the first successful solution of this type, and the first micromechanical model of the interphase region. The approach can be applied to many such problems, which opens an entirely new door of opportunity in this essential area. This aspect of the investigation was complementary to a major program funded by the NSF which dealt with this problem on a more general level.

6. Several methods of characterizing the interface were examined. These include:

    • Dynamic Mechanical Thermal Analysis (DTMA)
    • Acoustic microscopy
    • Dielectric Analysis (DEA)
    • Nano-indentation in an SEM
    • Meso-indentation using a microhardness tester (a method developed during this program)
    • Stress Pattern Analysis from Thermal Emission (SPATE)
    • Acoustic Emission

    A new initiative to use and develop the mechanics analysis to interpret the results of meso-indentation with a standard microhardness tester was launched. The results were very encouraging. This technique may present a new method for the characterization of the shear-related properties of interfaces in-situ. This technique also shows correlation with compressive strength measurements, a very important finding. There is some reason to believe that this technique may provide a long-awaited method of relating the microdetails of

interfaces/interphases to the macro-engineering response of concern to performance, such as strength and life.

7. With assistance from Virginia Tech and the Virginia Institute for Material Systems, we have established a new "Interface Mechanics Laboratory." That laboratory has a new work surfaces and cabinets, a new bench metallograph, a new microhardness tester, new cutting and polishing equipment, and a variety of photography devices. Other additions are planned. This is a major addition to our capabilities in this area, and one of the few laboratories in the country to concentrate on the *mechanics* of interfaces.

8. A new method of characterizing the effect of interfaces/interphases on the long-term response of composite material systems, especially the fatigue response of laminated systems, has been developed. A dynamic signal analyzer has been interfaced to a servohydraulic testing machine and test methodology has been developed which produces dynamic characteristics of the response of specimens to cyclic loading at different load levels and frequencies. These data show special sensitivity to the shear properties (and matrix properties in general) of the material systems under test. We believe that interfacial effects will be clearly delineated by this method. The technique is a unique combination of equipment and interpretative approaches. Along with the indenter method, it is a second unique technique (one static, the other dynamic) that we have developed to characterize the effect of interfaces/interphases on the response of material systems, with special emphasis on bridging the gap between the micro-details and the engineering consequences. Both of these techniques produce data that are directly related to engineering properties and performance.

9. Initial progress has been made in the use of our representations of microbehavior in simulation models of the long-term response of composite material systems. Progress has been made on two fronts. Under another research program conducted in parallel with this one, micromechanics models of tensile and compressive strength have been developed which reflect the effect of interfaces on those properties, for continuous-fiber reinforced material systems. (The compression model is not yet complete.) The tensile model also includes the time-dependent behavior of the matrix, and its' influence on the dynamic properties. These models were prepared for, and are being entered into, the MRLife code series developed by the Materials Response Group at Virginia Tech. That code uses mechanistic representations of damage and failure processes to predict remaining strength and life of composites under sustained and cyclic application of mechanical, thermal, and chemical loads. On another front, the concept of simulation has been carefully examined, and progress has been made in the manner in which that analytical method is used to represent the collective effect of the processes which define remaining strength and life. This subject was the text of two plenary lectures given by Dr. Reifsnider at two international conferences this Spring, one in Japan and one in Belgium. The plenary lecture in Japan was the only such lecture given by the U.S. side, as the U.S. representation to the Japan-U.S. Conference on Composite Materials, and the plenary lecture in Belgium is the lead-off plenary lecture for the Colloquium on "Durability of Polymer Based Composite Systems for Structural Applications" at the Free University of Belgium. This activity is clear evidence of leadership in this technical area. Most important, it provides a means of bringing the fundamental science generated in this program to the applied community in a form in which the rigor can be brought to bear on the technical problems of such importance to the economy and security of our country.

The present report briefly summarizes these activities, and provides a complete description of the fatigue investigations which are the final phase of the effort. In two sections which follow this one, "Salient Conclusions" and "Most Significant Findings" will be presented. That will be followed by a listing of "Publications" which resulted from this program. Detailed results of the research program will then be presented in the remainder of the report.

Salient Conclusions

1. Changing the interface, only, between the fiber and matrix in a fiber-dominated composite material can alter the fully-reversed, notched fatigue strength by more than an order of magnitude.

2. At least three mechanical properties appear to be important in the characterization of an interface or interphase region:

   - the stiffness of the region
   - the shear strength of the region
   - the tensile strength of the region.

   In addition, the geometry (thickness and any azimuthal distribution) is critical to the determination of the effect of the region on global properties and performance.

3. Interfaces are often finite regions--i.e., "interphases"--which may have properties which vary from point to point because of physical phenomena such as:

   - diffusion between the fiber and matrix
   - chemical reactions between the fiber, matrix, and interphase region
   - micromorphological growth kinetics
   - manufacturing effects

4. A meso-indentation technique based on "hardness" indentor concepts (developed by our research group) can be used to measure the shear strength of interface or interphase regions. The method has several advantages:

   - the test is simple, quick, and requires only a simple test device
   - the data developed by the test can be directly interpreted by a rigorous micromechanics analysis (elasticity) in terms of interfacial shear strength
   - the data can also be related to the compressive strength of many composite systems (in which the shear strength plays an important role in compression failure)
   - the data are closely grouped and consistent.

5. Several dynamic methods have shown considerable promise as nondestructive test techfniques for the characterization of interfaces and interphases. One method, which we developed, uses the dynamic signal outputs from servohydraulic test equipment, making it possible to monitor interface response during fatigue testing.

6. Performace simulation methods based on the "critical element concept" can be used to anticipate the effect of interfaces on the long-term cycle and time-dependent response of composite laminates.

7. Micromechanical models which do not consider fiber-fiber interactions do not correctly represent the influence of the interface or interphase on local stress fields and, therefore, on global properties.

Most Significant Findings

Two particularly important results of the program have been selected as "most significant findings." A brief description of these findings follows.

Development of a New Experimental Method and Micromechanical Model for the Determination of Interfacial Shear Strength in Composites

A newly developed experimental method and micromechanical model for data interpretation has provided the first practical method of measuring the interfacial shear strength in as-manufactured fiber-reinforced composite materials. The combined method/model development provides direct measurement of interface and interphase strength that correlates well with global composite properties and performance, in contrast to prior methods that are difficult (often impossible) to apply to engineering composites, and which give widely variable results that do not corelate with the global strength and life behavior which controls engineering applications.

Interfacial shear strength in fiber-reinforced materials is known to be critical to the determination of the strength, life, and damage tolerance of engineering components made from such materials. It has recently been found in our investigations, for example, that composites which have different interfacial strengths may have essentially the same static strength, but may have life times at a given load level which differ by more than an order of magnitude. This is a critical matter to the durability and damage tolerance of these materials, and a major oppoartunity for improved material design. However, prior methods of measuring the interfacial shear strength for such materials, such as nano-indentation, fragmentation tests, and the micro-bead test do not provide consistent data. Nor do those data correlate wsith the engineering properties affected by the interface of interphase region, such as strength, remaining strength, and life.

The present method uses a "mesoindentation" method wherein both the load on the indentor and the displacement of the indentor is measured as a function of time, as shown in Figure 1. The indentation covers many fiber diameters so that the data are averaged over many interfaces, as shown in Figure 2. The geometry of the indentor is arranged so that failure of the interfaces begins at a position below the surface of indentation, i.e., it is not influenced by the surface. A closed-form micromechanical mdoel of the local stress state under the indentor has been developed which is used to determine the actual stresses at the interface which ruptures, so that a direct measurement of the interfacial shear strength is provided by the method. It has also been found that other interpretations of the data can be made if the indentation is continued beyond first interfacial rupture. Indeed, the method shows considerable promise for the prediction of compressive strength, a very difficult property to measure at the global level. Among the important consequences of this new development is the unique ability to measure interfacial shear strength (and possibly compressive strength) on small smaples of trial materials for material development purposes, and the ability to measure those properties quickly and easily on as-manufactured bulk materials as a quality control

method. Finally, time-dependent properties may also be characterized by such a method. and current work is exploring the results of such measurements.

Isolation of the Influence of Interfaces and Interphases
on the Notched Fatigue Response of Composite Laminates

An experimental investigation has isolated the effect of different interfaces and interphases in fibrous composites on the notched fatigue life of laminates of such materials under fully-areversed loading. Micromechanical models are being used to identify the critical **parameters involved in creating observed changes in life of more than an order of magnitude in materials which show essentially identical static properties.**

A previous extensive investigation funded by the Air Force (conducted by a large group of other investigators over several years) studied the affect of various interfaces and interphases on the static properties of polymer matrix composites in coupon form. That study found significant differences in certain of those properties, but also found that many of the changes in the interfacial properties were not reflected in substantial changes in the global static properties. However, that study did not examine the fatigue response of those materials. We were successful in obtaining supplies of the original materials, as originally manufactured, with fourteen different combinations of constituent materials and interfaces, and manufactured coupons with center holes which were then subjected to fully-reversed fatigue loading. The results revealed that the fatigue response of these materials is greatly more sensitive to the interfacial strength and type than are the static properties. Moreover, as shown in Figure 3, it has also been found that these variations in life (of more than an order of magnitude for materials with essentially identical static properties) are **not** explained by the parameters usually used to "define" an interface, such as the interfacial strength. Indeed, correlations of fatigue performance with interfacial properties could not be made without recourse to analysis which includes a precise determination of the mode of failure, which can be altered by the interfacial properties and the details of the fatigue loading.

Efforts were made to put these results on a firm science base by developing and using micromechanical models of the local stress states, the development of damage, and the final (local) state of stress and state of material. These models represent micro-stability (as influenced by the support of the fibers by the surrounding matrix and interfacial material), micro-post-buckling (including plastic deformation), and damage development as an alteration of the micro-stress state. A "critical element" approach was also used to incorporate these models into a performance simulation code which can predict the remaining strength and life of composite materials with different interfacial strengths. A working version of the tensile failure part of that simulation model has been assembled and verified. Large dependency of remaining strength and life on interfacial strength, geometry, and mode of degradation is shown by the model.

Publications

A list of publications which have resulted from this program as of the date of this report. In every case, the support of the AFOSR is acknowledged in the published paper.

1. R.E. Swain, K.L. Reifsnider, K. Jayaraman, and M. El-Zein, "Interface/Interphase Concepts for Composite Material Systems," J. Thermoplastic Composite Materials, Vol. 3 (Jan 1990) pp. 13-23

2. K.L. Reifsnider and M. ElZein, "Mechanics of Thickness Effects on Laminate Strength and Performance," Proceedings of the Sagamore Conference, November, 1989.

3. K.L. Reifsnider, "Performance Simulation of Polymer Based Composite Systems," Proc. Predictive Technology Symposium, ADPA, 18-19 September, 1990, pp. 1-16.

4. D. Shalev and K.L. Reifsnider, "Study of the Onset of Delamination at Holes in Composite Laminates," J. Composite Materials, Vol. 24 (June 1990) pp.42-71

5. M. ElZein and K.L. Reifsnider, "On the Prediction of Tensile Strength After Impact of Composite Laminates," J. Comp. Technology and Research, in press.

6. K.L. Reifsnider, "Damage Tolerant Polymer Composite Systems," J. of Metals, Vol. 40 (Nov. 1988) pp. 51-54

7. K.L. Reifsnider, "Life Prediction Methodology for Composite Material Systems," Proc. Indo-U.S. Workshop on Composites, 21-42 July, 1990 (will be submitted to a journal shortly)

8. K.L. Reifsnider, "Interpretation of Laboratory Test Information for Residual Strength and Life Prediction of Composite Systems," Proc. of ASTM Symp. on Cyclic Deformation, Fracture, and Nondestructive Evaluation of Advanced Materials, 12-13 Nov. 1990, San Antonio; to be published in an STP.

9. K.L. Reifsnider, "The Use of Microcrack Analysis in Performance Simulation for Composite Materials Systems," Proc. of Conf. on Microcracking Induced Damage in Composites, 27-8 Nov. 1990, Dallas, Texas Winter Annual Meeting of ASME

10. K.L. Reifsnider, "Interpretation of Laboratory Test Information for Residual Strength and Life Prediction of Composite Systems," Proc. of Symp. on Cyclic Deformation, Fracture, and Nondestructive Evaluation of Advanced Materials, ASTM, San Antonio, 12-13 Nov. 1990.

11. K.L. Reifsnider, "Life Prediction in Advanced Material Systems," Proc of Conf. on Mechanical Fatigue in Advanced Materials, Engin. Foundation Meeting, 13-18 january, 1991.

12. K.L. Reifsnider and Z. Gao, "A Micromechanics model for Composites Under Fatigue Loading," Int. J. of Fatigue, Vol. 13 No. 2 (1991) pp. 149-156.

13. Z. Gao and K.L. Reifsnider, "Micromechanics of Tensile Strength in Composite Material Systems," in Composite Materials: Fatigue and Fracture (4th Symposium) ASTM, in press.

14. K.L. Reifsnider, Z. Gao, and R. Swain, "Micromechanical Concepts for the Estimation of Property Evolution and Remaining Life," Proc. of Program Review & Workshop, Virginia Tech Center for Composite Materials and Structures, 23-26 Sept. 1990, pp. I-1 - I-16.

15. K. Jayaraman & K. L. Reifsnider, "The interphase in Unidirectional Fiber-Reinforced Epoxies: Effect on Residual Thermal Stresses," submitted to J. Composites Science and Technology.

16. K. Jayaraman, & K.L. Reifsnider, "Residual Stresses in a Composite with Continuously Varying Youngs Modulus in the Fiber/Matrix Interphase," J. of Composite Materials, in press (expected in Fall 1991 issue)

17. K.L. Reifsnider, Z. Gao, and R. Swain, "Micromechanical Concepts for the Estimation of Property Evolution and Remaining Life," Proc. Intl. Conf. on Spacecraft Structures and Mechanical Testing, Noordwijk, Netherlands, 24-26 April 1991, (ESA SP-321, October 1991), pp. 653-658.

18. J.J. Lesko, G. Carman, D. Dillard, & K. Reifsnider, "Fiber/Matrix interface interrogation by Means of Meso-Indentation Testing," Proc. 15th Annual Meeting, American Adhesion Society, Hilton Head, Feb. 16-19, 1992.

19. Fatigue of Composite Materials K.L. Reifsnider, Editor, Elsevier, 1991.

20. C. Bakis and K. Reifsnider, "The Adiabatic Thermoelastic Effect in Laminated Fiber Composites," J. Composite Materials, Vol. 25 (1991) pp. 809-830.

21. K.L. Reifsnider, "Performance Simulation: A New Approach to the Prediction of Remaining Strength and Life of Material Systems," in Achievements in Composites in Japan and the United States, Japan Society for Composite Materials, Tokyo, (1990) pp. 3-14.

22. K.L. Reifsnider and Z. Gao, "Micromechanics for Performance Simulation," Proc. IUTAM Symp. on Local Mechanics Concepts for Composite Material Systems, 27-31 Oct. 1991, Blacksburg, VA, in press.
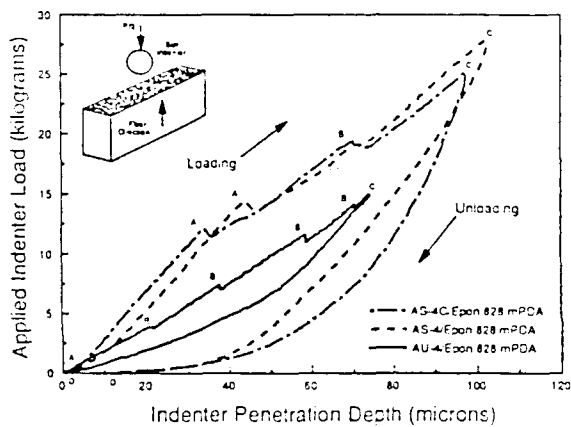
- A 1/16" diameter ball is pressed in the fiber direction of the composite while load and indenter penetration are monitored

- Interpretive micromechanics assist in determining the interfacial stresses from the penetration responses

- Understanding micro-phenomena (interfacial properties) are key to the optimum design & performance of composite materials

- First method that allows direct measurement of interface properties from as-fabricated commercial composites with a simple and inexpensive method
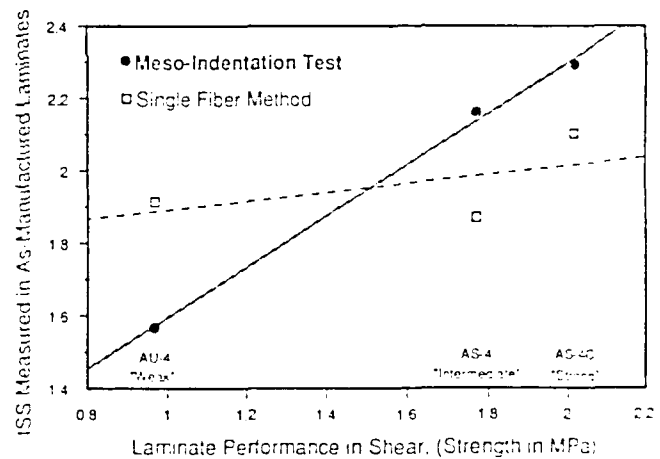
New technique shows improved ability to monitor interfacial shear strength over single fiber micro-indentation test (data shown relative to composite performance)

Figure 1. Summary of Meso-Indentation method of interface characterization.
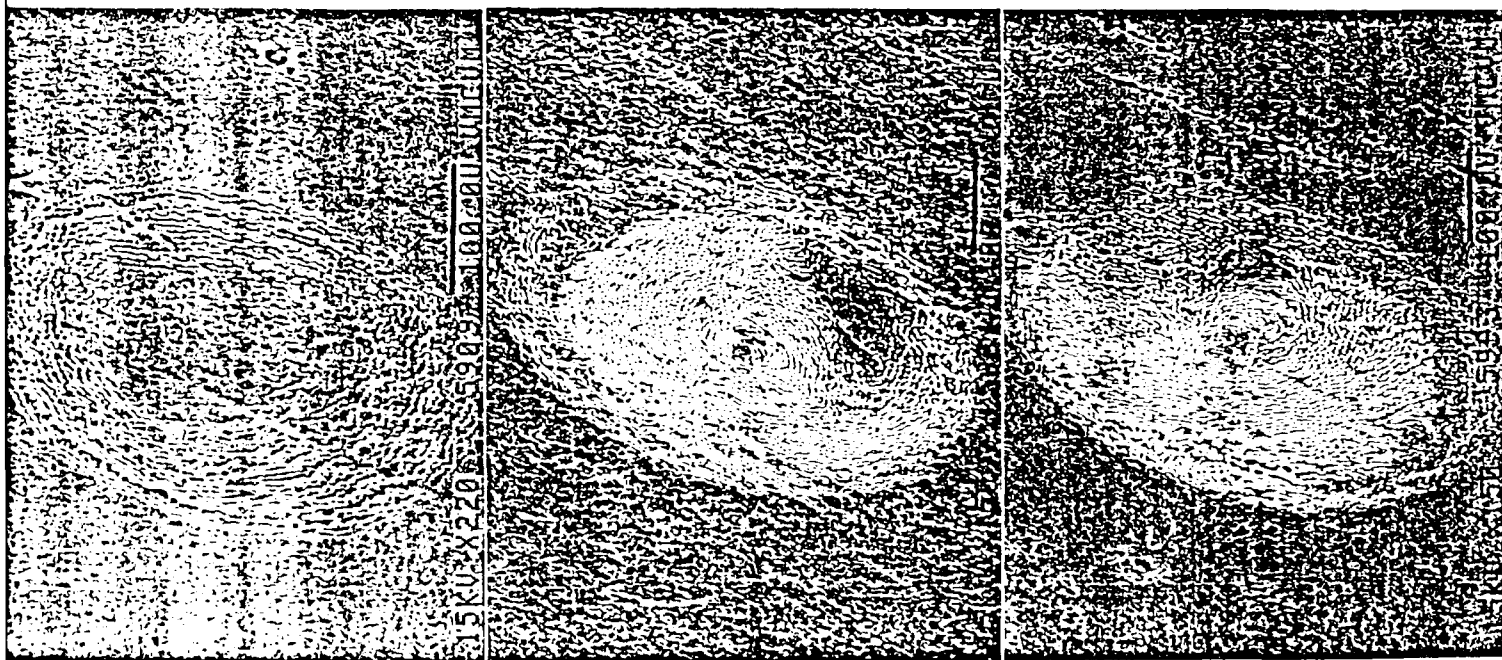
AU-4/828 mPDA   AS-4/828 mPDA   AS-4C/828 mPDA
"Weak" Interface   "Intermediate" Interface   "Strong" Interface

Figure 2. Examples of indentation in polymer-based composites.
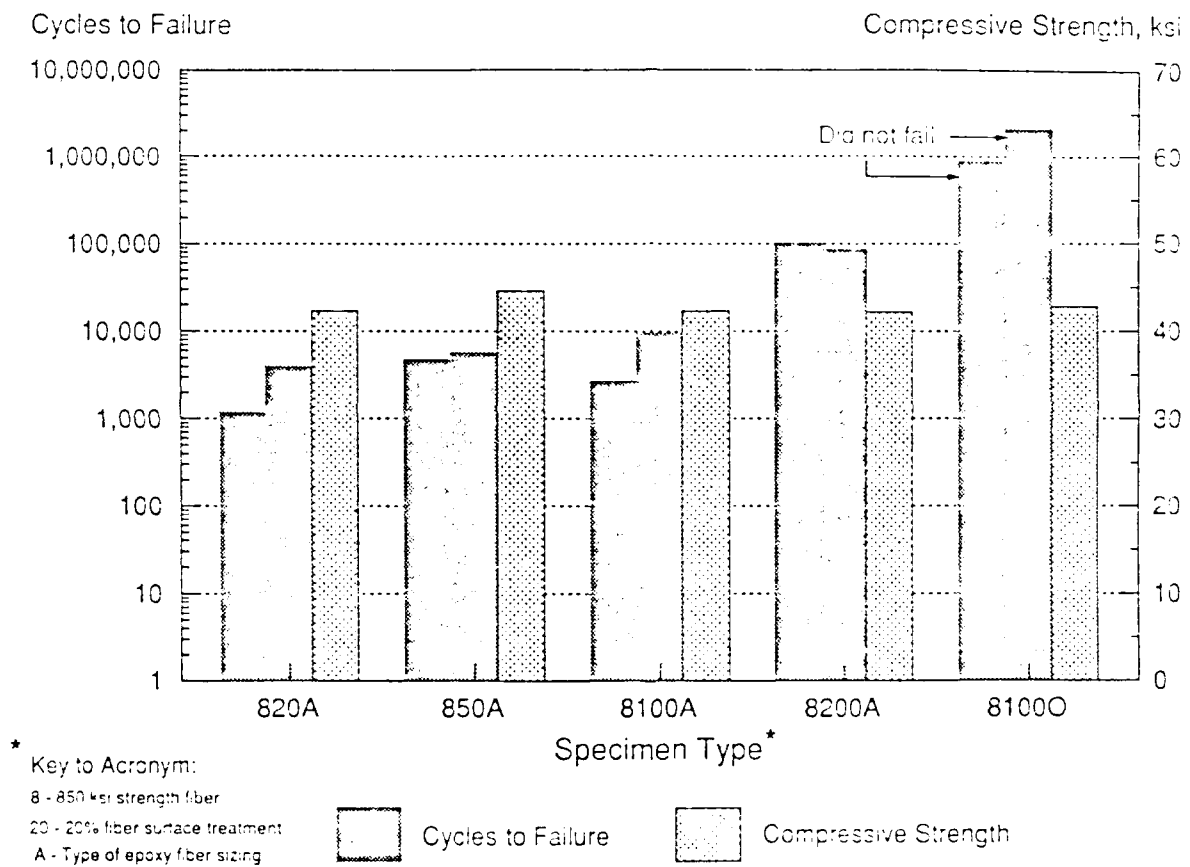
Figure 3. Comparison of fatigue life as influenced by fiber-matrix interface.

2. The Role of the Fiber/Matrix Interphase in the Static and Fatigue Behavior of Polymeric Matrix Composite Laminates

Robert E. Swain and Kenneth L. Reifsnider

This report summarizes the results and conclusions from the doctoral research of the first author, funded, in part, by the Air Force contract, "Evolution Mechanics of Material Systems: The Role of Interfaces and Interphases." The title of this chapter is identical to the title of the dissertation that details the broad scope of the research performed [1]. The following report is a nearly verbatim reproduction of the fifth chapter (entitled "Summary and Conclusions") of the aforementioned dissertation. Those interested in the fine detail that exists behind this general summary are urged to examine Ref. [1].

Introduction and Literature Review

The Interphase

- Researchers [2] have detected a third "phase" of the material between the bulk fiber phase and bulk matrix phase of a polymeric matrix composite. This finite-thickness region — termed the *interphase* — possesses mechanical, physical, and chemical properties that are distinct from the fiber and the matrix constituents. Thus, the interphase embodies the characteristics of the fiber matrix bond, including strength and stiffness (possibly tensorial in nature) that may be functions of position [2]. One should consider the interphase as a third constituent within a composite material system.
- The term, *interphase*, by emphasizing that a third phase exists between the fiber and matrix, replaces the outdated term, *interface*, which describes an idealized two-dimensional boundary.
- The interphase is created in the process of bonding the bulk fibers together with a matrix system. The nature of the fiber and matrix, the processing conditions, etc., can affect the character of the interphase. Engineers and chemists have sought to improve bond strength (or, equivalently, interphase strength) by developing fiber surface treatments and fiber sizings. The effect of a fiber surface treatment is to remove weak, unordered graphitic layers from the fiber surface [3]. The treatments tend to implant oxygen and nitrogen species that encourage chemical bonding with the matrix systems. Fiber sizings typically consist of a partially-cured epoxy that

is deposited onto the fiber surface. This coating — estimated to be between 100-500 nm in thickness [4,5] — aids in the handleability of the fibers and acts as a "primer" to further encourage bonding between the fiber and matrix.

The Interphase and its Influence on Composite Properties

- Having identified the interphase as a third constituent of a composite, researchers have sought to determine the relationship between the mechanical properties of the interphase and the resultant performance of the host composite. Several investigators have published work reporting that changes in interphase properties — achieved mainly through the presence or absence of fiber surface treatment and or sizing — *do* influence the quasi-static behavior of composites, especially when testing for "matrix-dominated" properties [6-17].
- The work mentioned above shares a common feature: laminate configurations have been extremely simple (almost exclusively unidirectional) in order to attribute composite behavior directly to the interphase. While considerable knowledge has been gained in this pursuit, there is a need to study the effect of interphase behavior on the response of engineering laminates, i.e., multi-directional laminates that possess stress raisers. In addition, *no* work has been published that studies the role of the interphase in the *fatigue response* of *carbon* fiber polymeric matrix composites.
- Another common feature that exists among every study that attempts to formulate an interphase composite performance relationship is the necessity to characterize the interphase strength. Techniques for measuring interphase strength are generally separated into two groups: single fiber tests and laminate tests. Single fiber tests are performed on model composite systems and fail to address the nature of the interphase in real, as-processed, standard fiber volume fraction composites. Laminate tests depend upon a necessary level of *inference*, i.e., a macroscopic strength property is assumed to correspond to the strength of the highly local interphase region. There is an overwhelming need within the composite community to find a technique that accurately assesses the strength of the interphase in real composite systems.

Opportunities

- Recently, an Air Force contract entitled, "The Development of Ultralightweight Materials," was awarded to the McDonnell Aircraft Company (abbreviated as McAir throughout this work) [18] and to the Northrop Corporation [19] (contract numbers F33615-88-C-5452 and F33615-88-C-5447, respectively). Each company supervised the creation of over twenty material systems specifically altered with respect to the fiber matrix interphase. The materials possessed different fiber systems, matrix systems, gradations of surface treatment, and different fiber sizing formulations. A considerable amount of quasi-static property data were published from these systems [20-22]. Noticeably absent from the test regimen was the characterization of the dynamic (fatigue) response of these materials. Each company provided the present investigation with a selection of materials from their material systems. This provided a unique opportunity to study the role of the interphase in the static and fatigue performance of carbon fiber polymeric matrix composites.

2. The Role of the Fiber/Matrix Interphase in the Static and Fatigue Behavior of Polymeric Matrix Composite Laminates

16

Experimental Techniques

Material Systems

- Eight McAir material systems arrived in panel form as two fiber systems bound with the same HC 9106-3 toughened epoxy system. The fibers, Courtaulds's 45-850 fibers (45 Msi tensile modulus, 850 ksi tensile strength) and 32-550 fibers (32 Msi tensile modulus, 550 ksi tensile strength) were surface treated at levels ranging from 20% to 200% of the industry standard treatment. Three of the systems had unsized fibers, four of the systems received an "A" epoxy sizing, and one system received an "O" "organic" sizing. The reader is encouraged to refer to Table 1 for the complete details of these systems including the coding scheme adopted in order to abbreviate the system descriptions.
- Six Northrop material systems arrived in pre-preg form as two fibers systems bound in two distinct matrix systems. Amoco's Thornel T650-35 fibers (35 Msi tensile modulus, 650 ksi tensile strength) were bound with a standard epoxy, ERLX 1901, and an amorphous thermoplastic, Radel-X (presently designated as Radel-8320 [21]). Amoco's Thornel T650X-50 fibers (50 Msi tensile modulus, 650 tensile strength) were bound only with the ERLX 1901 standard epoxy. The fibers in every Northrop system received were unsized. Northrop chose to compare the performance of systems possessing either 100% surface treatment or 0% surface treatment. The reader is encouraged to refer to Table 2 for the complete details of these systems including the coding scheme adopted in order to abbreviate the system descriptions.

Laminate Configurations and Test Specimens

- Laminate configurations tested in this investigation include 32-ply cross-ply specimens, $[\pm 45]_{ns}$ specimens (where n = 4 and 8), and unidirectional specimens containing 28 and 32 plies. A 0.25" diameter center hole was cut into a majority of the cross-ply specimens (giving a hole diameter-to-width ratio of 1:4).
- The unidirectional material was cut into diminutive 90° coupons for use in 3-point flexure testing. Other unidirectional coupons were cut and mounted in a room-cure epoxy such that the fiber ends could be polished for subsequent indentation testing and SEM work. Unidirectional McAir specimens were configured for compression testing in a Wyoming IITRI compression fixture.

Mechanical Testing

Quasi-static Strength and Stiffness Testing

- Quasi-static tension and compression strength testing was performed on notched cross-plied specimens from all fourteen material systems. The strength and modulus of each specimen was recorded. The axial tensile stiffness was measured on the McAir cross-plied specimens in the unnotched condition; these numbers were needed for future modelling work. Strength

testing was performed on the McAir ±45° laminates, allowing for the measure of tensile shear strength and shear stiffness. The unidirectional compressive strength, failure strain, and stiffness of six of the eight McAir systems were measured to serve as a comparison to the data obtained by Northrop on their material systems [21].

- Inspired by the work of Madhukar and Drzal [8] and Adams, et al. [23], transverse flexure testing was performed on the fourteen material systems under investigation in an attempt to characterize their bond strength. Strength, failure strain and flexural stiffness (derived from crosshead displacement) data were collected.

Fatigue Testing

- Notched cross-plied specimens from every material system were subjected to fully-reversed (R = -1), tension-compression, axial fatigue at a maximum applied stress level of 75% of their respective ultimate compressive strength. The stress level was chosen so that one could compare the performance of all fourteen systems on a common basis. Since there was a considerable range of compressive strengths, testing at a fixed stress level would unfairly tax many of the specimens. A wide range of fatigue lives indicated that the present decision to test at a fixed percentage of ultimate strength had some merit.

- During each notched cross-plied fatigue test the following data were collected: cycles to failure, modulus (with strain measured *across* the hole) as a function of cycles, notch temperature (measured with a thermocouple positioned at the point of maximum longitudinal stress) as a function of cycles, and phase and gain data collected from a Dynamic Signal Analysis program written in-house (by Ahmad Razvan).

- Unnotched McAir ±45° coupons were cycled at a stress ratio of R = 0.1 in tension-tension fatigue. Since this is a "matrix-dominated" laminate and the matrix was the same in each material system, it was decided to test each system under the same applied maximum stress of 24 ksi. Cycles to failure, specimen temperature as a function of cycles, and phase and gain data were collected during these tests.

Indentation Testing

- A novel indentation technique, the Continuous Ball Indentation Test [24], was performed as another approach to characterizing the interphase strength. Values reflecting the maximum indentation pressure and the depth of the indentation were used to quantify the response of the fourteen material systems.

Measurements of Strain Gradients

- A ten-gage strip gage (see Figure 1) was adhered to an 810A and an 8100 specimen in an attempt to detect the influence of the interphase on the longitudinal strain field in a ligament next to the center hole. Each specimen endured a number of tensile and compressive ramp loadings equal to the number of gages. This enabled the operators to monitor each gage without the luxury of having a myriad of strain amplifiers.

Non-destructive Testing

Fiber Volume Fraction Determination

- A fairly new technique to measure the fiber volume fraction of a composite was adopted in this study. This technique calculates the density of a composite by monitoring the weight of a coupon suspended in isopropyl alcohol (IPA) and applying Archimedes' principle. The test set-up employed is shown in Figure 2. Given that the matrix density and fiber density are known *a priori*, one can calculate the fiber volume fraction from these values, the "wet" weight of the composite (wet from the immersion in IPA), and the "dry" weight of the composite. This technique is seen as a *vast* improvement over the standardized matrix digestion technique [25].

Penetrant-enhanced X-ray Radiography

- Penetrant-enhanced X-ray radiography was employed to determine the extent and location of various damage modes within a fatigued laminate. The penetrant consisted of a zinc iodide solution. Optimum X-ray exposure times were determined for the material systems under investigation.

Scanning Electron Microscopy (SEM)

- A SEM was used for two distinct studies within this investigation. Unidirectional samples of the 810A, 820A, and 810O material were mounted such that the cross-section of the fibers were perpendicular to the viewing surface. These samples were polished and etched using an etchant formula typically employed in PEEK matrix studies [26]. Magnifications approaching $\times 21,000$ were used in order to focus on the interphase region of these 5 micron fibers. The other SEM study involved examining the fracture surface of an 810A tensile specimen and an 810O tensile specimen. An attempt was made to infer the quality of bonding by visually assessing the amount of matrix remaining on the fibers.

Experimental Results and Discussion

Characterization of Interphase Strength

Transverse Flexure Testing

- Transverse flexural strength (TFS) appeared to be a sensitive measure of bond strength (see Figure 3). In the McAir material, where the interphase was altered by gradations in the level of fiber surface treatment, an increase in TFS was noted to correspond to an increase in the percentage of surface treatment. In the Northrop material, where the interphase was altered by the presence or absence of fiber surface treatment, *large* differences in TFS were seen as the fiber went from the untreated to the surface treated condition. This observation concurs with

the findings of other researchers who claim that bond strength increases by a discrete "jump" when one surface treats the fiber by as little as 10% of the industry-standard process; only moderate increases in strength are witnessed upon the application of higher levels of surface treatment [9,12,14,17,27].

- Other variables besides the level of surface treatment seem to affect the TFS results (Figure 3). The "O" sizing appeared to cause a slight increase in TFS over its "A" sizing counterpart. Differences in TFS were attributable to the matrix systems. The largest TFS was seen in the 3RSN system. It was hypothesized that the processing temperature of this thermoplastic system contributes to the formation of large compressive residual stresses in the interphase that must be overcome during transverse tensile loading.

- It appeared that fiber type also played a role in determining a material's TFS (Figure 3). In two separate cases the matrix and surface treatment remained constant while the fiber type changed. Noticeable differences in TFS were noted in each case. Possible explanations were given for this behavior.

- Failure strain results revealed the same trends as the strength results. There was some reservation about the precision of these numbers since the failure strain was calculated from the crosshead displacement. Flexural stiffness data was relatively insensitive to the bond condition. This observation concurs with the findings of Madhukar and Drzal [8].

- Every surface treated specimen snapped into two distinct pieces upon failure. This is in stark contrast to the untreated specimens; in every instance they remained intact upon failure.

Indentation Testing

- Large differences in the Maximum Mean Hardness Pressure (MMHP) and representative strain (d/D at MMHP) were seen among the fourteen material systems (see Figure 4). The correlation between indentation performance and the level of surface treatment was not nearly as clear as with the TFS results. Two general observations were apparent, however. Instances where a material's MMHP was high and its d/D was low (as in the 820A system) indicate that the material possesses a quality of "brittleness", while low values of MMHP accompanied by high values of d/D is indicative of a "ductile" quality of the material. These trends were later confirmed in fracture surface studies of failed notched tensile specimens. The other general observation is that MMHP is greater in surface treated specimens than it is untreated specimens. This was true in two of three instances, yet, is usually seen in the systems tested thus far by Lesko [24].

- The explanation of the lack of definitive correlation between the indentation results and the TFS results (see Figure 5) centered about the differences in the failure mechanisms in each test. It was felt that the indentation test may represent a "shear" response of the interphase rather than the "tensile" response seen in the TFS results. This explanation requires further proof, however.

Quasi-static Strength and Stiffness Testing

Notched Cross-plied Specimens

- A wide variability in the notched tensile strengths was observed for the fourteen systems (see Figure 6). In general, the notched strength correlates with the unnotched strength of the material, yet, a definite dependence on interphase strength was noted. Systems that revealed high MMHP values seemed to perform poorly in the notched strength tests.
- The notched compressive strengths of the fourteen material systems (see Figure 6) were, without exception, much lower than the notched tensile strengths (in one instance, lower than 50% of the tensile strength). This *was not* attributed to bending failures in the laminates.
- Unlike the tensile case, the compressive strengths were remarkable in their *lack* of variability between systems whose fiber surface treatment had been altered. The compressive strength *did* differ, however, as one went from one *fiber system* to another. In every instance, if one kept the matrix system the same, as the fiber diameter increased, the strength increased. Strength differences were also attributed to the matrix system; the strength of the "3" fibers in the thermoplastic matrix was noticeably less than the strength of the same fibers in the epoxy matrix.
- There seemed to be a correlation between system modulus and the interphase condition. As surface treatment levels increased, the modulus was observed to increase in six of the eight McAir systems (see Figure 7). The 810O specimens displayed an obvious *decrease* in modulus over their 810A counterparts, leading one to believe that sizing formulation can affect the interphase's contribution to laminate stiffness. It was unclear whether the modulus values (obtained by measuring strain across the center hole) reflected a material response or a geometric response. The tensile stress-strain curves of surface treated and untreated systems clearly revealed differences in performance (see Figure 8).

Unnotched Cross-plied Specimens

- In contrast to the notched cross-plied 8A&O specimens, where the tensile modulus generally increased as the level of surface treatment increased, the *unnotched* stiffness was observed to decrease (see Figure 9). The 810O system, however, still revealed a lower stiffness than its 810A counterpart.

Unnotched ±45° Specimens

- Prior to collecting data, ±45° tensile strength (45TS) data culled from References [20,21] were plotted against their respective transverse flexural strength data. Surprisingly, a nearly linear relationship was observed between these two sets of data (see Figure 10). This result was more stunning when one recognized the distinct damage sequence that each laminate endured prior to failure. Possible explanations for this behavior were submitted.
- Bolstered by the above results, the published 45TS data were compared to published short beam shear strength data and edge delamination strength (EDS) data [21]. A general correlation was observed for the former data set (see Figure 11). The 45TS and the EDS data sets displayed an amazing degree of correlation (see Figure 12).

- The ±45° tension strengths measured from the McAir material generally correlated with their respective TFS data.
- Each ±45° tensile specimen displayed the same failure process. After sustaining an applied longitudinal strain of approximately 5%, a gross "yielding" of the laminate would occur, wherein the 45° fiber angles would align towards the loading axis. This yielding would result in an increase of nearly 10% in the longitudinal strain with no further increase in load (see Figures 13 and 14). Afterwards, the laminate would begin to carry load once again until failure. An incredible *lack* of matrix cracking was observed in an X-ray radiograph of a fatigued specimen that had undergone yielding (see Figure 15), leading one to believe that this behavior is related to matrix deformation rather than interphase (or matrix) failure.
- The ±45° tensile strengths recorded in these labs were considerably higher than the strengths published in Ref. [20]. There was no obvious explanation for this behavior.
- Measured shear stiffness values appeared insensitive to differences in the bond condition. This observation concurs with the findings of Madhukar and Drzal [7].

Unidirectional Compressive Specimens

- *No* correlation was seen between interphase strength and unidirectional IITRI compression strength of the McAir systems. Another troubling result was the occurrence of an average unidirectional compressive strength of the 55U system that was nearly equivalent to several of the 8A&O systems (see Figure 16). This finding did not concur with the trends observed in the notched cross-plied strength results and in the published results of McAir [20]; in these instances, the 5U series compressive strength was consistently higher than the 8A&O series strength.
- The IITRI compression strength values were considerably lower than the strength values published from the Northrop systems [21]. This may reflect the fact that different test fixtures were used in each case to determine the compressive strengths.

Fatigue Testing

Notched Cross-plied Specimens

- The interphase was shown to significantly influence the cyclic life of the 8A&O series (see Figure 17). In the 82A, 85A, and 810A systems — whose cyclic lives were nearly indistinguishable — microbuckling failure emanated from the center hole and grew towards the specimen edges (see Figure 18). The early presence of this microbuckling severely limited the life of these specimens. The 820A specimen also failed due to microbuckling formation, yet, in this instance, the initiation and progression of the failure was delayed. It was postulated that the stronger bonding of the system (observed in both TFS and MMIIP results) may have aided in the suppression of the microbuckle failures.
- The 810O specimen *never failed* when subjected to fully-reversed cyclic loading at a maximum applied stress level of 75% of its ultimate compressive strength (UCS). An X-ray radiograph taken after 2.1 million cycles revealed a complete absence of microbuckling (see Figure 19). This finding spawned several smaller investigations into why such an astonishing difference

occurs between the behavior of the 810O system and the 810A system — two systems differing *only in the sizing applied to the fiber.*

- The 5U series fatigue life did not reveal the same dramatic differences as the 8A&O series (see Figure 20). One is tempted to conclude for the 5U series that an increase in surface treatment caused an increase in life. More data is needed to confirm this suspicion. X-ray radiographs taken at 70% of the estimated life of each system failed to reveal the presence of microbuckling (for instance, see Figure 21). It was confirmed, however, that final failure of the laminate was in a sublaminate buckling mode. It was noted that all three 5U systems displayed fatigue lives rivaling the 820A specimens, yet, the applied stress level was significantly higher.

- Only one of the three material series in the Northrop selection of materials revealed a difference in fatigue life that was attributable to the bond condition (see Figure 22). The 3NN system performed poorly when fatigued at 75% UCS. The unusually high stress level that it endured was held responsible for its performance. Yet, when the stress level was lowered to correspond to the level applied to the 3SN specimens, its fatigue life was indistinguishable from its 3SN counterpart. It was felt that the high applied stress level limited the possible damage modes the two material systems could experience, thus dictating their fatigue lives.

- The 3RN series systems displayed comparable fatigue lives. X-ray radiography of the specimens revealed intense cross-cracking (as an example, see Figure 23). This cracking was thought to have occurred during the "cool-down" from their inordinately high processing temperatures. It was postulated that this cracking may have severely reduced the interphase strength of the two systems. No confirmation of this point was available, however.

- While differences in the fatigue life of the 5NN and 5SN systems were recorded, these results were hampered by the presence of significant data scatter that may have resulted from differences in panel quality.

- Strain levels were recorded as a function of cycles for each of the material systems and converted into plots of normalized modulus versus normalized life (see Figure 24). These plots were very effective in characterizing the amount of fatigue life expended and remaining. The normalized modulus response seemed to indicate the presence (or absence) of key damage modes such as microbuckling.

- Notch temperature readings as a function of life displayed an unusual degree of reproducibility and, therefore, could be used to predict the stage of life a laminate was enduring (see Figure 25). This data was used in conjunction with the normalized modulus measurements to terminate specimens at a fixed percentage of remaining life in order to perform damage analysis.

- It was anticipated that the interphase would play a role in the dissipation of mechanical energy that would become manifest as specimen heating. The average temperature achieved at specimen failure (coinciding with the maximum temperature) was recorded for each material system (see Figure 26). Temperatures, in some instances, reached over 200°F. It appeared that the variation in the average failure temperature among the fourteen systems was related to the variation in the notched cross-plied compressive strength of the systems — the value that dictated the applied fatigue stress level. A simple analysis of rate-dependent heating was performed. It was seen that the variations in specimen heating among the systems could be accurately accounted for by considering the product of the applied stress amplitude and the resulting strain amplitude measured across the notch (the response for the Northrop materials possessing the standard epoxy are shown in Figure 27). These effects overwhelmed any effects that could be attributed to differences in the bond condition.

2. The Role of the Fiber/Matrix Interphase in the Static and Fatigue Behavior of Polymeric Matrix Composite Laminates

- A new and novel technique, Dynamic Signal Analysis (DSA) [28], was employed in an attempt to detect differences in dynamic performance that could arise from differences in the interphase. In its most basic form, the DSA resembles a macroscopic Dynamic Mechanical Analysis (DMA) instrument, enabling the operator to monitor dynamic phase lag and dynamic compliance. It was hoped that the phase lag signal would indicate the presence of differing bond conditions. Unfortunately, the data from the technique was not reproducible to a satisfying degree, precluding any comparative measures. Several sources of error in the test set-up were identified and corrected. More effort and experience will be required before the DSA technique can be successfully used to interrogate dynamic behavior that arises from differences in the interphase.

- The DSA technique *did* edify its position as an effective tool in failure prediction. The gain signal, which resembles the dynamic compliance, — with few exceptions — increases dramatically as the laminate faces imminent demise. This quality will be very useful to those investigators studying late-life damage states. It should be emphasized that the primary benefit of this interrogative technique lies in the fact that it is *non-contact*. This is a very appealing attribute in those instances when one is studying the fatigue behavior of laminates in demanding environments where strain monitoring is impractical.

- In an attempt to explain the difference in the fatigue behavior between the 810A, 820A, and 810O specimens, an SEM investigation of the interphase was performed. A chemical etch was used to assist in the identification of the two-phase toughened epoxy matrix system. The 810A and 820A systems displayed a nearly uniform "honeycomb" pattern of continuous epoxy surrounding empty capsules of eroded thermoplastic (see, as an example, Figure 28). There were no distinguishing traits to indicate differences in the interphase between these two systems. The 810O micrograph was stunningly different from its counterparts, however (see Figure 29). A distinct region different from the fibers and the honeycomb structure seen in the two previous micrographs was visible. The presence of this region helps explain the differences seen in the moduli of the 810O and 810A systems (provided that the modulus of this region is less than the matrix region). It also provides a clue as to why the fatigue life was so dramatically different in the 810O system. Detailed work should be performed to aid in understanding the structure property relationship that may arise in systems possessing different sizings or coatings.

- Inspired by the SEM results, the thought occurred that differences in local interphase moduli may influence the manner in which the stress is distributed away from the global stress concentrator. A strip gage was applied to one 810A specimen and one 810O specimen. The strain readings confirmed that the 810O specimen was the more compliant of the two (see Figure 30). After applying a regimen of fatigue cycles, the strain field of each specimen was monitored to detect the effect of stress relaxation. Surprisingly, the strain field in the 810A specimen changed only slightly. The gage nearest the hole was disabled by fatigue damage. The 810O specimen, on the other hand, had its first *three* gages disabled. This was completely unexpected since X-ray radiographs of 810O specimens after millions of cycles fail to reveal damage away from the hole. Though the strip gage technique proved highly effective at monitoring the gradient of strain arising from the center hole, the results of the tests could not be easily explained.

Unnotched ± 45° Specimens

- The great differences in fatigue behavior seen in the notched cross-plied 8A&O series materials was not replicated in the unnotched ±45° fatigue tests (see Figure 31). In the 8A&O series, unnotched ±45° *strength* seemed to be a good indicator of fatigue performance, i.e., the stronger the laminate, the longer the life. This theory did not apply to the 5U specimens, however. It was generally concluded that despite the differences seen in the fatigue behavior of the McAir systems, one would be hard-pressed to correlate the performance to the to influence the fatigue behavior of these systems.

- The temperature of each specimen was monitored during fatigue. The temperature at failure was recorded and compared among the systems (see Figure 32). In this case, the heating analysis developed for the notched cross-plied case failed to predict the variations in the temperature response. It was clear that the two 32-ply laminates (the 820A and 55U specimens) displayed the highest temperatures at failure. It was postulated that the fiber type may play a role in explaining the differences between the 8A&O and 5U temperature response.

- The investigators were, again, unable to utilize the DSA data collected from the fatigue tests due to poor reproducibility.

Modelling Considerations

Introducing the Interphase into Predictions of Notched Cross-plied Tensile Strength

Review of Notched Tensile Strength Theories

- Prior to introducing the interphase into a micromechanical model of notched tensile strength, it was prudent to review the current theories. Two approaches, the Whitney-Nuismer model [29] and the "terminal damage state" approach of Kortschot and Beaumont [30], were addressed. It is the author's opinion that these two seemingly disparate approaches are entirely reconcilable.

Discussion of Data

- Attempts to incorporate interphase behavior into micromechanical models of notched strength were temporarily discouraged by indications that unidirectional tensile strength and interphase strength (characterized by TFS and MMIIP results) seemingly fail to correlate with one another (see Figures 33 and 34, respectively).

- Data published by McAir and Northrop [20-22], along with data collected in the present investigation were used to calculate the "average-stress criteria parameter", a_o, of Whitney and Nuismer. This parameter can qualify the "notch sensitivity" of a material, i.e., a high value of a_o indicates an insensitivity to the presence of the notch, and, therefore, relatively high notched strengths. Low values of a_o indicate a heightened sensitivity to the presence of the notch, and, therefore, relatively low values of notched strength. The values for a_o were calcu-

lated for all fourteen systems under investigation (see Figure 35). It was seen that this parameter reveals a nearly linear dependence on the transverse flexural strength (see Figure 36). In other words, the stronger the interphase, the more notch sensitive the laminate. This is thought to be the first instance where this relationship has been formed so convincingly; *the notched tensile strength of a cross-plied laminate strongly depends on the strength of the fiber/matrix interphase.*

Introducing the Interphase into Predictions of Notched Cross-plied Compressive Strength

A Survey of the Micromechanical Theories of Compressive Strength

- The lamina level served as the starting point for the introduction of the interphase into notched compressive strength. It was necessary, therefore, to review the large number of compression models that have been published in order to identify the salient features of each approach. These models neatly separate themselves into two groups: instability analyses and constituent failure theories. Arguments were presented towards favoring the constituent failure theory approach to unidirectional compressive strength modelling. From among the many models, it was felt that the model of Hyer [31] incorporated a number of key variables an ideal (two-dimensional) model should possess.

Adaptation of the Present Unidirectional Micromechanical Model

- Unidirectional compressive failure is dictated by one of two variables in Hyer's model [31]: shear failure of the matrix (or, in the present case, the interphase) or fiber failure due to bending. A parameter representing the influence of the interphase was introduced into each scenario. It was determined that the "shear failure" scenario failed to represent the actual compressive data measured by Northrop [21]. The "bending scenario", on the other hand, predicted the compressive response of *many* of the diverse material systems with engineering accuracy (see Figure 37). Several systems failed to be represented by this theory, however.

Prediction of Unnotched Cross-plied Compressive Strength

- Cross-plied compressive strength of nearly twenty material systems culled from Northrop's published report [22], were plotted against their respective unidirectional compressive strength values. It was seen that a nearly linear relationship existed between the two variables beyond a certain unidirectional strength value (see Figure 38). Below this value, cross-ply compressive strength was seen to be nearly constant, perhaps reflecting the role of the 90° plies as laminate stabilizers. It is felt that once unidirectional strength is predicted, unnotched cross-plied compressive strength can be predicted with reasonable accuracy.

Prediction of Notched Cross-plied Compressive Strength

- Attempts at correlating a compressive "average-stress criteria parameter" with the transverse flexural strength (as was done successfully in the tensile case) proved entirely unsuccessful for the fourteen material systems under investigation.
- Another attempt was made, however, using "open-hole" compressive data supplied by Northrop [21]. Since the unnotched strength of their laminate configuration was not available, the notched strength of their materials were normalized by the unnotched cross-ply compressive strength of the respective systems; this permitted the calculation of an "adjusted" parameter, a_0^*. This parameter was plotted against the $\pm 45°$ tensile strength [21] (shown in Figure 10 to be linearly related to the TFS) of its respective system (see Figure 39). As in the tensile case, several systems revealed a strong dependence on the characterization of the interphase strength. This indicates that notched compressive strength is also dependent on the degree of fiber/matrix bonding.

Evolution Concepts as Applied to Fatigue Performance Modelling

- Fatigue behavior is dictated by how the states of stress and strength *evolve* over cyclic time. If one assumes that intrinsic fiber strength does not degrade as a function of fatigue, then one would normally be forced to admit that the matrix system is largely responsible for the fatigue performance of composite laminates. This thought is not completely satisfying, however. The idea that the *interphase* is critical to the fatigue performance of composites has been introduced. The next investigation into the role of the interphase in the fatigue performance of composite laminates should focus on the *degradation* of interphases as a function of cyclic time. The indentation technique used in the present investigation could be modified to allow for the interrogation of interphase strength in as-damaged *laminates*.

Future Recommendations

Several questions remained unanswered that beg for more research to be performed. The following is a brief list of research issues the author feels would illuminate the role of the interphase in the performance of composite laminates:

- A thorough investigation should follow the work of Lesko [24] to address the many questions that arose while using the indentation technique to characterize the interphase. What *exactly* is the indentation test measuring? Shear response? Compressive response?
- Once such an investigation has taken place, considerable work could be focused on using the technique to monitor the *degradation* of interphases in as-damaged *laminates* (as opposed to unidirectional specimens).
- The transverse flexure test would benefit immensely from a careful and detailed SEM analysis of the failure surfaces. Is the failure in the interphase? In the matrix? In the fiber? Is the failure ductile or brittle? These answers will help researchers understand why the TFS results mirror the bond condition so well.

- Another test technique aimed at characterizing the "shear response" of the interphase should be pursued. This approach could be modelled after the works of Newaz [32] and Naim [33,34]. Their attempts to quantify shear behavior by analyzing longitudinal splitting has immediate applicability to the fatigue response of notched composites. It is quite possible that shear response of the present systems measured in this manner could correlate to the notched cross-plied fatigue behavior or to the ±45° fatigue behavior.

- A whole research project could be devoted to the study of why the presence of the "O" sizing affected the fatigue (and static) performance of the 810O specimen. This study would involve intense physical and chemical analyses of the distinct region seen in the SEM micrographs. Lessons learned from this study could possibly change how composite scientists design materials for fatigue resistance.

- It is quite necessary to understand how the interphase influences the fatigue behavior at *low applied stress levels*. Several systems in this investigation failed after only a few thousand cycles. Perhaps at this high stress level, the effect of the interphase was overwhelmed by the other mechanisms that instigated rapid laminate failure.

- Finally, there is a great need for the interphase to enter micromechanical models of composite behavior in a rigorous manner. Several avenues have been opened within this study. The physics of the interphase must be described with our mathematical tools in order to accurately predict the performance of composites subjected to static and dynamic loading.

References

1. Swain, R. E., "The Role of the Fiber/Matrix Interphase in the Static and Fatigue Behavior of Polymeric Matrix Composite Laminates," Ph.D. Dissertation, Dept. of Engineering Science and Mechanics, College of Engineering, Virginia Polytechnic Institute and State University, Blacksburg, Virginia, Feb. 1992.

2. Javaraman, K., Reifsnider, K. L., and Swain, R. E., "The Interphase in Unidirectional Fiber-Reinforced Composites, I. A Review of Characterization Methods," submitted to *Journal of Composites Technology and Research*, 1991.

3. Drzal, L. T., Rich, M. J., Lloyd P. F., "Adhesion of Graphite Fibers to Epoxy Matrices: I. The Role of Fiber Surface Treatment," *Journal of Adhesion*, Vol. 16, No. 1, 1983, pp. 1-30.

4. Drzal, L. T., Rich, M. J., Koenig, M. F., "Adhesion of Graphite Fibers to Epoxy Matrices: II. The Effect of Fiber Finish," *Journal of Adhesion*, Vol. 16, No. 2, 1983, pp. 133-152.

5. Hughes, J. D. H., "The Carbon Fiber Epoxy Interface - A Review," *Composites Science and Technology*, Vol. 41, 1991, pp. 13-45.

6. Madhukar, M. S., and Drzal, L. T., "Effect of Fiber-Matrix Adhesion on the Longitudinal Compressive Properties of Graphite Epoxy Composites," *Proceedings of the Fifth Technical Conference of the American Society for Composites*, 1990, pp. 849-858.

7. Madhukar, M. S., and Drzal, L. T., "Fiber-Matrix Adhesion and its Effects on Composite Mechanical Properties. I. In-plane and Interlaminar Shear Behavior of Graphite Epoxy Composites," *Journal of Composite Materials*, Vol. 25, Aug. 1991, pp. 932-957.

8. Madhukar, M. S., and Drzal, L. T., "Fiber-Matrix Adhesion and its Effects on Composite Mechanical Properties. II. Tensile and Flexural Behavior of Graphite Epoxy Composites," *Journal of Composite Materials*, Vol. 25, Aug. 1991, pp. 958-991.

9. Curtis, P. T., Morton, J., "The Effect of Fibre Surface Treatment on the Compressive Strength of CFRP Laminates," *Progress in Science and Engineering of Composites*, T. Hayashi, K. Kawata, and S. Umekawa, Eds., ICCM-IV, 1982, pp. 219-226.

10. Lehmann, S., Megerdigian, C., and Papalia, R., "Carbon Fiber Resin Matrix Interphase: Effect of Carbon Fiber Surface Treatment on Composite Performance," *SAMPE Quarterly*, April 1985, pp. 7-13.

11. Lehmann, S., Robinson, R., and Tse, M. K., "Characterization of Carbon Fiber Resin Matrix Interphase," *Materials Sciences for the Future: 31st International SAMPE Symposium*, 1986, pp. 291-302.

12. Norita, T., Matsui, J., and Matsuda, H. S., "Effect of Surface Treatment of Carbon Fiber on Mechanical Properties of CFRP," *Composite Interfaces*, H. Ishida and J. L. Koenig, Eds., Elsevier, 1986, pp. 123-132.

13. Robinson, R., Lehmann, S., Askew, G., Wilford, D., Megerdigian, C., and Papalia, R., "A Preliminary Assessment of the Role of Fiber Surface Properties in Controlling Composite Performance," *High Tech - The Way into the Nineties*, K. Brunsch, H.-D. Gödilden, and C.-M. Herkert, Eds., Elsevier, 1986, pp. 299-310.

14. Robinson, R., Lehmann, S., Wilford, D., Askew, G., Coulthard, R., Megerdigian, C., and Kirby, J., "Surface Characteristics Influencing Carbon Fibre Matrix Adhesion Performance," *Looking Ahead for Materials and Processes*, J. de Bossu, G. Briens and P. Lissac, Eds., Elsevier Science Publishing, 1987.

15. Megerdigian, C., Robinson, R., and Lehmann, S., "Carbon Fiber Resin Matrix Interphase: Effect of Carbon Fiber Surface Treatment and Environmental Conditioning on Composite Performance," *Materials — Pathway to the Future:* Proceedings of the International SAMPE Symposium and Exhibition, G. Carrillo, E. Newell, W. Brown, and P. Phelan, Eds., Vol. 33, 1988, pp. 571-582.

16. Verpoest, I., Desaeger, M., and Ivens, J., "The Influence of the Fiber-Matrix Interface on Damage Development in Composite Materials," *Academia Analecta*, Jan. 1989.

17. Ivens, J., Wevers, M., Verpoest, I., and De Meester, P., "The Influence of the Interface on Damage Development in CFRP," *ICCM VII: The Proceedings of the Seventh International Conference on Composite Materials*, Vol. 2, W. Yunshu, G. Zhenlong, and W. Renjie, Eds., Pergamon Press, 1989, pp. 447-453.

18. Beck, A. R., and Yen, A., "Development of Ultralightweight Materials," First Interim Technical Report, Air Force Contract No. F33615-88-C-5447, Aug. 1988.

19. Tung, C., and Yen, A., "Development of Ultralightweight Materials," Tenth Interim Technical Report, Air Force Contract No. F33615-88-C-5447, Nov. 1990.

20. Hahn, G., Wong, R., Hwang, W.-F., Hartness, T., Drzal, L., Robinson, R., and Smith, S., "Development of Ultralightweight Materials," Tenth Quarterly Interim Technical Report, Air Force Contract No. F33615-88-C-5452, Nov. 1990.

21. Tung, C., and Yen, A., "Development of Ultralightweight Materials," Eighth Interim Technical Report, Air Force Contract No. F33615-88-C-5447, May 1990.

22. Tung, C., and Yen, A., "Development of Ultralightweight Materials," Ninth Interim Technical Report, Air Force Contract No. F33615-88-C-5447, Aug. 1990.

23. Adams, D. F., King, T. R., Blackketter, D. M., "Evaluation of the Transverse Flexure Test Method for Composite Materials," submitted for publication in *Composites Science and Technology*, 1991.

24. Lesko, J. J., Carman, G. P., Dillard, D. A., Reifsnider, K. L, "Indentation Testing of Composite Materials as a Tool for Measuring Interfacial Quality," *Composite Materials: Fatigue and Fracture (Fourth Conference), ASTM STP 1156*, accepted for publication, Nov. 1991.

25. ASTM Standard D 3171-76, "Standard Test Method for the Fiber Content of Resin-Matrix Composites by Matrix Digestion," *Annual Book of ASTM Standards*, Vol. 15.03, 1991, pp. 123-125.

26. Olley, R. H., Bassett, D. C., Blundell, D. J., "Permanganic Etching of PEEK," *Polymer*, Vol. 27, March 1986, pp. 344-348.

27. Peters, P. W. M., and Albertsen, H., "The Fiber Matrix Interphase in CFRP with a Phase-Separating Matrix System," *Interfacial Phenomena in Composite Materials*, Leuven, Sept. 17-19, 1991, pp. 101-104.

28. Elahi, M., Razvan, A., Reifsnider, K. L., "Characterization of Composite Materials Dynamic Response Using Load Stroke Frequency Response Measurement," presented at the *ASTM Fourth Symposium on Composite Materials: Fatigue and Fracture*, Indianapolis, Indiana, May 7, 1991.

29. Whitney, J. M., and Nuismer, R. J., "Stress Fracture Criteria for Laminated Composites Containing Stress Concentrations," *Journal of Composite Materials*, Vol. 8, July 1974, pp. 253-265.

30. Kortschot, M. T., and Beaumont, P. W. R., "Damage Mechanics of Composite Materials: II - A Damage-Based Notched Strength Model," *Composite Science and Technology*, Vol. 39, 1990, pp. 303-326.

31. Hyer, M. W., "Micromechanics of Compression in Unidirectional Laminates," Technical Report 86-9 prepared for Martin Marietta, Baltimore Division, Aug. 1986.

32. Newaz, G. M., "Evaluation of Fiber-Matrix Interphasial Toughness in Unidirectional Composites," *Polymer Composites*, Vol. 7, No. 6, 1986, pp. 421-425.

33. Nairn, J. A., "Fracture Mechanics of Unidirectional Composites Using the Shear-Lag Model, I. Theory," *Journal of Composite Materials*, Vol. 22, June 1988, pp. 561-588.

34. Nairn, J. A., "Fracture Mechanics of Unidirectional Composites Using the Shear-Lag Model, II. Experiment," *Journal of Composite Materials*, Vol. 22, June 1988, pp. 569-600.

35. Goodman, C., "Percent Fiber Volume Fraction in Composite Laminates," Celion Carbon Fibers Application & Product Development Specification No. CS-200-T, Nov. 1988.

Table 1.   List of the McAir Material Systems.

MATERIAL TYPE ACRONYM	FIBER MODULUS (Msi)	FIBER STRENGTH (ksi)	PERCENT SURFACE TREATMENT	FIBER SIZING	MATRIX TYPE	MATERIAL SERIES ACRONYM
52U	32	550	20	Unsized	T. Epoxy	
55U	32	550	50	Unsized	T. Epoxy	5U
510U	32	550	100	Unsized	T. Epoxy	
82A	45	850	20	"A" sized	T. Epoxy	
85A	45	850	50	"A" sized	T. Epoxy	
810A	45	850	100	"A" sized	T. Epoxy	8A&O
820A	45	850	200	"A" sized	T. Epoxy	
810O	45	850	100	"O" sized	T. Epoxy	

Table 2.   List of the Northrop Material Systems.

MATERIAL TYPE ACRONYM	FIBER MODULUS (Msi)	FIBER STRENGTH (ksi)	PERCENT SURFACE TREATMENT	FIBER SIZING	MATRIX TYPE	MATERIAL SERIES ACRONYM
3NN	35	650	0	Unsized	S. Epoxy	3N
3SN	35	650	100	Unsized	S. Epoxy	
3RNN	35	650	0	Unsized	T-plastic	3R
3RSN	35	650	100	Unsized	T-plastic	
5NN	50	650	0	Unsized	S Epoxy	5N
5SN	50	650	100	Unsized	S. Epoxy	
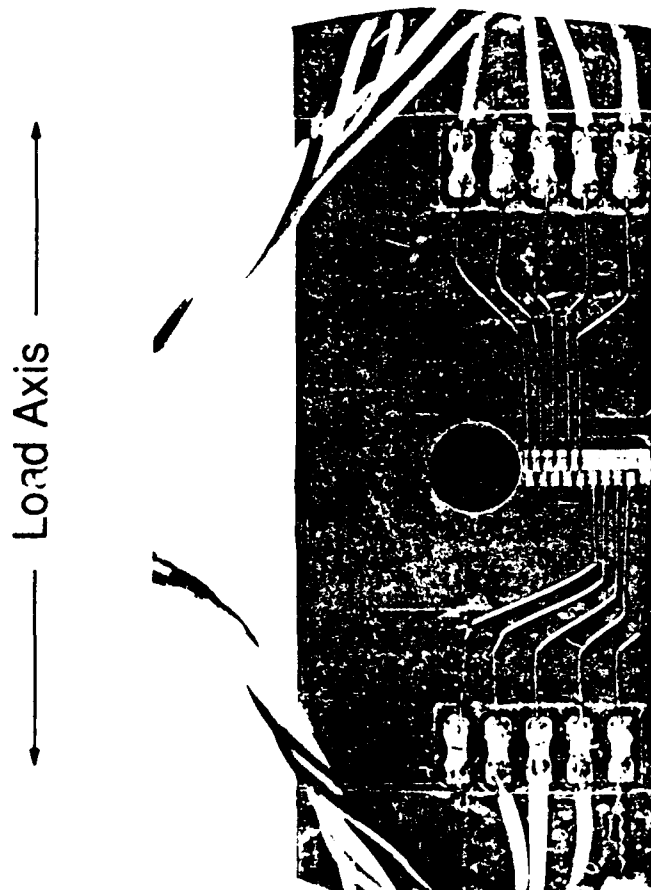
Figure 1.   Photograph of a Strip Gage Applied to an 810A Specimen.
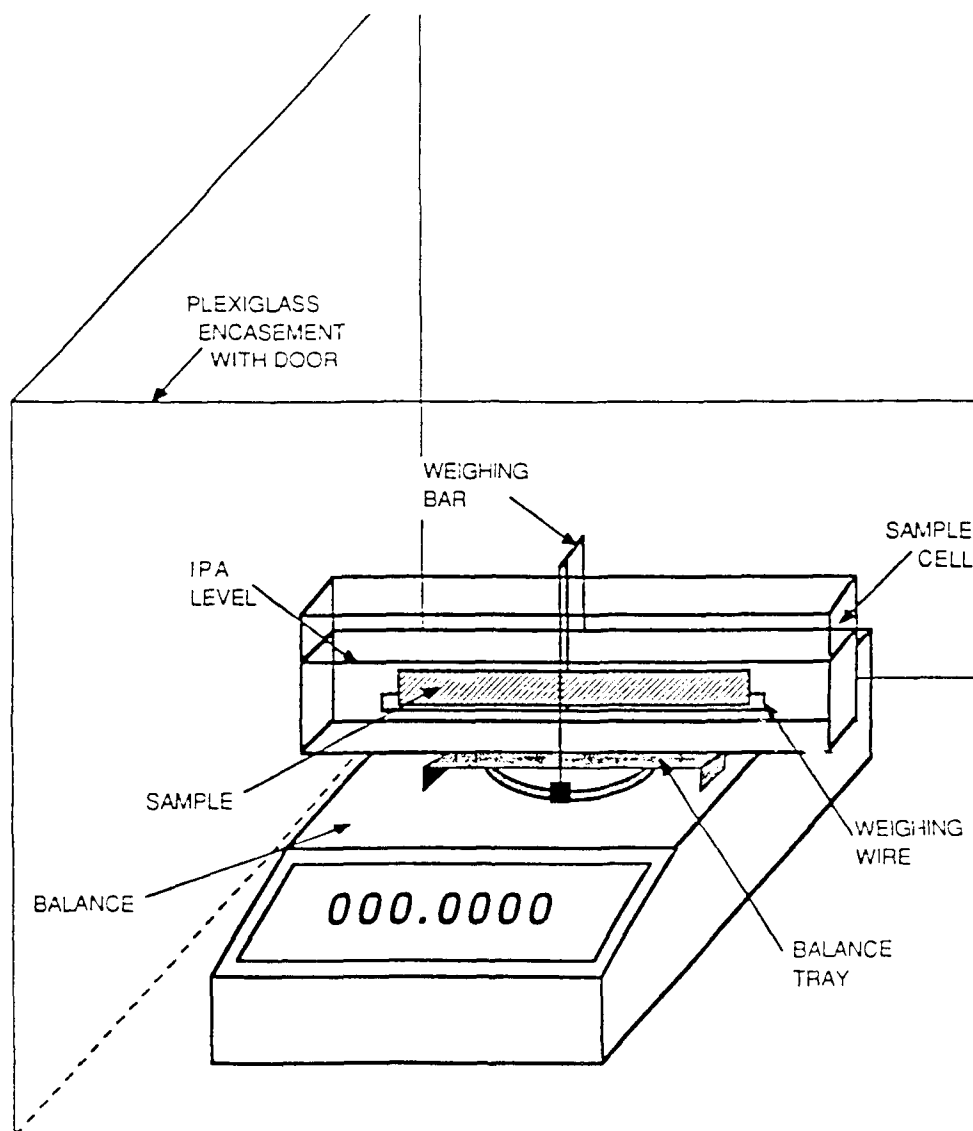
Figure 2.   Set-up for Isopropyl Alcohol (IPA) Technique for Measuring Fiber Volume Fraction (taken from [35]).

Transverse Flexural Strength (ksi)

Material Type
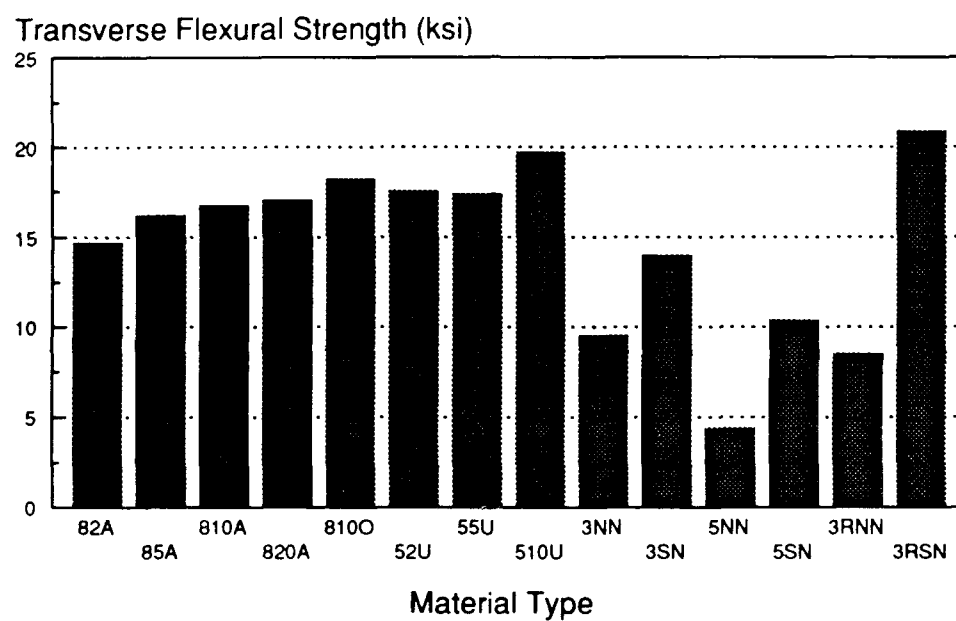
Figure 3. Average Transverse Flexural Strength of the McAir and Northrop Materials.

MMHP (ksi)   Representative Strain, d/D
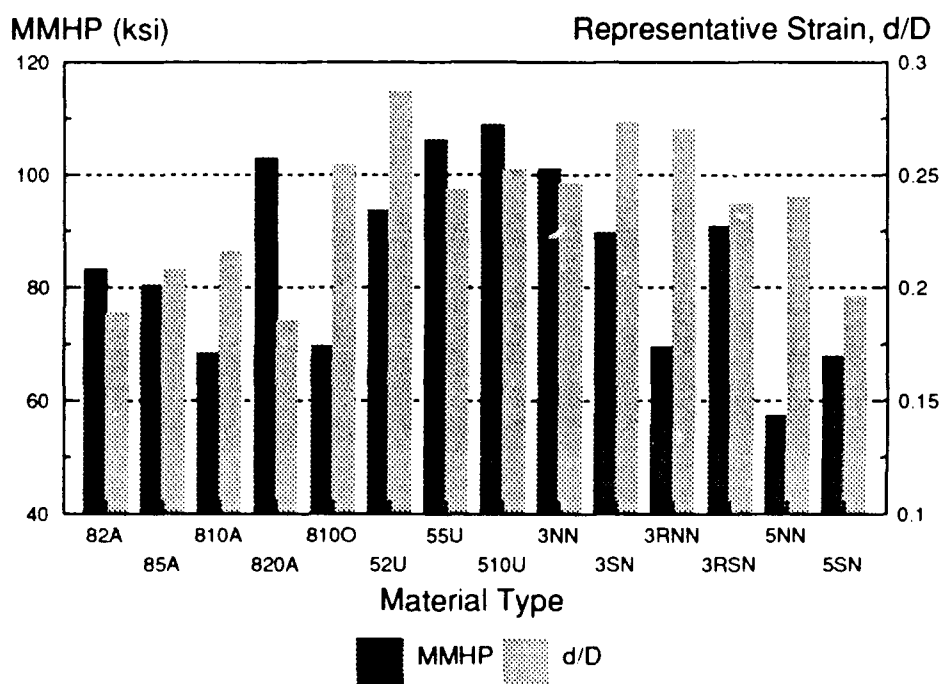
Figure 4.   Average Maximum Mean Hardness Pressure and Representative Strain of the McAir and
            Northrop Materials.
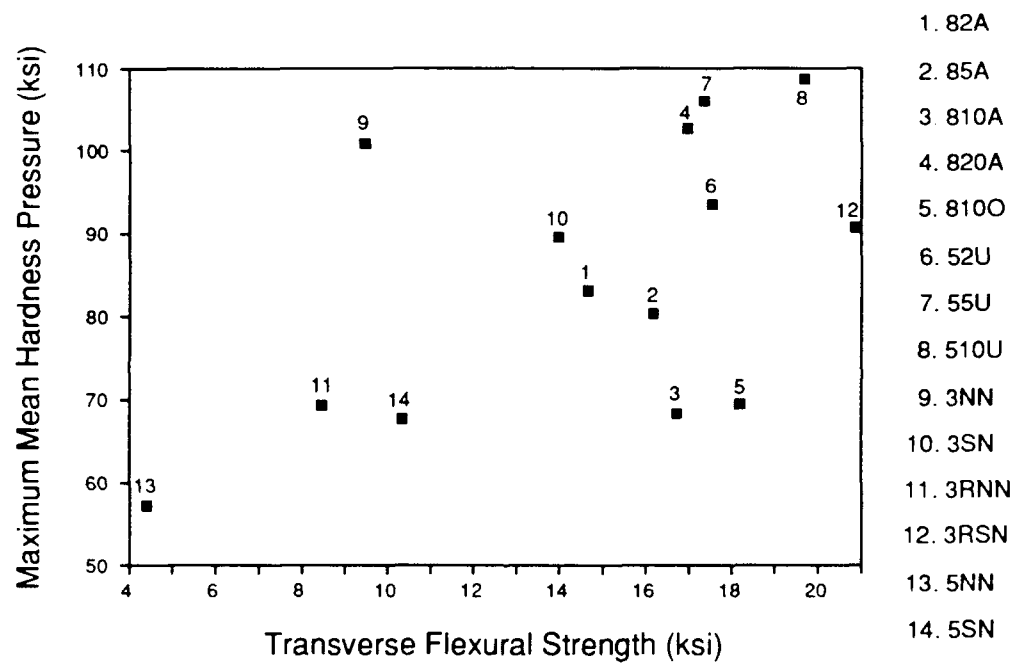
Figure 5.   Maximum Mean Hardness Pressure versus Transverse Flexural Strength of the McAir and Northrop Materials.

2. The Role of the Fiber/Matrix Interphase in the Static and Fatigue Behavior of Polymeric Matrix Composite Laminates
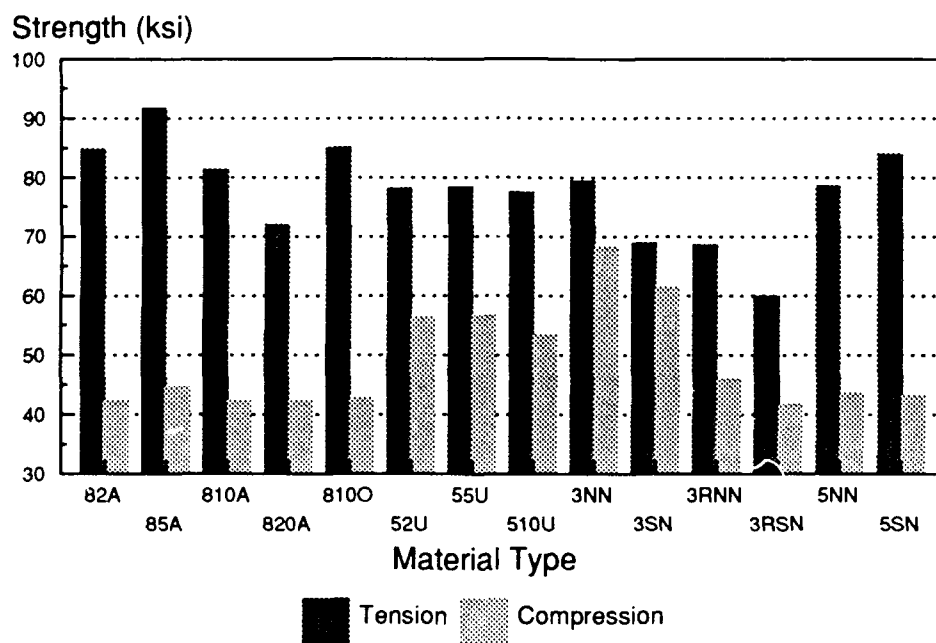
Figure 6.   Average Gross-section Tensile and Compressive Strengths of the Notched Cross-plied McAir and Northrop Materials.
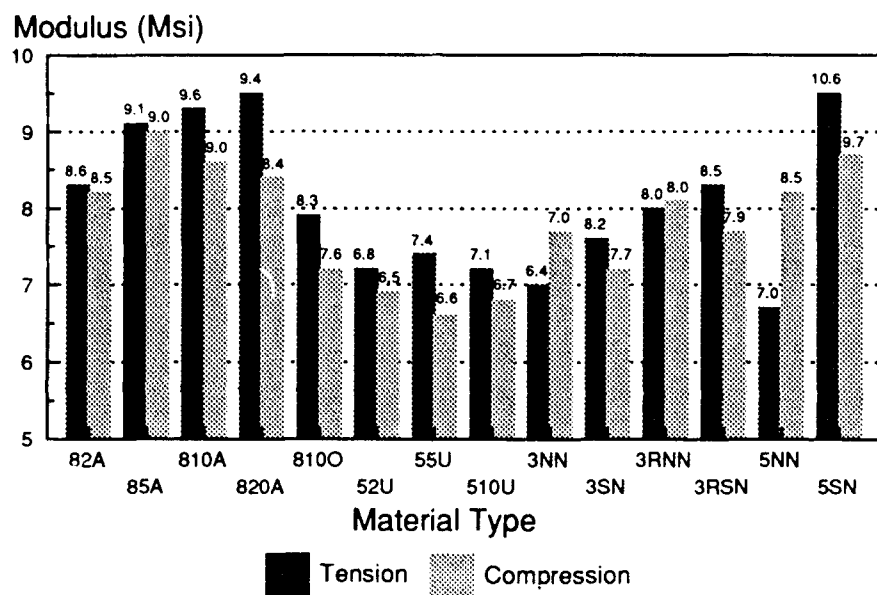
Modulus (Msi)

Column height represents measured value

Numbers above column represent values adjusted by fiber volume fraction

Figure 7. Average Gross-section Tensile and Compressive Moduli of the Notched Cross-plied McAir and Northrop Materials.
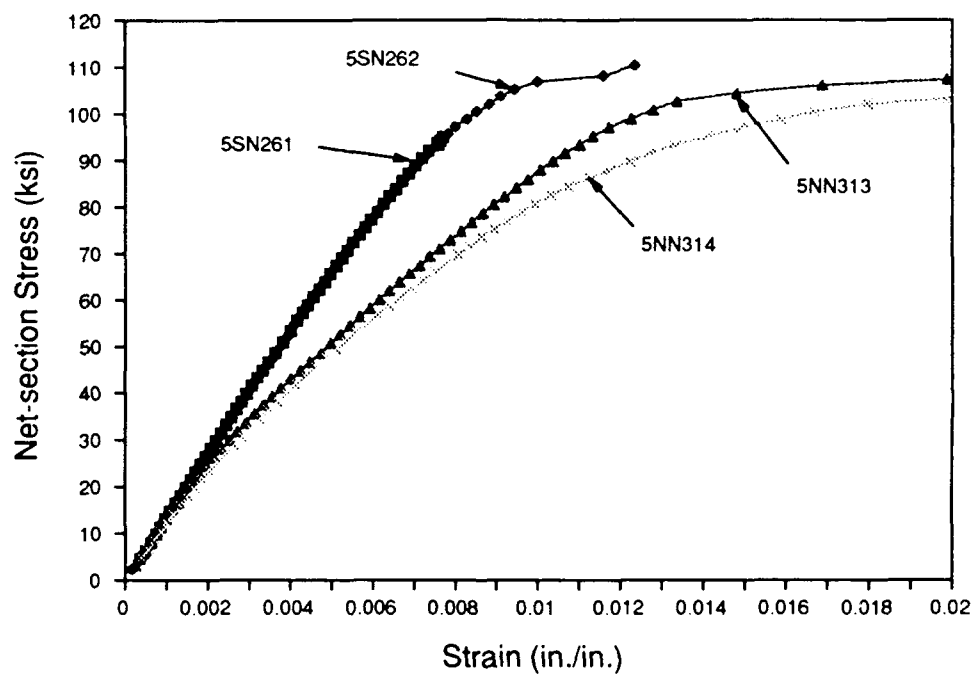
Figure 8. Net-Section Tensile Stress vs. Measured Strain for Two 5NN Specimens and Two 5SN Specimens.
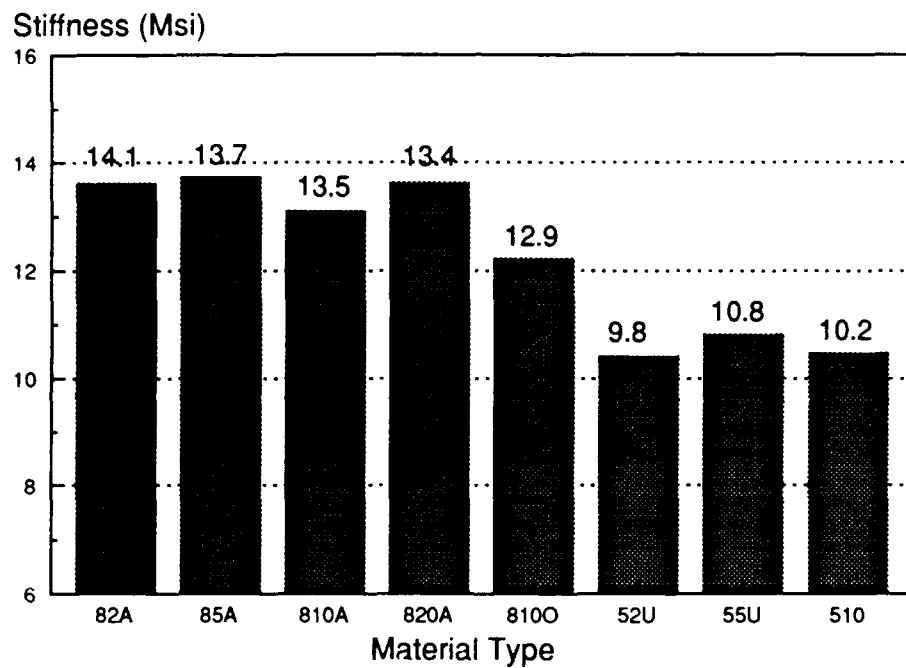
2. The Role of the Fiber/Matrix Interphase in the Static and Fatigue Behavior of Polymeric Matrix Composite Laminates

40

Stiffness (Msi)

Column height represents measured value

Numbers above column represent values adjusted by fiber volume fraction

Figure 9.   Tensile Moduli of the Unnotched Cross-plied McAir Materials.
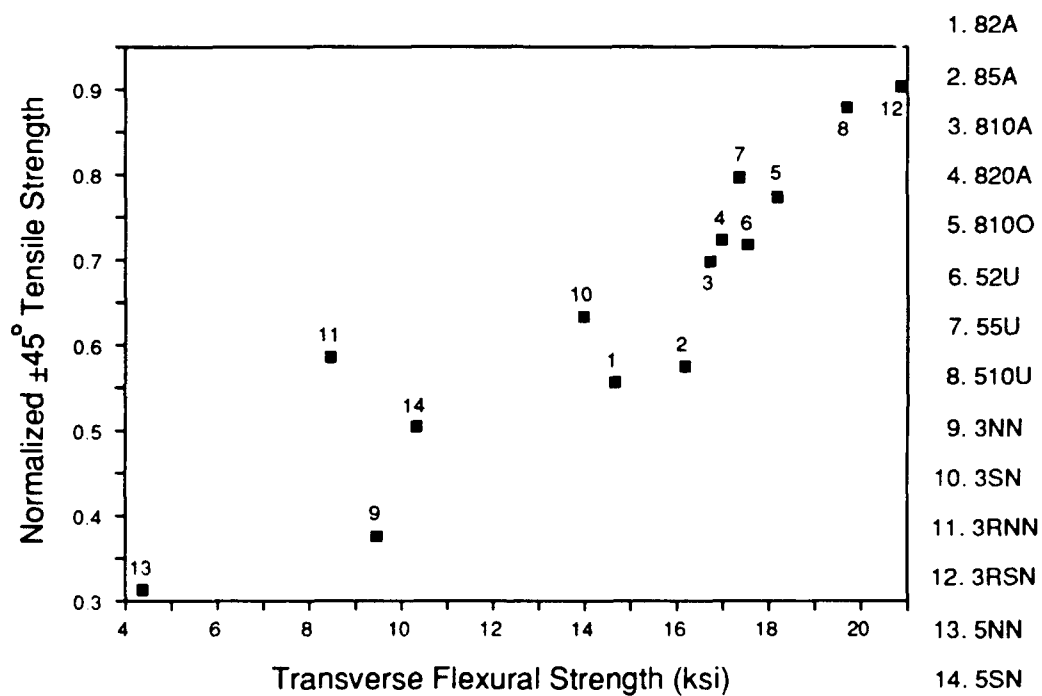
Figure 10. Normalized ± 45° Tensile Strength versus Transverse Flexural Strength of the McAir and Northrop Materials [20,21].
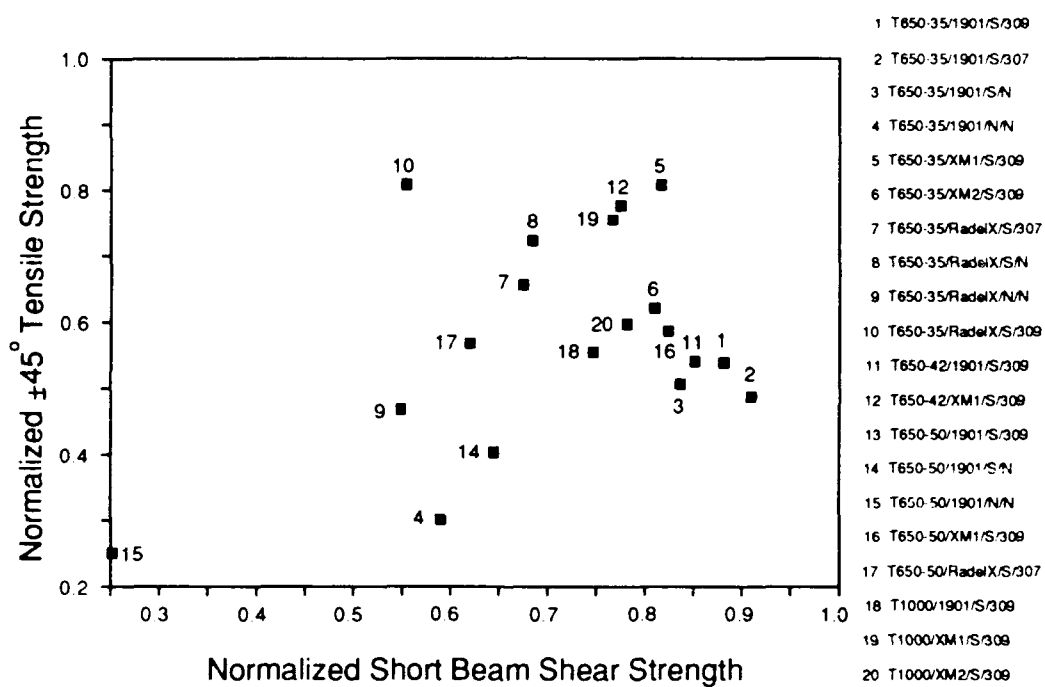
Figure 11. Normalized ±45° Tensile Strength versus Normalized Short Beam Shear Strength of the Northrop Materials [21].
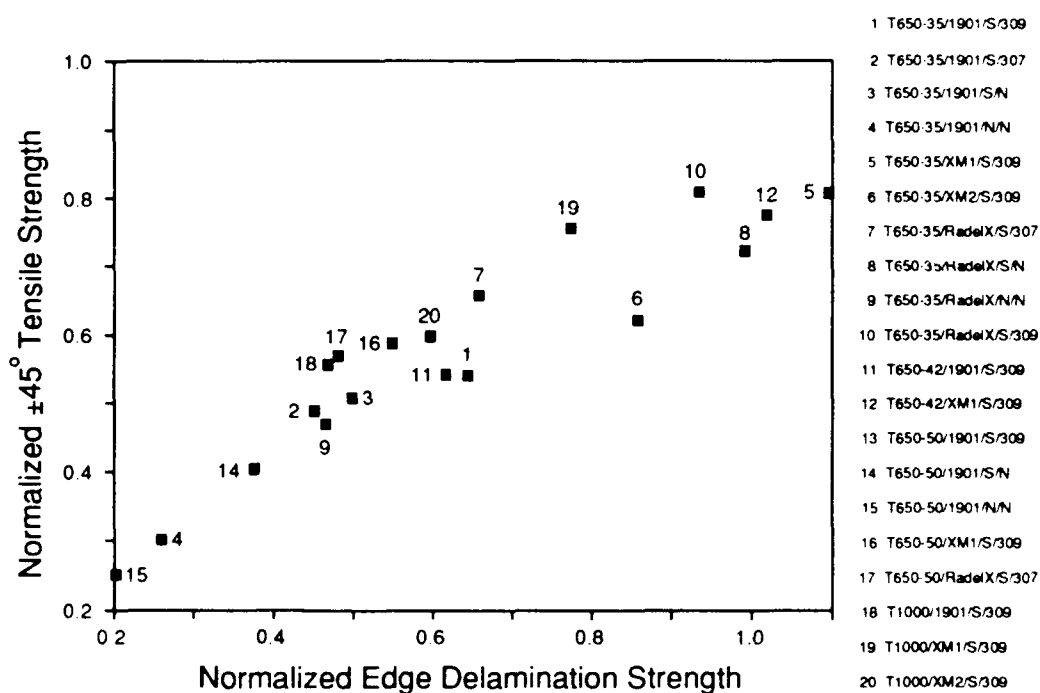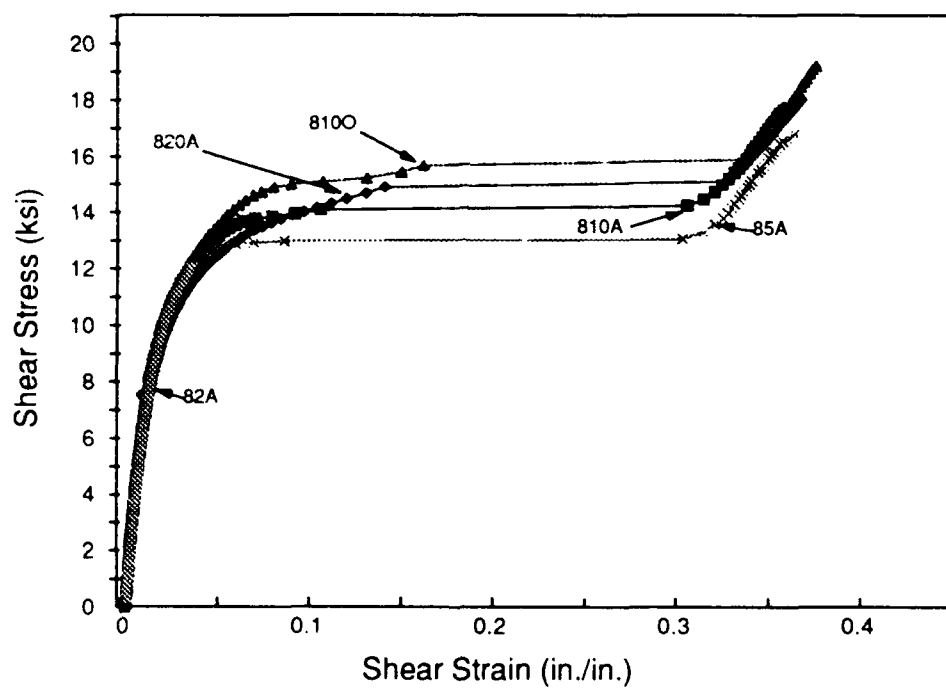
Figure 12. Normalized ±45° Tensile Strength versus Normalized Edge Delamination Strength of the Northrop Materials [21].

Legend:
1. T650-35/1901/S/309
2. T650-35/1901/S/307
3. T650-35/1901/S/N
4. T650-35/1901/N/N
5. T650-35/XM1/S/309
6. T650-35/XM2/S/309
7. T650-35/RadelX/S/307
8. T650-35/RadelX/S/N
9. T650-35/RadelX/N/N
10. T650-35/RadelX/S/309
11. T650-42/1901/S/309
12. T650-42/XM1/S/309
13. T650-50/1901/S/309
14. T650-50/1901/S/N
15. T650-50/1901/N/N
16. T650-50/XM1/S/309
17. T650-50/RadelX/S/307
18. T1000/1901/S/309
19. T1000/XM1/S/309
20. T1000/XM2/S/309

2. The Role of the Fiber/Matrix Interphase in the Static and Fatigue Behavior of Polymeric Matrix Composite Laminates

Figure 13. Shear Stress versus Shear Strain for Five Specimens in the 8A&O Series.
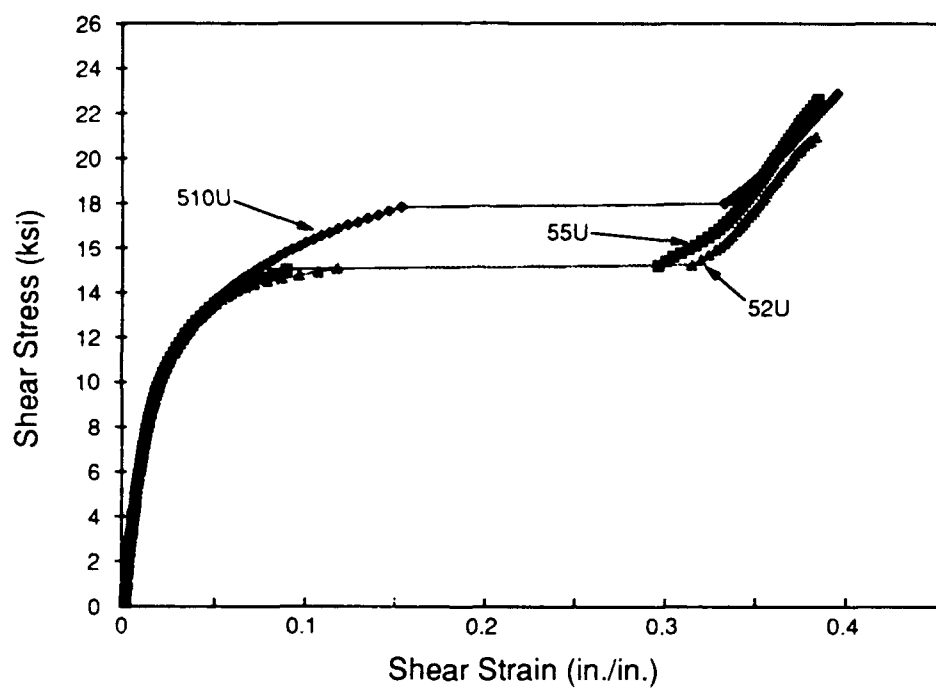
Figure 14.   Shear Stress versus Shear Strain for Three Specimens in the 5U Series.
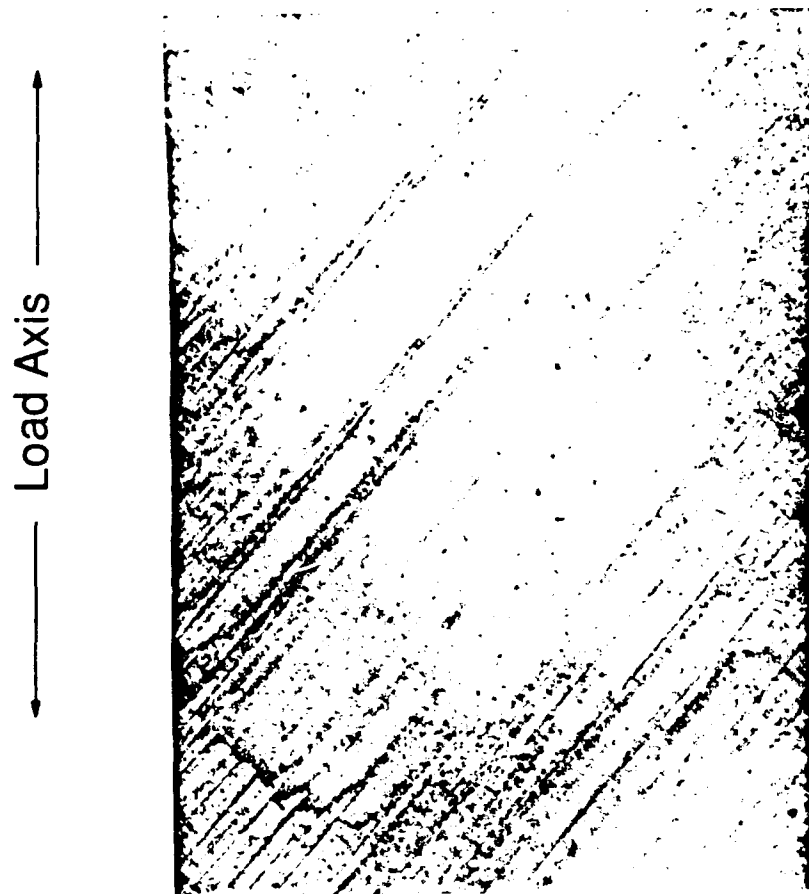
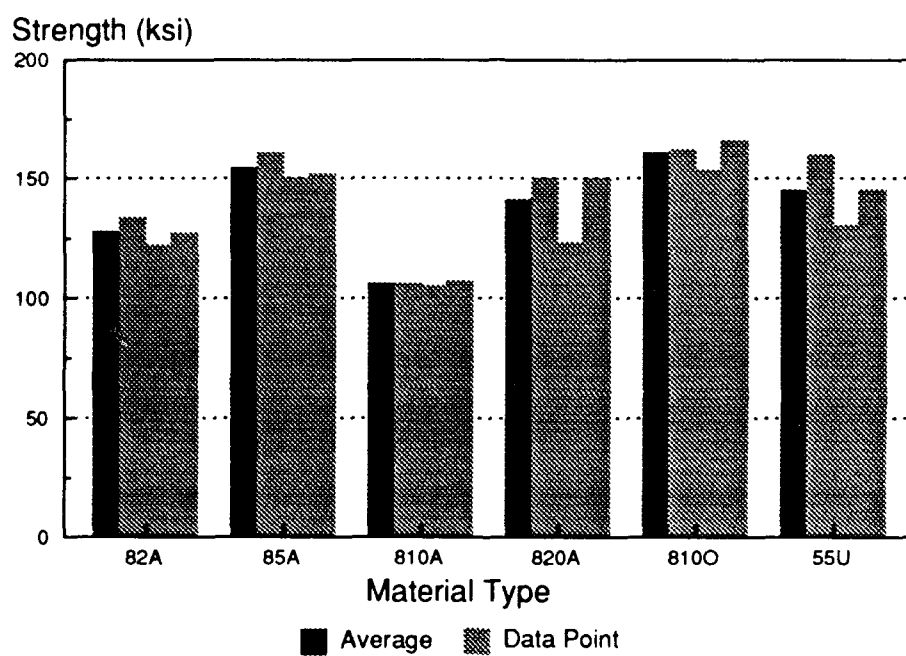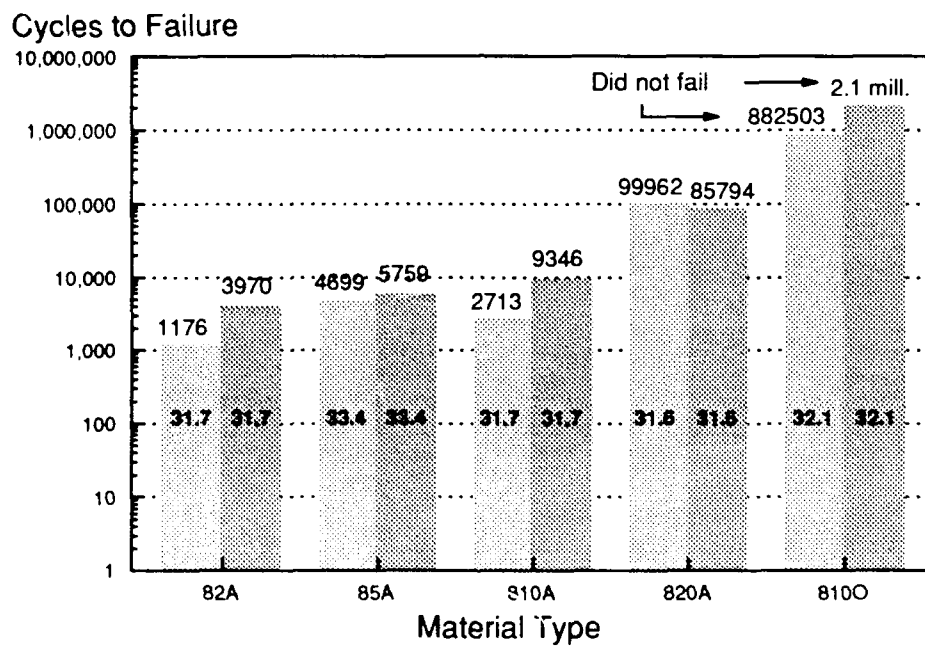Figure 15. X-ray Radiograph of a ±45° 510U Specimen after 1 Million Cycles; Max. Stress = 24 ksi; R = -1 at 10 Hz.

Figure 16.   Average Strength and Strength of Individual Unidirectional Compressive Specimens from the McAir Materials.

Cycles to Failure

Numbers above bar: actual cycles

Numbers inside bar: applied stress level (ksi)

Figure 17. Cycles to Failure of the Notched Cross-plied Specimens in the 8A&O Series; Max. Applied
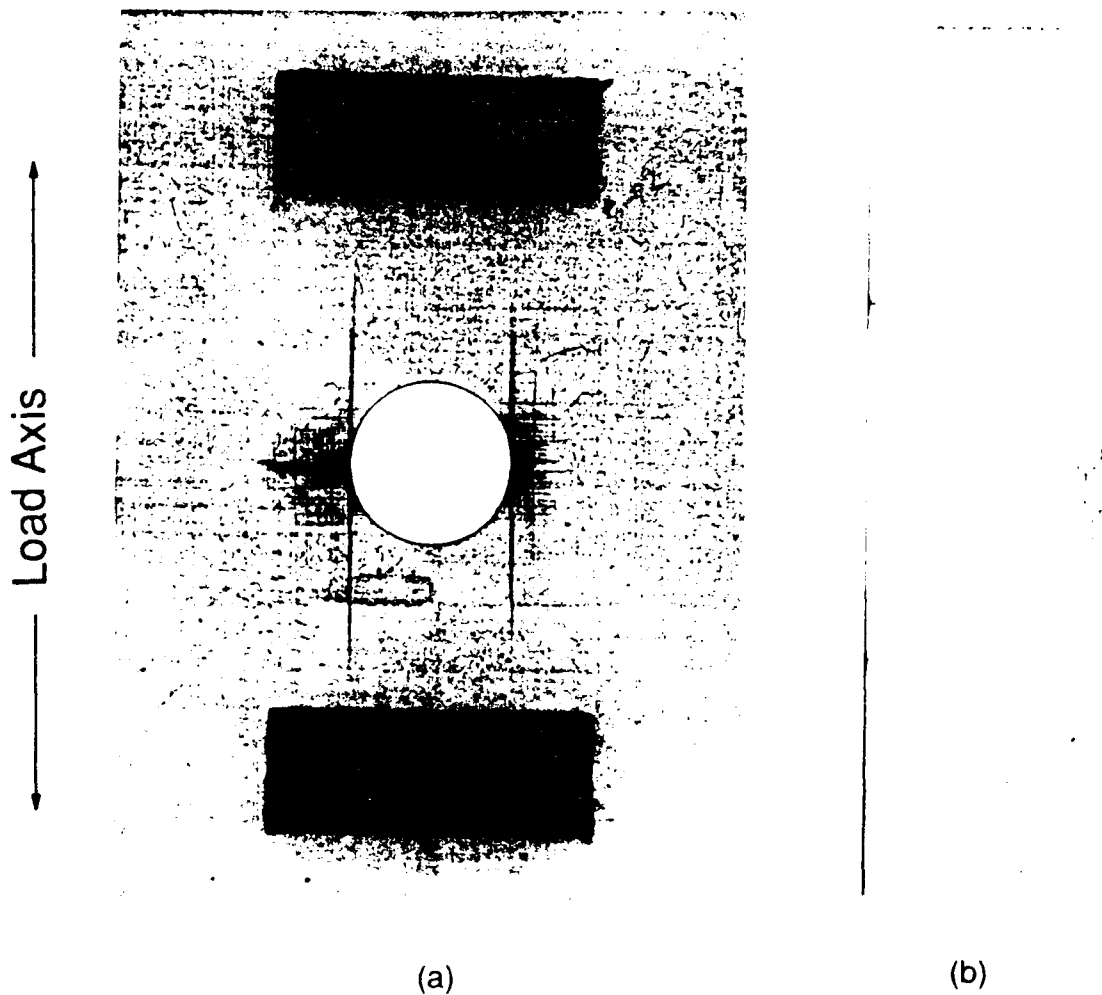Stress = 75% UCS; R = -1 at 10 Hz.

(a)   (b)

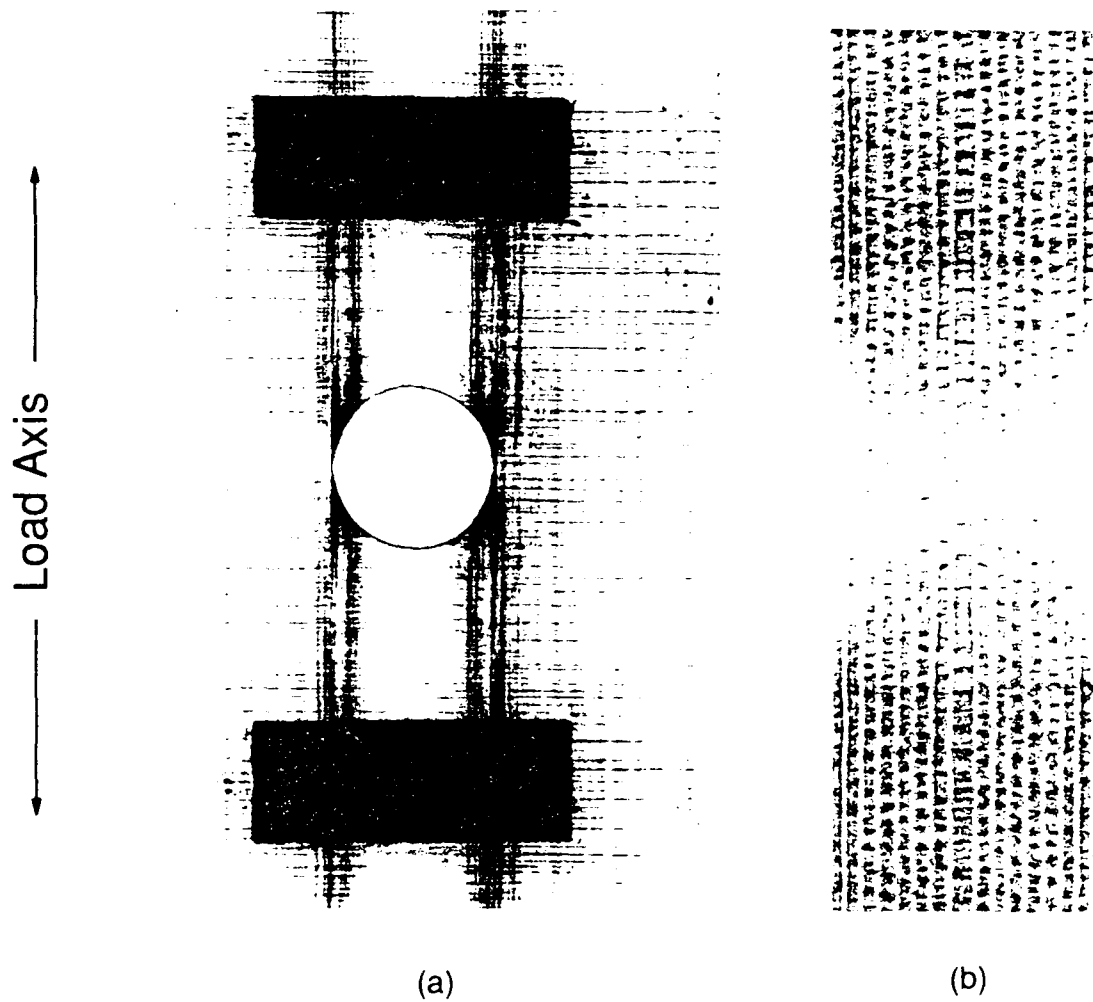Figure 18.   X-ray Radiograph of an 810A Specimen after 3000 Cycles; a.) Front View, b.) Edge View.

Figure 19. X-ray Radiograph of an 810O Specimen after 2.1 Million Cycles; a.) Front View, b.) Edge View.
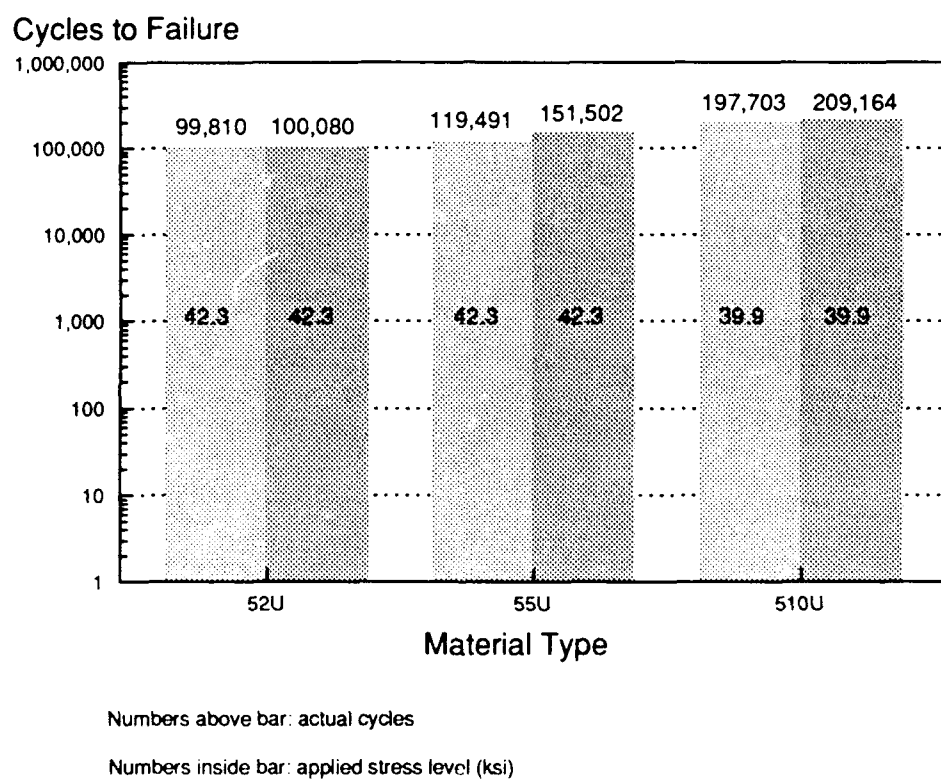
Cycles to Failure

Figure 20. Cycles to Failure of the Notched Cross-plied Specimens in the 5U Series; Max. Applied
Stress = 75% UCS; R = -1 at 10 Hz.

Load Axis

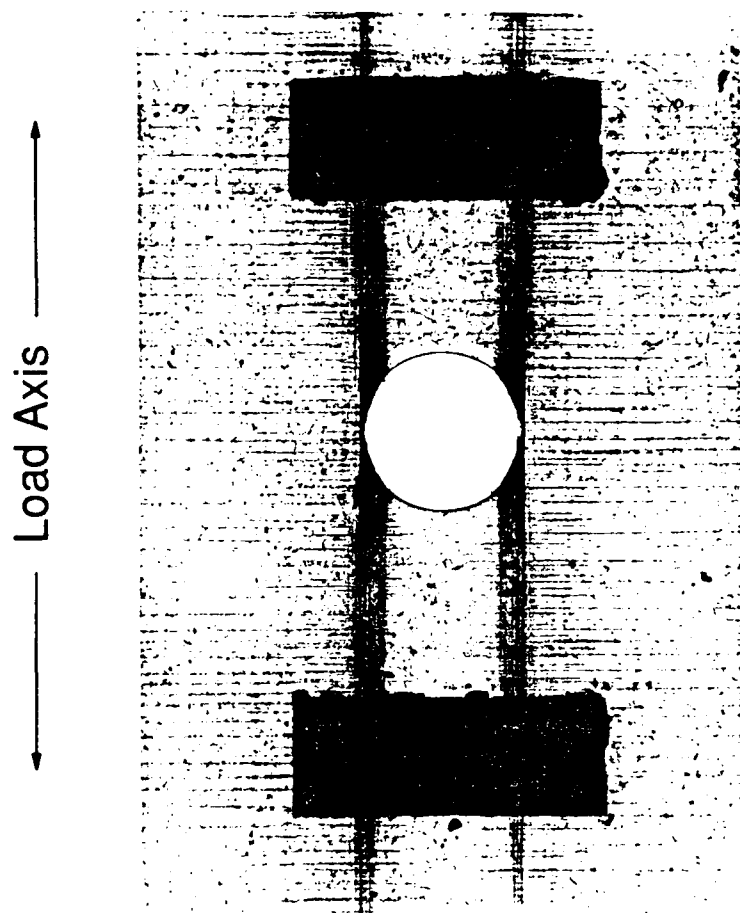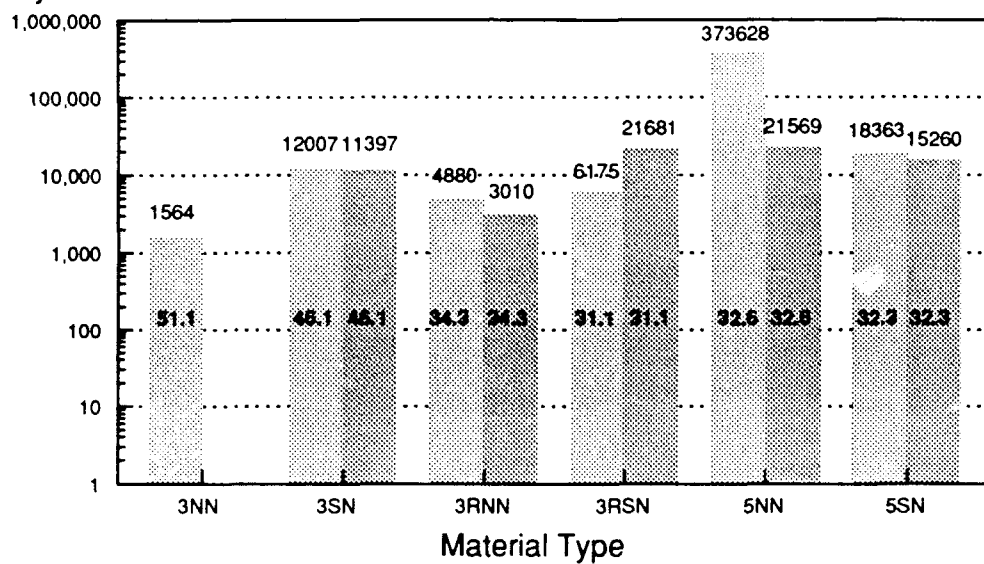Figure 21. X-ray Radiograph of a 510U Specimen after 136,100 Cycles.

Cycles to Failure

Numbers above bar: actual cycles

Numbers inside bar: applied stress level (ksi)

Figure 22.   Cycles to Failure of the Northrop Notched Cross-plied Specimens; Max. Applied Stress = 75% UCS; R = -1 at 10 Hz.
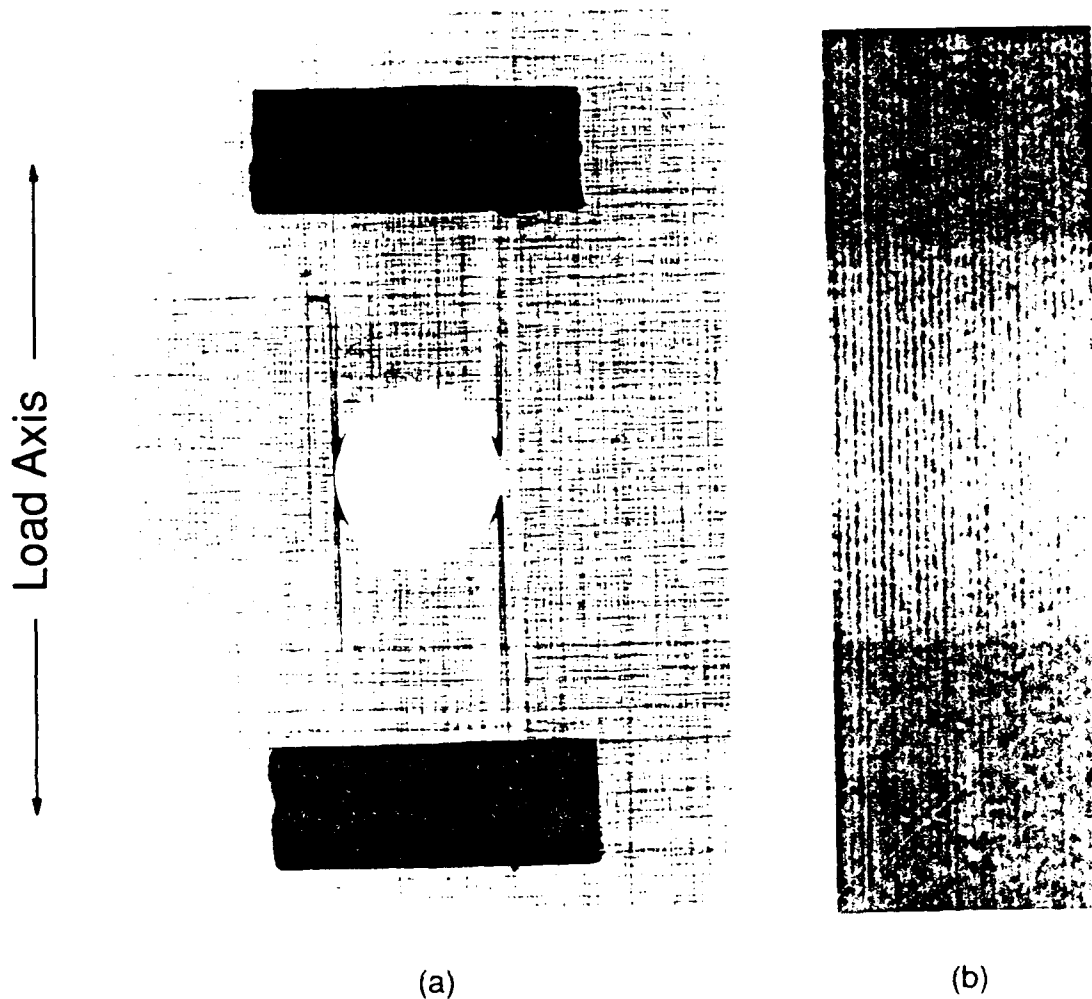
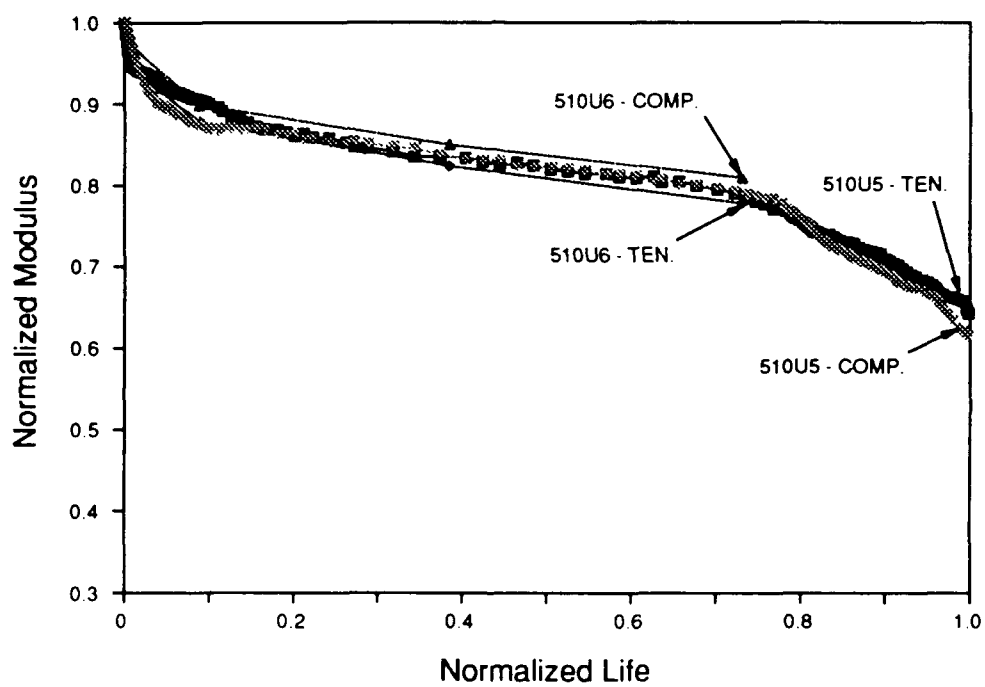**Figure 23.** X-ray Radiograph of a 3RSN Specimen after 5500 Cycles: a.) Front View, b.) Edge View.

Figure 24. Plot of Normalized Modulus versus Normalized Life for Two 510U Specimens; Max. Stress = 75% UCS; R = -1 at 10 Hz.
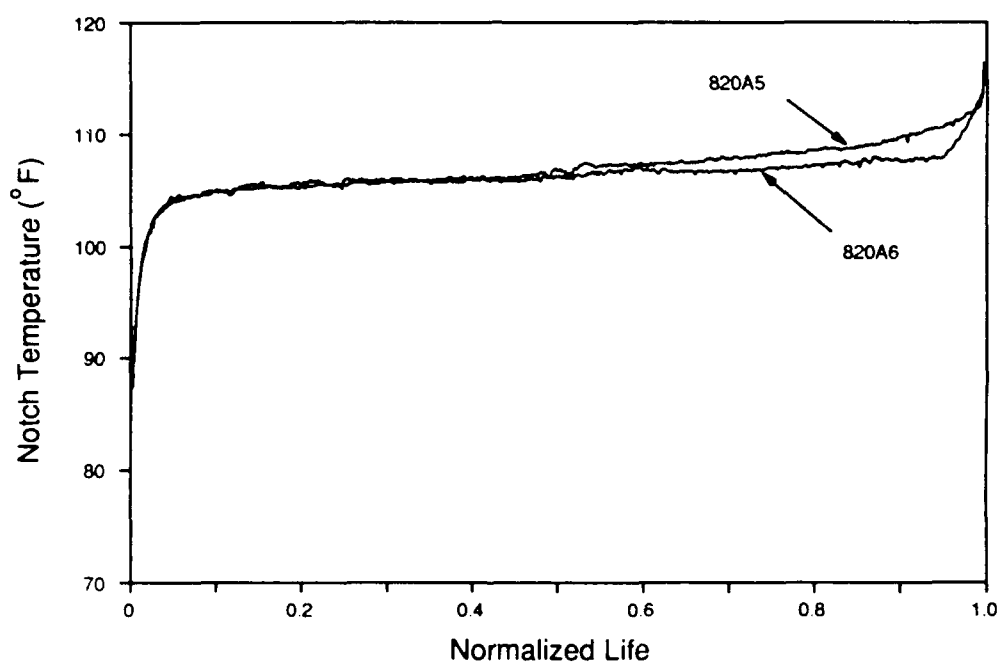
Figure 25.   Plot of Notch Temperature versus Normalized Life for Two 820A Specimens; Max.
Stress = 75% UCS; R = -1 at 10 Hz.
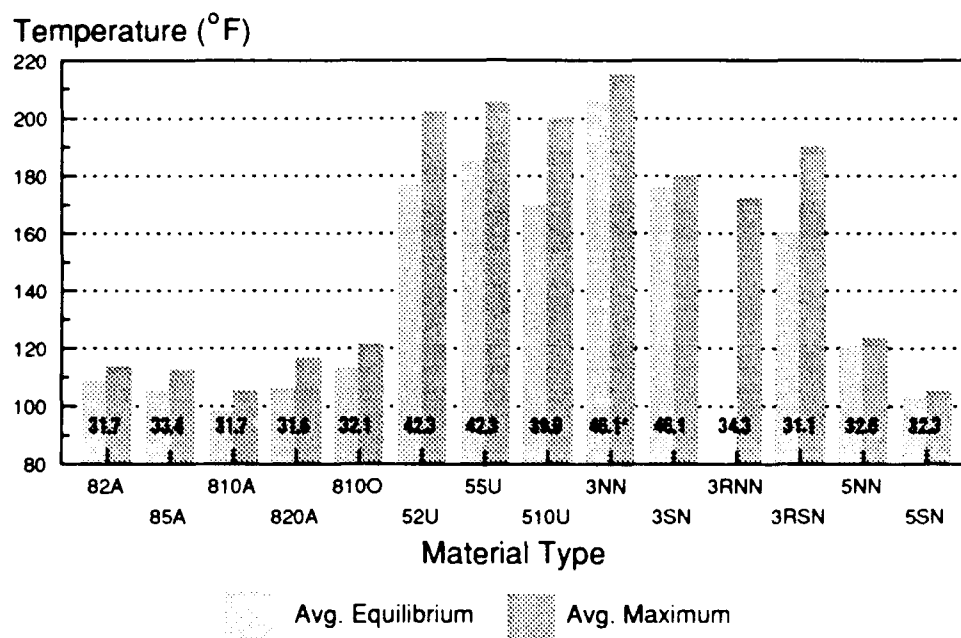
Temperature (°F)

Numbers in bars: applied stress level (ksi)

* Actually less than 75% UCS

Figure 26.   Average Equilibrium Temperature and Maximum Temperature of the McAir and Northrop Materials during Fatigue Loading.

2. The Role of the Fiber/Matrix Interphase in the Static and Fatigue Behavior of Polymeric Matrix Composite Laminates   58

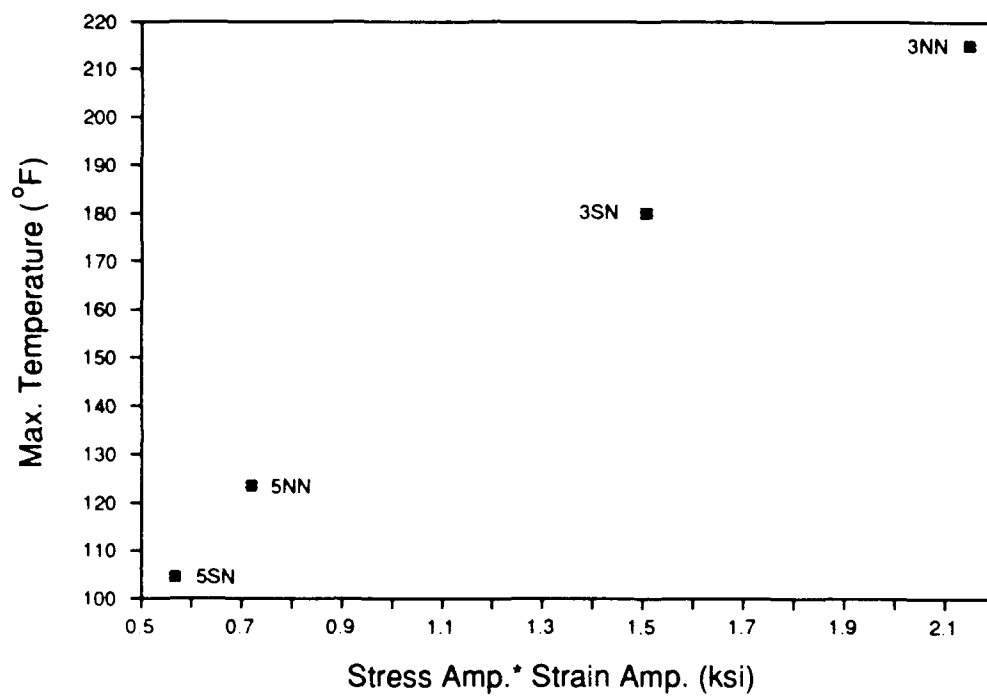Figure 27. Plot of Maximum Specimen Temperature versus Specific Energy Term for Northrop Materials; Max. Stress = 75% UCS; R = -1 at 10 Hz.
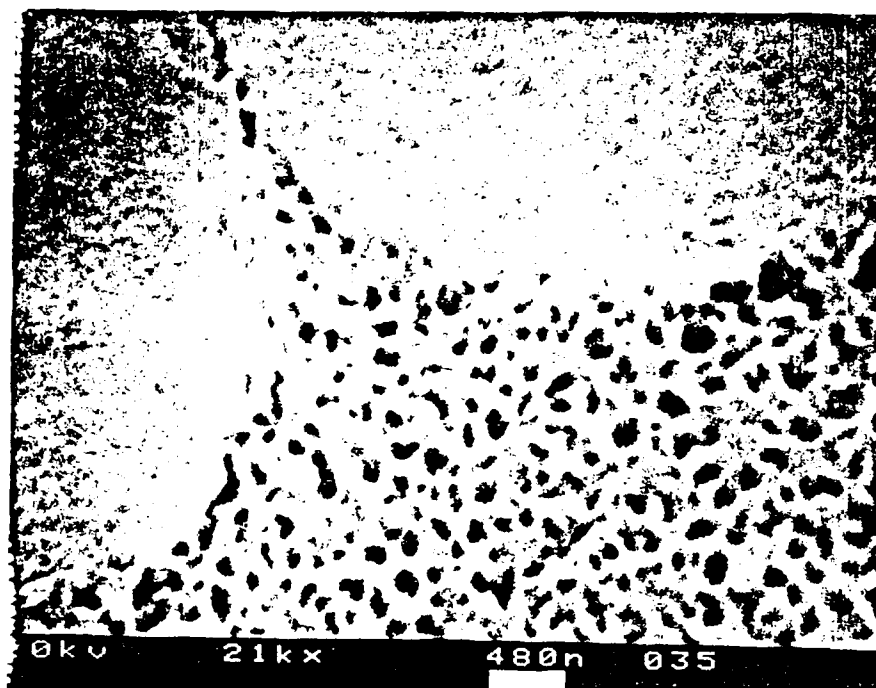
Figure 28.   SEM Micrograph of an Etched 810A Specimen (x 21,000).
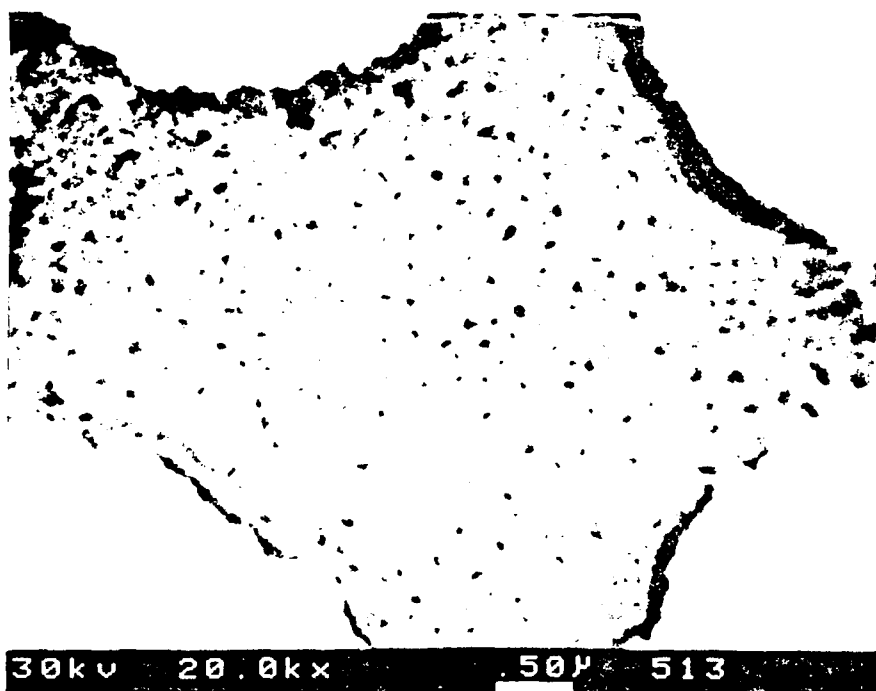
Figure 29.   SEM Micrograph of an Etched 810O Specimen (x 20,000).
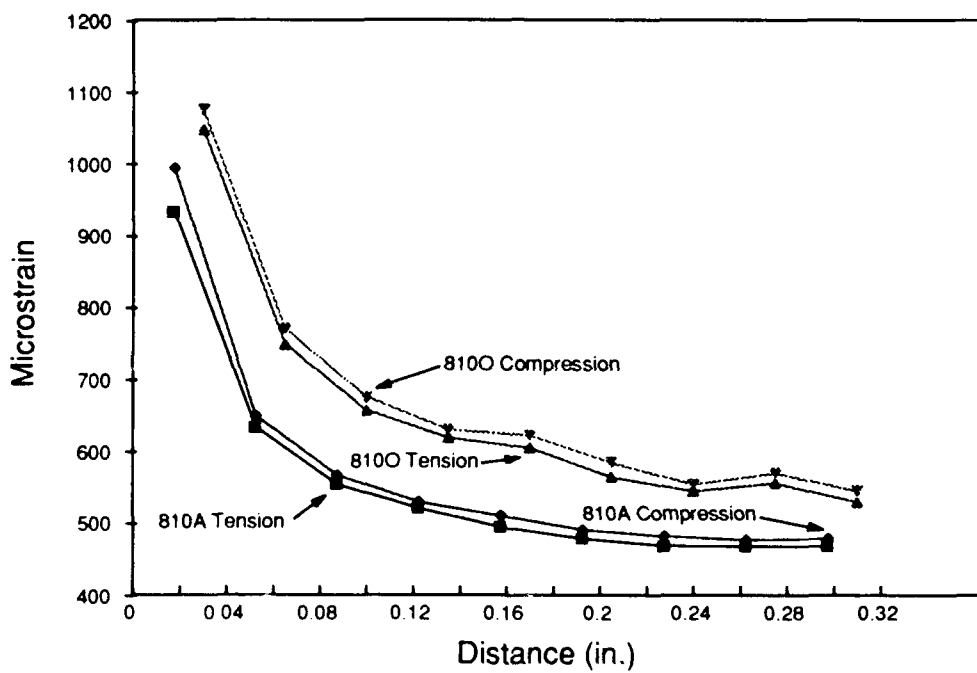
Figure 30.   Longitudinal Strain Measurements as a Function of Distance from the Hole; 810A and 810O under 1000 & -1000 lb.
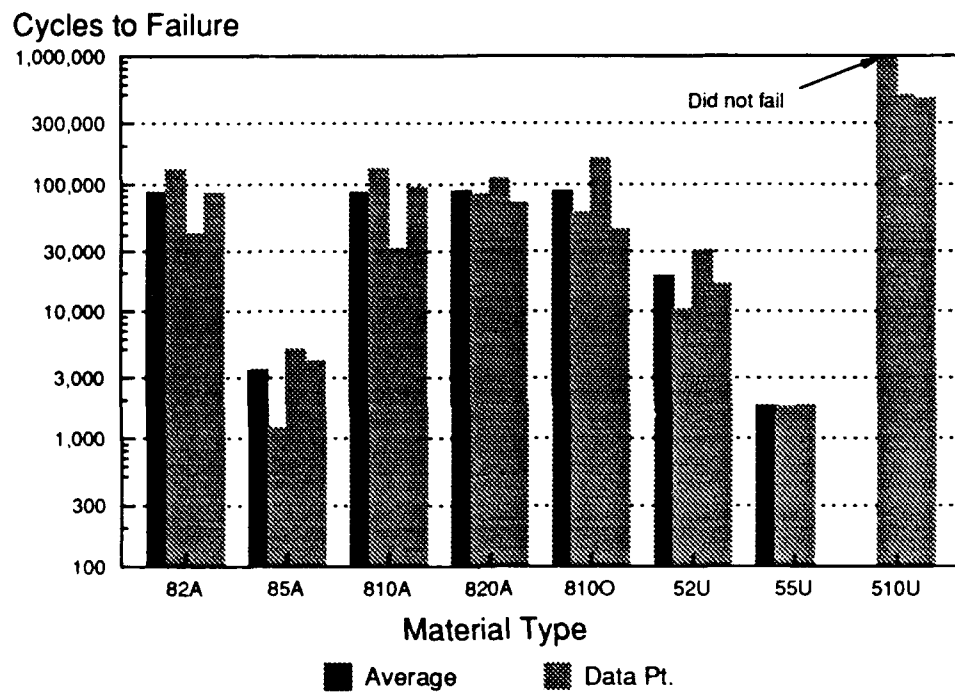
Cycles to Failure

Figure 31. Cycles to Failure of the ±45° McAir Specimens; Max. Stress = 24 ksi; R = 0.1 at 10Hz.

2. The Role of the Fiber/Matrix Interphase in the Static and Fatigue Behavior of Polymeric Matrix Composite Laminates
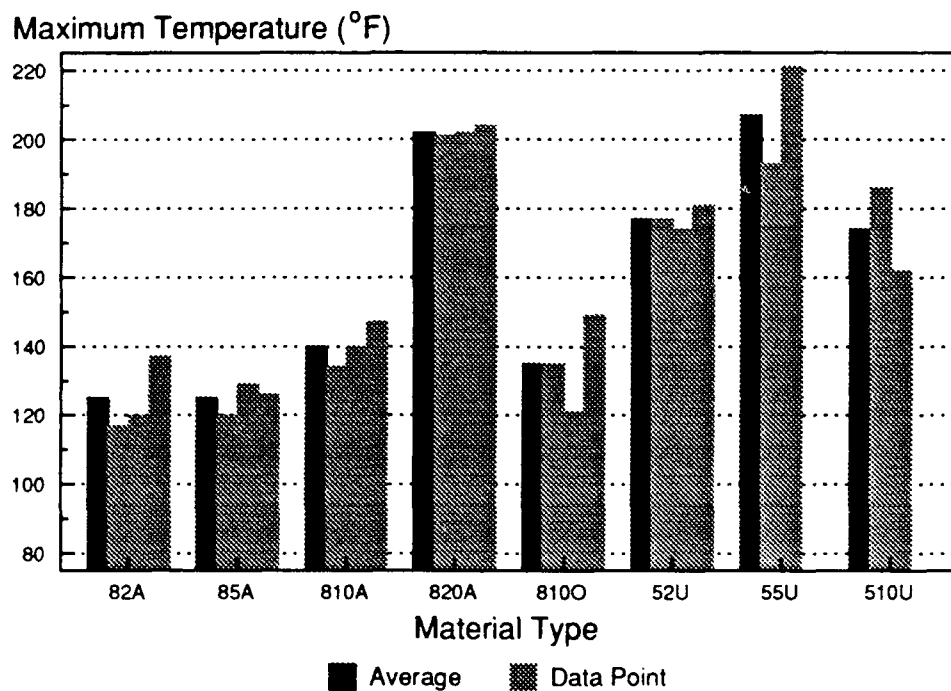
Figure 32. Temperature at Failure of the ±45° McAir Specimens; Max. Stress = 24 ksi; R = 0.1 at 10Hz.
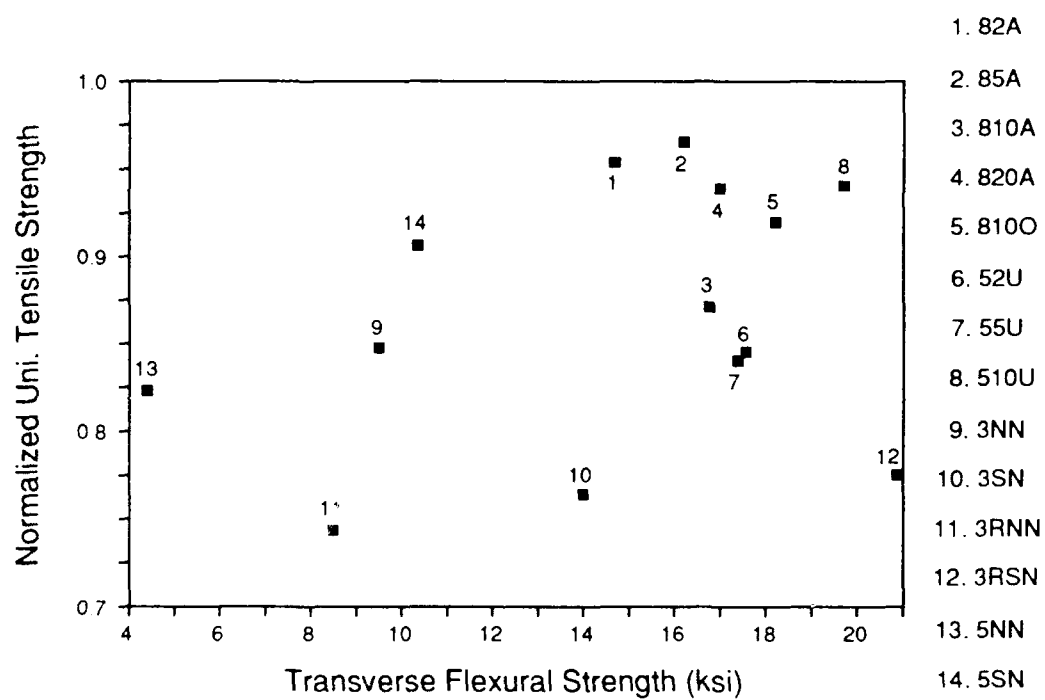
Figure 33. Normalized Unidirectional Tensile Strength versus Transverse Flexural Strength of the McAir and Northrop Materials [20,21].
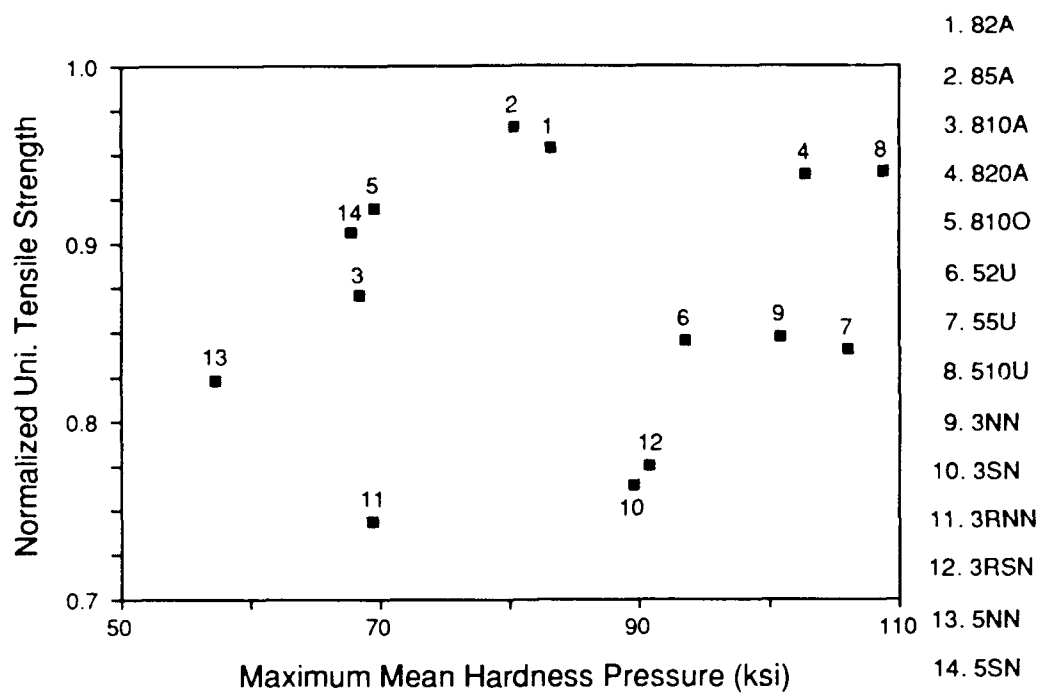
Figure 34.   Normalized Unidirectional Tensile Strength versus Max. Mean Hardness Pressure of the McAir and Northrop Materials [20,21].
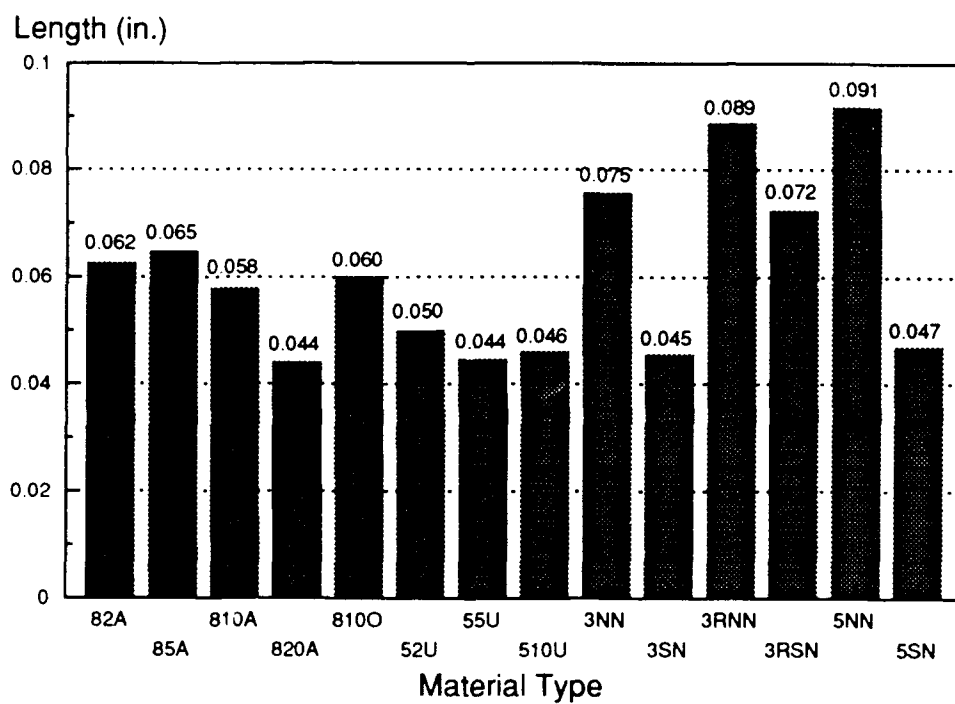
Figure 35. The Calculated Average-Stress Criteria Parameters of the McAir and Northrop Materials.
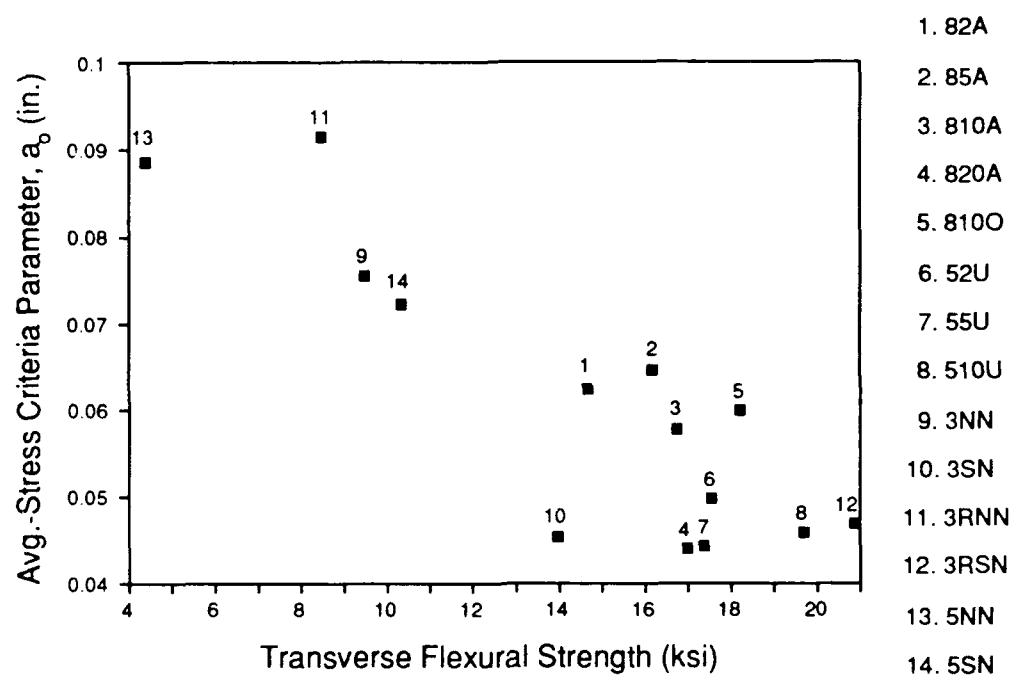
Figure 36. The Calculated Average-Stress Criteria Parameter versus the Transverse Flexural Strength of the McAir & Northrop Materials.
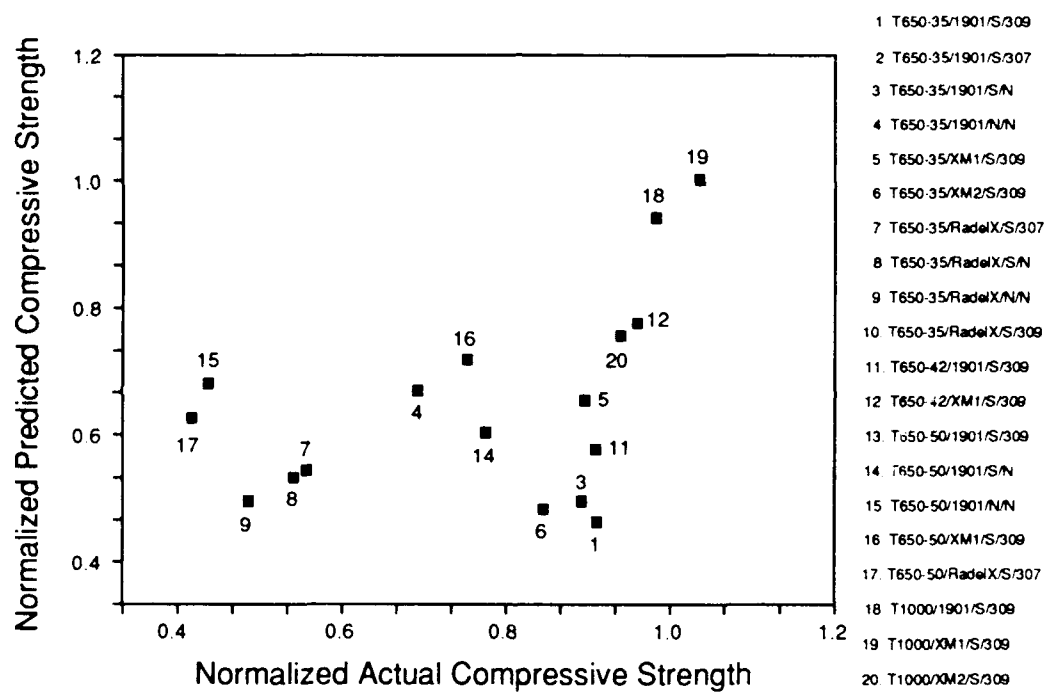
Figure 37. Normalized Unidirectional Compressive Strength; Predicted Values versus Actual Values (Bending Failure Scenario) [21].

The data points and legend in the figure:

Y-axis: Normalized Cross-plied Compressive Strength (0.2 to 1.0)
X-axis: Normalized Unidirectional Compressive Strength (0.4 to 1.0)

Legend:
1 T650-35/1901/S/309
2 T650-35/1901/S/307
3 T650-35/1901/S/N
4 T650-35/1901/N/N
5 T650-35/XM1/S/309
6 T650-35/XM2/S/309
7 T650-35/RadelX/S/307
8 T650-35/RadelX/S/N
9 T650-35/RadelX/N/N
10 T650-35/RadelX/S/309
11 T650-42/1901/S/309
12 T650-42/XM1/S/309
13 T650-50/1901/S/309
14 T650-50/1901/S/N
15 T650-50/1901/N/N
16 T650-50/XM1/S/309
17 T650-50/RadelX/S/307
18 T1000/1901/S/309
19 T1000/XM1/S/309
20 T1000/XM2/S/309

Figure 38.   Normalized Cross-plied Compressive Strength vs. Normalized Unidirectional Compressive Strength; Northrop Materials [21,22].

Figure 39.   Adjusted Average-Stress Criteria Parameter versus Normalized ±45° Tensile Strength; Northrop Materials [21].

3. The Interphase in Unidirectional Fiber-Reinforced Epoxies: Mori-Tanaka Analysis of the Effect on Local Stress Fields

Krishnan Jayaraman, Zhanjun Gao and Kenneth L. Reifsnider
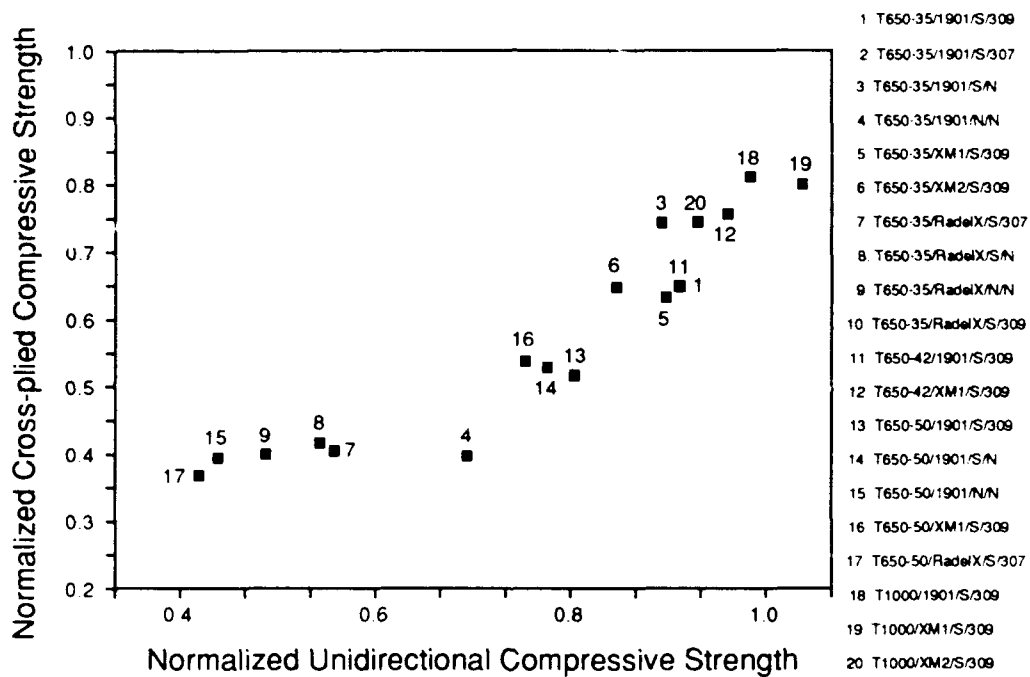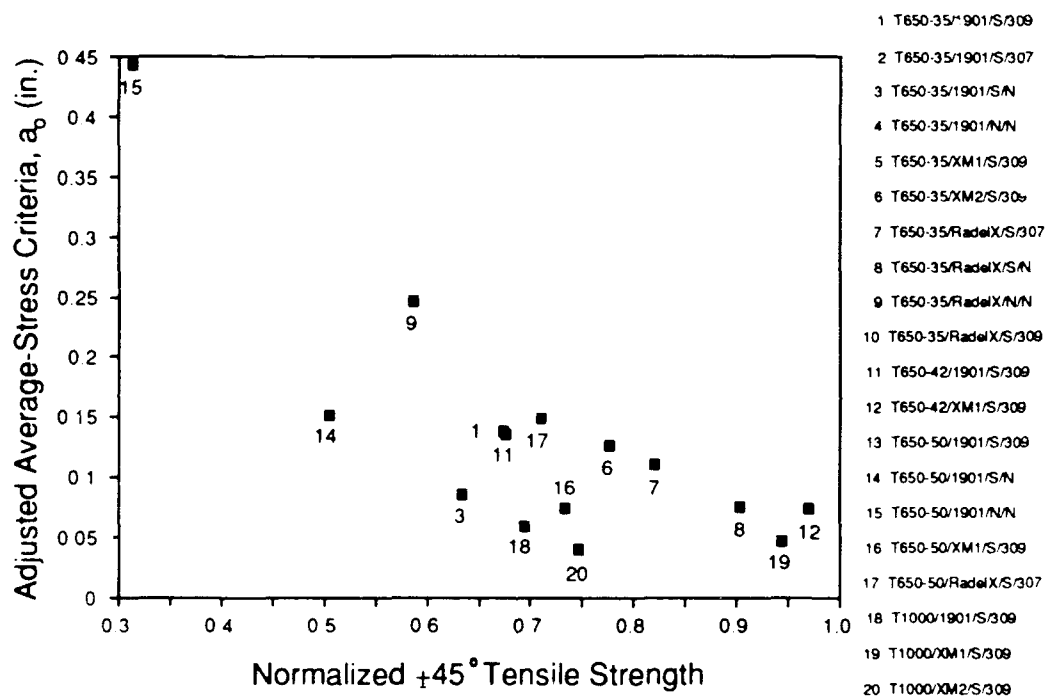
Abstract

The "interphase", in a composite, is usually modeled as a homogeneous region, despite the fact that it may have spatial property variations. However, it is important to the understanding of composite behavior to incorporate a realistic interphasial region into the micro-mechanical analyses of composite systems. The authors have recently proposed a model for the interphase properties in fiber-reinforced thermosets: the Young's modulus and coefficient of thermal expansion of the interphase are assumed to vary as functions of distance from the fiber in this model. In the current study, the authors' model is utilized along with Mori-Tanaka analyses for the determination of *non-dilute* local stress fields in unidirectional fiber-reinforced epoxies under thermo-mechanical loading situations. The governing field equations in terms of displacements are solved in "closed form". It is found that property variations in the interphase have a u... : effect on the local stresses. This is significant, considering the fact that local stresses play an important role in controlling the structural perform-ance of a composite. The ideas behind this study can be extended to characterize and analyze the interphase in metal matrix and ceramic matrix composites.

Introduction

Mechanics representations of the micro-details of fiber-reinforced composites have generally assumed the existence of two phases, namely the fiber and matrix. However, in reality, an additional phase may exist between the fiber and matrix. This phase, commonly known as the interphase, is the local region that results when the matrix bonds with the fiber surface or the fiber sizing. The interphase region is often the product of processing conditions involved in composite manufacture. Hence, the properties of the region depend directly upon the chemical, mechanical and thermodynamical nature of the bonding process between the matrix material and fiber material, and any subsequent changes in those local conditions. As a direct result of this dependence, the interphase may have spatially non-uniform properties, i.e., the properties may vary from point to point through the thickness of the interphase. Its realistic incorporation into the micro-mechanical analyses of composite systems is critical to the understanding of composite behavior because:

- The interphase is responsible for transmitting any interaction between the fiber and the matrix.
- Interphasial degradation has a definite effect on the global properties and response of the composite material.
- Interphasial failure may often lead to global composite material failure.

The authors have reviewed, in previous publications, the methods available for the experimental characterization of the interphase [1] and the studies available on interphase models [2], and have presented their own model for the interphase in a fiber-reinforced thermoset. The effect of an interphase on the residual thermal stresses in fiber-reinforced epoxies has also been studied using concentric cylinder assemblages [3]. The present article attempts to evaluate the effect of interphases on the local stresses in fiber-reinforced epoxies under various loading conditions using Mori-Tanaka analysis.

Several researchers [4-11] have investigated the local stresses occurring in composite materials under thermo-mechanical loading situations using the classical elasticity theory. They have also made some of the following simplifying assumptions:

- The composite is unidirectional and the fibers are continuous.

- The composite can be modeled by a representative volume element consisting of concentric cylinders representing the various phases.

- The phases are linearly elastic.

- The phase between fiber and matrix in coated composites has the bulk material properties of the coating.

- There is perfect bonding between phases.

- The composite end conditions are satisfied only in the sense of the St.Venant's principle.

Mikata and Taya [4] have used a four-phase model (fiber/coating matrix/surrounding body) to evaluate the constituent stresses in coated fiber composites (Ni-coated T300/Al 6061 and SiC-coated T300/Al 6061) under thermo-mechanical loading situations. The fiber and the surrounding body were considered to be transversely isotropic, and the coating and matrix were considered isotropic; the properties of the surrounding body were obtained using the rule-of-mixtures. The composite was subjected to three independent loading conditions — axisymmetric temperature change, uniaxial stress applied parallel to the fiber direction, and equal biaxial stresses applied perpendicular to the fiber direction. The effect of volume fraction and thickness of the coating on the constituent stresses was also studied.

Tandon and Pagano [5] have utilized a three-phase model (fiber/coating/matrix) to examine the constituent stresses in a coated Nicalon BMAS composite under mechanical loading conditions. The fiber, coating, and matrix were considered isotropic and the composite was subjected to two different loading conditions — transverse stress and longitudinal shear stress. The tractions acting on the radial boundary of each concentric cylinder assemblage were approximated by the boundary conditions on the composite. The Nicalon fibers were assumed to be coated by a hypothetical coating material; the Young's modulus and the thickness of the coating were used as variables and their effect on the constituent stresses was studied. Pagano and Tandon [6, 7] have also used a similar analytical framework to calculate the constituent residual thermal stresses in a coated Nicalon BMAS composite. The coating materials and their thicknesses were used as variables, and their effect on the constituent stresses was studied.

Benveniste, Dvorak and Chen [8] have used a three-phase model (fiber/coating/matrix) to predict the local stresses in a carbon-coated SiC/Titanium Aluminate composite under thermomechanical loading situations. A simple variation of the formulations of Eshelby [12, 13] and Mori and Tanaka [14], called the *Equivalent Inclusion - Average Stress (EIAS) concept* by Benveniste [15], was used and the composite was subjected to six different loading conditions -- uniform change in temperature, axial normal stress, transverse hydrostatic stress, longitudinal shear stress, transverse shear stress, and transverse normal stress. The local stresses in the fiber, coating and the adjacent matrix in the composite were approximated by the solution for a single coated fiber in infinite matrix subjected to average matrix stresses. The fiber-fiber interaction was approximately taken into account through the average matrix stresses.

Zhang [9] has developed an analytical procedure for the determination of constituent stresses in a unidirectional n-layered composite, comprising of a single fiber surrounded by n-cylindrical matrices under mechanical loading conditions. The material of all the cylinders were considered cylindrically anisotropic and the composite was subjected to two different loading conditions — uniaxial strain applied parallel to the fibers and equal biaxial stresses applied perpendicular to the fibers. The original problem, requiring the solution of a linear, simultaneous, algebraic equation set of the order $2n + 2$, was reduced to a problem of finding the inverse of a nxn matrix, using the matrix resolution technique. While Zhang [9] has not considered a surrounding body with composite properties as the $n + 1^{th}$ layer, it will be quite simple to add that layer to the existing analytical framework.

Lo, Schmitz and Gottenberg [10] have considered a four-phase model (fiber/flexible interlayer/matrix/surrounding body) to investigate the constituent stresses in a glass/epoxy composite under a transverse tensile load applied perpendicular to the fibers. The interlayer modulus and thickness were used as variables and their effect on the constituent stresses was studied. Based on the results of the analysis, a criterion was provided for the selection of optimal interlayer thickness.

Dasgupta and Sirkis [11] have used a three-phase model (optical fiber/coating/surrounding host) to determine the constituent stresses in a composite (T300/5208 epoxy) structure embedded with

optical (glass) fiber sensors, under a tensile strain applied parallel to the fiber. Optimizing criteria were used to determine the optimal coating material properties (Young's modulus and coefficient of thermal expansion) and thickness.

Although the *in situ* properties of the constituents may be strongly influenced by processing conditions, this effect is usually neglected in the analyses mentioned above, owing to the lack of definitive data; bulk material properties are used instead [6]. There are some analyses [16, 17, 18, 19], where material property variations have been considered, although some of these are not directly related to composite micro-mechanics.

Lekhnitskii [16] has considered the problem of a continuously non-homogeneous, orthotropic hollow cylinder under internal and external pressures, and fixed at the ends. The compliance coefficients were assumed to be

$$a_{ij} = \alpha_{ij} r^{-n} \tag{1}$$

where α_{ij} are constants, r is the radial distance, and n is any constant real number. Expressions for stresses have been derived under the assumption of plane strain, using a stress function approach. Numerical results have also been given for the problem of a oak wood tube, loaded on the inner contour and having the following material properties:

$$E_r = 2 \times 10^5 \rho^n \; \text{Kgf cm}^2$$

$$E_\theta = 0.95 \times 10^5 \rho^n \; \text{Kgf/cm}^2$$

$$v_{r\theta} = 0 \tag{2}$$

where ρ is the radial distance, and n is any constant real number. Several other cylinder problems with non-homogeneous elastic characteristics have also been considered.

Subbaraman and Reifsnider [17, 18] have touched upon this subject while analytically evaluating the stress-strain behavior of a thin cylindrical fuel clad under fission gas (internal) pressure in a Liquid Metal Fast Breeder Reactor. The stainless steel alloy fuel cladding has been observed to

undergo property variations in the radial direction due to long-time exposure to liquid sodium under high temperature, varying impurity concentrations and neutron fluxes. The through-the-thickness material stiffness has been modeled by a general function, f(r). Some specific functions have been considered for f(r) and stresses and strains have been found under the assumption of plane strain.

Van Fo Fy [19] has used a three-phase model (fiber/binder/matrix), with the fiber-binder assemblages distributed in the matrix in a regular hexagonal array, to evaluate the constituent stresses in a glass fiber-reinforced plastic under an applied longitudinal shear stress. The following expressions were considered for the shear modulus of the interphase:

$$G_i = G_0 \, e^{g(\lambda - \rho)}, \tag{3}$$

$$G_i = G_0 \, e^{-g(\lambda - \rho)}, \tag{4}$$

where λ represents the radius of the fiber, ρ represents the radial coordinate, g represents a constant, and G_0 represents the value of the interphase shear moduli at $\rho = \lambda$. Equation (3) characterizes an interphase where the shear modulus decreases as a function of distance from the fiber surface while Equation (4) characterizes the opposite of the above case. Expressions for the stresses have been derived using a series formulation of the displacements.

In this publication, the EIAS concept of Benveniste, Dvorak and Chen [8] is employed to evaluate the constituent stresses in a unidirectional fiber-reinforced composite subjected to thermo-mechanical loading situations. The composite consists of three phases — the fiber, interphase and matrix; the interphase Young's modulus and coefficient of thermal expansion are non-uniform as outlined in the next section. The general formulation of the *EIAS concept*, the formulation of the auxiliary problems and their solution methods, the solution methods to the resulting Navier equations, the results, and the conclusions are presented in subsequent sections.

Fiber-Interphase-Matrix Model

The present model considers the interphase in a fiber-reinforced epoxy; the model follows some of the ideas set forth in the models available in the literature [2] and includes the following assumptions:

- The interphase is simulated by a circular cylindrical shell of inner radius, r_f (also the radius of the fiber) and outer radius, r_i as shown in Figure 1(a); the fiber, simulated by a solid circular cylinder of radius, r_f lies inside the shell, while the matrix lies outside. The matrix, interphase and the fiber are denoted by m, i and f, respectively. The properties of the matrix, interphase and the fiber are denoted by subscripts m, i and f, respectively. The interphase thickness and fiber diameter are denoted by c and d, respectively. The variable ϕ is defined as the ratio of the interphase thickness to the fiber diameter.

- The fiber is transversely isotropic (or isotropic) and linearly elastic.

- The interphase and the matrix are isotropic and linearly elastic.

- The values of the Young's modulus (E_i) and the coefficient of thermal expansion (α_i) at the interphase-matrix interface are equal to the bulk matrix values (E_m and α_m).

- The values of the Young's modulus and the coefficient of thermal expansion at the fiber-interphase interface are ratios of the values in the bulk matrix. These ratios are denoted by ξ_y and ξ_c, where y and c represent the Young's modulus and the coefficient of thermal expansion respectively (see Figure 1(b)). The ratios are, to a certain extent, suggested by the cure chemistry of epoxy. If a higher cross-linking density is present at the fiber-interphase interface than in the bulk matrix, then this is expected to result in a higher elastic modulus and a lower coefficient of thermal expansion at that interface. Thus, if $\xi_y > 1$, then $\xi_c < 1$.

- The Young's modulus and the coefficient of thermal expansion of the interphase are functions of the radial coordinate.

- The Young's modulus and the coefficient of thermal expansion of the interphase follow the same functional form. They are given by

$$ L_i = P_i \left(\frac{r}{r_f} \right)^{C_i} $$

$$x_i = P_c \left(\frac{r}{r_i} \right)^{Q_c} \tag{5}$$

where P_i, Q_i, P_c and Q_c are constants and r is the radial distance. The constants P_i, Q_i, P_c and Q_c are determined from the values of the properties at the fiber-interphase and interphase-matrix interfaces.

- The interface conditions for the Young's modulus and coefficient of thermal expansion are given by :

$$E_i(r_i) = E_m ; \quad E_i(r_f) = \xi_v E_m ; \quad \alpha_i(r_i) = \alpha_m ; \quad \alpha_i(r_f) = \xi_c \alpha_m . \tag{6}$$

- The Poisson's ratio of the interphase (v_i) is assumed to be constant and the same as that of the matrix (v_m).

- The bonding between the phases is perfect.

Many different interphases can be modeled by varying the parameters ϕ (representing the interphase thickness), and ξ (representing the values of the properties at the fiber-interphase interface).

Stress Fields by the "Equivalent Inclusion - Average Stress concept"

The following assumptions are used in the formulation:

- The fiber-interphase assemblage is simulated by two concentric, long, circular cylinders. The radii of the interphase and the fiber are denoted by r and r_s, respectively.

- The continuous fiber composite is represented by a material system consisting of an infinite matrix in which the fibers are aligned and distributed in a statistically homogeneous manner.

- A cylindrical coordinate system (r, θ, z) is considered with z as the axial coordinate and r-θ as the transverse plane (see Figure 1 a)).

- The temperature change is uniform in all the phases.

The *Equivalent Inclusion idea* of Eshelby [12, 13] and the *Average Stress concept* of Mori and Tanaka [14] have received wide attention in the micro-mechanics research community. Many important micro-mechanics problems have been dealt with using one or both of the above methods; the reader is urged to refer to Mura [20] for a comprehensive introduction to different topics in micro-mechanics as related to these problems. Recently, Benveniste [12] has provided a simple re-examination of the *Equivalent Inclusion idea* and the *Average Stress concept*, called the *EIAS concept*; the formulation for the stress fields given below will closely follow the work of Benveniste [12] and Benveniste, Dvorak and Chen [8].

The cross-section of a unidirectional composite with a distribution of fiber-interphase assemblages in a matrix is shown in Figure 2(a). The boundary conditions for the general thermo-mechanical loading of this composite are given by

$$\lim_{r \to \infty} \sigma_{ij}(r, \theta, z) = \sigma_{ij}^{o} \qquad T(r, \theta, z) = T^{o} \qquad (7)$$

where $\sigma_{ij}(r, \theta, z)$ and $T(r, \theta, z)$ are the stress field and uniform temperature change respectively and the superscript "o" indicates known quantities associated with the composite problem. The local stress fields associated with the composite can now be written as

$$\tau_{ij}^{(n)}(r, \theta, z) = \tilde{M}_{ijkl}^{(n)}(r, \theta, z) \sigma_{kl}^{o} + \tilde{N}_{ij}^{(n)}(r, \theta, z) T^{o} \qquad n = f, i, m \qquad (8)$$

where $\tilde{M}_{ijkl}^{(n)}$ and $\tilde{N}_{ij}^{(n)}$ represent fourth and second order tensors related to the composite, respectively. m, i and f represent quantities related to the matrix, interphase and fiber, respectively. Determination of $\tilde{M}_{ijkl}^{(n)}$ and and $\tilde{N}_{ij}^{(n)}$ in closed-form is difficult due to the interactions of fiber-interphase assemblages. Hence, different models have been introduced in the literature to approximately evaluate $\tilde{M}_{ijkl}^{(n)}$ and $\tilde{N}_{ij}^{(n)}$. The *EIAS concept* is one such formulation and can be explained by considering:

- a fiber-interphase assemblage embedded in an infinite matrix medium, and
- a fiber-interphase assemblage embedded in a deformed infinite matrix medium.

3. The Interphase in Unidirectional Fiber-Reinforced Epoxies: Mori-Tanaka Analysis of the Effect on Local Stress Fields

Consider a fiber-interphase assemblage embedded in an infinite matrix medium as shown in Figure 2(b). The boundary conditions for the general thermo-mechanical loading of this body is given by

$$\lim_{r \to \infty} \sigma_{ij}(r, \theta, z) = \sigma_{ij}^{d} \qquad \begin{array}{c} T(r, \theta, z) = T^{d} \\ \forall (r, \theta, z) \end{array} \tag{9}$$

where the superscript "d" indicates known quantities associated with the single fiber-interphase-infinite matrix problem. The stress fields associated with this body can now be written as

$$\sigma_{ij}^{(n)}(r, \theta, z) = M_{ijkl}^{(n)}(r, \theta, z) \sigma_{kl}^{d} + N_{ij}^{(n)}(r, \theta, z) T^{d} \qquad n = f, i, m \tag{10}$$

where $M_{ijkl}^{(n)}$ and $N_{ij}^{(n)}$ represent fourth and second order tensors related to the single fiber-interphase embedded in an infinite matrix, respectively; $M_{ijkl}^{(n)}$ and $N_{ij}^{(n)}$ can be determined in closed-form for this body under different loading conditions.

Consider a typical fiber-interphase assemblage in the dotted portion of Figure 2(a), which is shown separately in Figure 2(c). The matrix region in this portion of the composite is already deformed and possesses an average stress, σ_{ij}^{av}. Therefore, the boundary conditions for the general thermo-mechanical loading of this portion of the composite can be approximately expressed as

$$\lim_{r \to \infty} \sigma_{ij}(r, \theta, z) = \sigma_{ij}^{av} \qquad \begin{array}{c} T(r, \theta, z) = T^{o} \\ \forall (r, \theta, z) \end{array} \tag{11}$$

The stress fields associated with this body can now be written as

$$\sigma_{ij}^{(n)}(r, \theta, z) = M_{ijkl}^{(n)}(r, \theta, z) \sigma_{kl}^{av} + N_{ij}^{(n)}(r, \theta, z) T^{o} \qquad n = f, i, m \tag{12}$$

where $M_{ijkl}^{(n)}$ and $N_{ij}^{(n)}$ are known once the problem of single fiber-interphase assemblage embedded in an infinite matrix medium, shown in Figure 2(b) is solved.

The volume average stresses in the fiber and interphase are found from Equation (12) as

$$\{\sigma_{ij}^{(f)}\}_{av} = \{M_{ijkl}^{(f)}\}_{av} \sigma_{kl}^{av} + \{N_{ij}^{(f)}\}_{av} T^{o} \tag{13}$$

$$\{\sigma_{ij}^{(i)}\}_{av} = \{M_{ijkl}^{(i)}\}_{av}\,\sigma_{kl}^{av} + \{N_{ij}^{(i)}\}_{av}\,T^o \tag{14}$$

where the subscript "av" denotes the average values over the volume of the respective constituents. The following relation is then used along with Equations (13) and (14) to determine the average matrix stresses:

$$V_f\{\sigma_{ij}^{(f)}\}_{av} + V_i\{\sigma_{ij}^{(i)}\}_{av} + V_m\,\sigma_{ij}^{av} = \sigma_{ij}^o \tag{15}$$

where V_f, V_i and V_m represent the volume fractions of the fiber, interphase and matrix, respectively. Once the average matrix stresses are known, the local stress fields are determined from Equation (12).

Formulation and Solution Methods for the Auxiliary Problems

The solutions for the auxiliary problems (single fiber-interphase-unbounded matrix assemblage subjected to uniform temperature and boundary loads) are discussed in this section; the application of the *ELAS concept* to determine the local stresses follows the description in the previous section. The loading situations under consideration are a uniform temperature change and boundary loads (longitudinal shear stress and transverse shear stress) as shown in Figure 3. Some other cases of boundary loads (axial normal stress in the direction of the fibers, transverse hydrostatic stress perpendicular to the fibers, and transverse normal stress perpendicular to the fibers) can be dealt with using the formulation of the three cases described above. Furthermore, since the general thermo-mechanical loading problem is linear, it can be solved as a superposition of the loading cases mentioned above [8].

The following methodology is used to solve the auxiliary problems:

- A displacement field is assumed based on the loading condition.

- The Navier's (governing differential) equations are found for each of the domains of the problem.

- The governing differential equations are solved to find the the displacements in the constituents in terms of constants.

- The strains and the stresses in the constituents are determined by making use of the strain-displacement and the constitutive relations, respectively.

- The constants are determined by using the boundary and interface conditions.

Uniform Change in Temperature

The composite is assumed to experience an axisymmetric generalized plane-strain. Due to axisymmetry and the absence of shear in the concentric cylinder assemblage model, the displacement field in the n-th domain (n = m, i, f) can be expressed by

$$u_r^{(n)} = u^{(n)}(r)$$

$$u_\theta^{(n)} = 0$$

$$u_z^{(n)} = w^{(n)}(z) \tag{16}$$

where $u^{(n)}$ are the components of displacement.

Matrix (n = m) and Fiber (n = f) Domains

The Navier's equations of elasticity are :

$$\frac{d^2 w^{(n)}}{dz^2} = 0 \tag{17}$$

$$\frac{d^2 u^{(n)}}{dr^2} + \frac{1}{r} \frac{du^{(n)}}{dr} - \frac{u^{(n)}}{r^2} = 0. \tag{18}$$

The general solution to Equation (17) is given by

$$w^{(n)}(z) = C^{(n)} z + D^{(n)} \tag{19}$$

and the general solution to Equation (18) is found by the Cauchy-Euler method (see section on "Solution Methods for the Governing Differential Equations") to be

$$u^{(n)}(r) = A^{(n)}r + \frac{B^{(n)}}{r}. \tag{20}$$

$A^{(n)}$, $B^{(n)}$, $C^{(n)}$ and $D^{(n)}$ are unknown constants which will be determined by the boundary/interface conditions. The expressions for $u^{(m)}$ and $u^{(f)}$ are consistent with the work of Hashin and Rosen [21].

Interphasial Domain (n = i)

The Navier's equations of elasticity are:

$$\frac{d^2 w^{(i)}}{dz^2} = 0 \tag{21}$$

$$\frac{d^2 u^{(i)}}{dr^2} + \left[\frac{Q_y + 1}{r} \right] \frac{du^{(i)}}{dr} + \left[\frac{Q_y \frac{v_i}{1 - v_i} - 1}{r^2} \right] u^{(i)} + \left[\frac{v_i}{1 - v_i} \frac{Q_y}{r} \right] \frac{dw^{(i)}}{dz}$$

$$- \left[\frac{1 + v_i}{1 - v_i} \frac{P_c(Q_y + Q_c)r^{Q_c - 1}}{r_f^{Q_c}} \right] T^d = 0. \tag{22}$$

The general solution to Equation (21) is given by

$$w^{(i)}(z) = C^{(i)}z + D^{(i)} \tag{23}$$

and the general solution to Equation (22) is found by the Cauchy-Euler method to be

$$u^{(i)}(r) = A^{(i)}r^{m_1} + B^{(i)}r^{m_2} - C^{(i)}v_i r + \frac{\frac{1 + v_i}{1 - v_i} P_c(Q_y + Q_c)r^{Q_c + 1}T^d}{\left\{ Q_c^2 + 2Q_c + Q_v Q_c + Q_y + Q_v \frac{v_i}{1 - v_i} \right\} r_f^{Q_c}} \tag{24}$$

where

$$m_1, m_2 = \frac{1}{2} \left[-Q_y \pm \sqrt{\frac{Q_y^2(1 - v_i) - 4v_i(Q_y + 1) + 4}{1 - v_i}} \right].$$

$A^{(i)}, B^{(i)}, C^{(i)}$ and $D^{(i)}$ are unknown constants which will be determined by the boundary/interface conditions.

Solution Method

The boundary and interface conditions for this loading situation are given by

$$\lim_{r \to \infty} \frac{1}{\pi r^2} \left[2\pi \int_0^{r_f} \sigma_{zz}^{(f)} r\, dr + 2\pi \int_{r_f}^{r_i} \sigma_{zz}^{(i)} r\, dr + 2\pi \int_{r_i}^{r} \sigma_{zz}^{(m)} r\, dr \right] = 0 \tag{25}$$

$$\lim_{r \to \infty} \sigma_{xx}^{(m)} = 0 \quad \equiv \quad \lim_{r \to \infty} \sigma_{yy}^{(m)} = 0 \quad \equiv \quad \lim_{r \to \infty} \sigma_{rr}^{(m)} = 0 \tag{26}$$

$$u^{(m)} = u^{(l)} \quad w^{(m)} = w^{(l)} \quad \sigma_{rr}^{(m)} = \sigma_{rr}^{(l)} \quad at \ \ r = r_l \tag{27}$$

$$u^{(i)} = u^{(f)} \quad w^{(i)} = w^{(f)} \quad \sigma_{rr}^{(i)} = \sigma_{rr}^{(f)} \quad at \ \ r = r_f, \tag{28}$$

where σ_{rr} and σ_{zz} represent the radial and axial stresses, respectively.

The required end conditions are given by:

$$\sigma_{zz}^{(m)}(r, \pm l/2) = \sigma_{zz}^{(i)}(r, \pm l/2) = \sigma_{zz}^{(f)}(r, \pm l/2) = 0 \tag{29}$$

where l is the length of the cylinder assemblage. Since end conditions (29) are difficult to enforce, condition (25), "equivalent in the St.Venant sense" to conditions (29) is enforced. Equation (25) will be satisfied if $\sigma_{zz}^{(i)} = 0$ is imposed. The boundaries of the matrix, parallel to the fiber direction, are stress free; boundary condition (26) is a direct consequence of this assumption. Interface conditions (27) and (28) are dictated by the assumption of perfect bonding at the fiber-interphase and interphase-matrix interfaces.

The interface conditions on w dictate that $C^{(m)} = C^{(i)} = C^{(f)} = C$ and $D^{(m)} = D^{(i)} = D^{(f)} = D$. Since D represents a rigid body displacement, it can be set to zero without loss of generality. Thus, we have

$$w^{(m)}(z) = w^{(i)}(z) = w^{(f)}(z) = Cz. \tag{30}$$

3. The Interphase in Unidirectional Fiber-Reinforced Epoxies: Mori-Tanaka Analysis of the Effect on Local Stress Fields

$B^{(\cdot)}$ must be set equal to zero, since $|u^{(\cdot)}(0)| \neq \infty$. The remaining six boundary interface conditions are used to solve for the remaining constants $A^{(m)}$, $A^{(i)}$, $A^{(f)}$, $B^{(m)}$, $B^{(i)}$ and C. The displacements, the strains and the stresses in each of the constituents are determined using the values of the above constants.

Longitudinal Shear Load

The displacement field in the n-th domain (n = m, i, f) can be expressed by

$$u_r^{(n)} = 0$$

$$u_\theta^{(n)} = 0$$

$$u_z^{(n)} = w^{(n)}(r) \sin \theta \tag{31}$$

where $u^{(\cdot)}$ are the components of displacement.

Matrix (n = m) and Fiber (n = f) Domains

The Navier's equation of elasticity is:

$$\frac{d^2 w^{(n)}}{dr^2} + \frac{1}{r} \frac{dw^{(n)}}{dr} - \frac{w^{(n)}}{r^2} = 0. \tag{32}$$

The general solution to Equation (32) is found by the Cauchy-Euler method to be

$$w^{(n)}(r) = A^{(n)}r + \frac{B^{(n)}}{r}. \tag{33}$$

$A^{(\cdot)}$ and $B^{(\cdot)}$ are unknown constants which will be determined by the boundary interface conditions. The expressions for $u_z^{(m)}$ and $u_z^{(f)}$ are consistent with the work of Benveniste, Dvorak and Chen [8].

Interphasial Domain (n = i)

The Navier s equation of elasticity is:

$$\frac{d^2 w^{(i)}}{dr^2} + \left[\frac{Q_y + 1}{r} \right] \frac{dw^{(i)}}{dr} - \frac{w^{(n)}}{r^2} = 0. \tag{34}$$

The general solution to Equation (34) is found by the Cauchy-Euler method to be

$$w^{(i)}(r) = A^{(i)} r^{m_1} + B^{(i)} r^{m_2} \tag{35}$$

where

$$m_1, m_2 = \frac{1}{2} \left[-Q_y \pm \sqrt{Q_y^2 + 4} \right].$$

$A^{(i)}$ and $B^{(i)}$ are unknown constants which will be determined by the boundary/interface conditions.

Solution Method

The boundary and interface conditions for this loading situation are given by

$$\lim_{r \to \infty} \sigma_{yz}^{(m)} = \sigma^d \quad \equiv \quad \frac{E_m}{2(1 + v_m)} A^{(m)} = \sigma^d \tag{36}$$

$$w^{(m)} = w^{(i)} \quad \sigma_{rz}^{(m)} = \sigma_{rz}^{(i)} \quad at \quad r = r_i \tag{37}$$

$$w^{(i)} = w^{(f)} \quad \sigma_{rz}^{(i)} = \sigma_{rz}^{(f)} \quad at \quad r = r_f \tag{38}$$

where σ_{yz} and σ_{rz} represent the shear stresses.

Boundary condition (36) is a direct consequence of the fact that the boundaries of the matrix, parallel to the fiber direction, experience the applied stress. Interface conditions (37) and (38) are dictated by the assumption of perfect bonding at the fiber-interphase and interphase-matrix interfaces. $B^{(f)}$ must be set equal to zero, since $|u^{(f)}(0)| < \infty$. The five boundary/interface conditions are used to solve for the remaining constants $A^{(m)}$, $A^{(i)}$, $A^{(f)}$, $B^{(m)}$ and $B^{(i)}$. The displacements, the strains and the stresses in each of the constituents are determined using the values of the above constants.

Transverse Shear Load

The composite is assumed to experience plane strain and the state of stress applied to the composite at infinity is pure shear. The displacement field in the n-th domain (n = m, i, f) can be expressed by

$$u_r^{(n)} = u^{(n)}(r) \cos 2\theta$$

$$u_\theta^{(n)} = v^{(n)}(r) \sin 2\theta$$

$$u_z^{(n)} = 0 \tag{39}$$

where $u^{(n)}$ are the components of displacement.

Matrix (n = m) Domain

The Navier's equations of elasticity are :

$$\frac{d^2 u^{(m)}}{dr^2} + \frac{1}{r}\frac{du^{(m)}}{dr} + \frac{5v_m - 3}{1 - v_m}\frac{u^{(m)}}{r^2} + \frac{1}{1 - v_m}\frac{1}{r}\frac{dv^{(m)}}{dr} + \frac{4v_m - 3}{1 - v_m}\frac{v^{(m)}}{r^2} = 0$$

$$\frac{d^2 v^{(m)}}{dr^2} + \frac{1}{r}\frac{dv^{(m)}}{dr} + \frac{10v_m - 9}{1 - 2v_m}\frac{v^{(m)}}{r^2} - 2\frac{1}{1 - 2v_m}\frac{1}{r}\frac{du^{(m)}}{dr} + 2\frac{4v_m - 3}{1 - 2v_m}\frac{u^{(m)}}{r^2} = 0 \tag{40}$$

The general solution to Equations (40) is found by the general solution of Pagano [22] (see section on "Solution Methods for the Governing Differential Equations") to be

$$u^{(m)} = A^{(m)} r^3 + \frac{B^{(m)}}{r^3} + C^{(m)} r + \frac{D^{(m)}}{r} \tag{41}$$

$$v^{(m)} = -\frac{3 - 2v_m}{2v_m} A^{(m)} r^3 + \frac{B^{(m)}}{r^3} - C^{(m)} r + \frac{2v_m - 1}{2(1 - v_m)}\frac{D^{(m)}}{r} \tag{42}$$

$A^{(m)}$, $B^{(m)}$, $C^{(m)}$ and $D^{(m)}$ are unknown constants which will be determined by the boundary interface conditions.

Fiber (n = f) Domain

The Navier's equations of elasticity are :

$$\frac{d^2 u^{(f)}}{dr^2} + \frac{1}{r}\frac{du^{(f)}}{dr} + \frac{2C_{23f} - 3C_{22f}}{C_{22f}}\frac{u^{(f)}}{r^2} + \frac{C_{22f} + C_{23f}}{C_{22f}}\frac{1}{r}\frac{dv^{(f)}}{dr} + \frac{C_{23f} - 3C_{22f}}{C_{22f}}\frac{v^{(f)}}{r^2} = 0$$

$$\frac{d^2 v^{(f)}}{dr^2} + \frac{1}{r}\frac{dv^{(f)}}{dr} + \frac{C_{23f} - 9C_{22f}}{C_{22f} - C_{23f}}\frac{v^{(f)}}{r^2} - 2\frac{C_{22f} + C_{23f}}{C_{22f} - C_{23f}}\frac{1}{r}\frac{du^{(f)}}{dr} + 2\frac{C_{23f} - 3C_{22f}}{C_{22f} - C_{23f}}\frac{u^{(f)}}{r^2} = 0 \qquad (43)$$

where C_{ijf} refer to fiber stiffnesses. The general solution to Equations (43) is found by the general solution of Pagano [22] to be

$$u^{(f)} = A^{(f)}r^3 + \frac{B^{(f)}}{r^3} + C^{(f)}r + \frac{D^{(f)}}{r} \qquad (44)$$

$$v^{(f)} = -\frac{3C_{22f} + C_{23f}}{2C_{23f}}A^{(f)}r^3 + \frac{B^{(f)}}{r^3} - C^{(f)}r + \frac{C_{23f} - C_{22f}}{2C_{22f}}\frac{D^{(f)}}{r} \qquad (45)$$

where C_{ijf} refer to fiber stiffnesses. $A^{(f)}$, $B^{(f)}$, $C^{(f)}$ and $D^{(f)}$ are unknown constants which will be determined by the boundary interface conditions. The expressions for $u_r^{(m)}$, $u_\theta^{(m)}$, $u_r^{(f)}$ and $u_\theta^{(f)}$ are consistent with the work of Christensen and Lo [23] and Theocaris and Varias [24].

Interphase (n = i) Domain

The Navier's equations of elasticity are :

$$\frac{d^2 u^{(i)}}{dr^2} + \frac{Q_\nu + 1}{r}\frac{du^{(i)}}{dr} + \frac{5\nu_i - 3 + Q_\nu \nu_i}{1 - \nu_i}\frac{u^{(i)}}{r^2} + \frac{1}{1 - \nu_i}\frac{1}{r}\frac{dv^{(i)}}{dr} + \frac{4\nu_i - 3 + 2Q_\nu \nu_i}{1 - \nu_i}\frac{v^{(i)}}{r^2} = 0$$

$$\frac{d^2 v^{(i)}}{dr^2} + \frac{Q_\nu + 1}{r}\frac{dv^{(i)}}{dr} + \frac{10\nu_i - 9 - Q_\nu(1 - 2\nu_i)}{1 - 2\nu_i}\frac{v^{(i)}}{r^2} - 2\frac{1}{1 - 2\nu_i}\frac{1}{r}\frac{du^{(i)}}{dr}$$

$$+ 2\frac{4\nu_i - 3 - Q_\nu(1 - 2\nu_i)}{1 - 2\nu_i}\frac{u^{(i)}}{r^2} = 0 \qquad (46)$$

The general solution to Equations (46) is found by the general solution of Pagano [22] to be

$$u^{(i)} = \mathcal{F}_r^{(i)}(A^{(i)}, B^{(i)}, C^{(i)}, D^{(i)}, r) \qquad (47)$$

$$v^{(i)} = \mathbb{P}_\theta^{(i)}(A^{(i)}, B^{(i)}, C^{(i)}, D^{(i)}, r) \tag{48}$$

where $\mathbb{P}_r^{(i)}$ and $\mathbb{P}_\theta^{(i)}$ are functions of the radial distance and constants. $A^{(i)}$, $B^{(i)}$, $C^{(i)}$ and $D^{(i)}$ are unknown constants which will be determined by the boundary/interface conditions.

Solution Method

The boundary and interface conditions for this loading situation are given by

$$\lim_{r \to \infty} \sigma_{xx}^{(m)} = \sigma^d \equiv \lim_{r \to \infty} \sigma_{yy}^{(m)} = -\sigma^d \equiv \frac{E_m}{1 + v_m} C^{(m)} = \sigma^d \tag{49}$$

$$u_r^{(m)} = u_r^{(i)} \quad u_\theta^{(m)} = u_\theta^{(i)} \quad \sigma_{rr}^{(m)} = \sigma_{rr}^{(i)} \quad \sigma_{r\theta}^{(m)} = \sigma_{r\theta}^{(i)} \quad at \ \ r = r_i \tag{50}$$

$$u_r^{(i)} = u_r^{(f)} \quad u_\theta^{(i)} = u_\theta^{(f)} \quad \sigma_{rr}^{(i)} = \sigma_{rr}^{(f)} \quad \sigma_{r\theta}^{(i)} = \sigma_{r\theta}^{(f)} \quad at \ \ r = r_f \tag{51}$$

where σ_{xx} and σ_{yy} represent the normal stresses, and $\sigma_{r\theta}$ represents the shear stress.

Boundary condition (49) is a direct consequence of the fact that the boundaries of the matrix, parallel to the fiber direction, experience the applied stress. Interface conditions (50) and (51) are dictated by the assumption of perfect bonding at the fiber-interphase and interphase-matrix interfaces. $B^{(f)}$ and $D^{(f)}$ must be set equal to zero, since $|u^{(f)}(0)| \neq \infty$. $A^{(m)}$ must be set equal to zero, since $|\lim_{r \to \infty} \sigma_{xx}^{(m)}| \neq \infty$ and $|\lim_{r \to \infty} \sigma_{yy}^{(m)}| \neq \infty$. The nine boundary/interface conditions are used to solve for the remaining constants $A^{(i)}$, $A^{(f)}$, $B^{(m)}$, $B^{(i)}$, $C^{(m)}$, $C^{(i)}$, $C^{(f)}$, $D^{(m)}$ and $D^{(i)}$. The displacements, the strains and the stresses in each of the constituents are determined using the values of the above constants.

Solution Methods for the Governing Differential Equations

Equations (18), (22), (32), and (34) are solved by the Cauchy-Euler method. The equations are transformed into equations with constant coefficients after making a change of variables

$$r = e^x \tag{52}$$

where x is the transformed independent variable. The differential equations are then solved by one of the basic methods [25].

The solution of Equations (40), (43) and (46) follows the general solution of Pagano [22] for a cylindrically anisotropic body under two dimensional surface tractions and involves the following steps:

- The following functional forms are assumed for u and v:

$$u = Mr^p \quad v = Nr^p \tag{53}$$

  where M and N are constants.

- u and v are substituted into the Navier equations (40), (43) and (46) resulting in two algebraic equations in M and N for each constituent.

- The determinant of the coefficients (M and N) of the algebraic equations is found for each of the constituents. They are given by:

$$D_m = D_m (p, E_m, v_m)$$

$$D_i = D_i (p, Q_v, v_i)$$

$$D_f = D_f (p, C_{ij}) \tag{54}$$

- The determinant is set to zero, in each case, resulting in a fourth order equation in p; the roots of this equation (p_1, p_2, p_3 and p_4) are determined.

- Relationships between M_k ($k = 1, 2, 3, 4$) and N_k ($k = 1, 2, 3, 4$) are also determined from the algebraic equations.

The expression for Q_v can be written as

$$Q_v = \frac{\ln\left(\frac{1}{v_v}\right)}{\ln\left(1 + \frac{2r}{d}\right)} \tag{55}$$

The determinant of the coefficients for the interphase is dependent on Q_y (and hence c and ξ_y) and v_i ($= v_m = 0.35$ [3], in this case). A three-dimensional plot of $D_i(p, Q_y)$ vs. p vs. Q_y is shown in Figure 4(a); the top surface of the plot represents the zero value of the determinant. Figure 4(b) shows the top surface of the three-dimensional plot as a contour plot and the roots (p_1, p_2, p_3 and p_4) can be determined for a given value of Q_y. Clearly, the roots p_k ($k = 1, 2, 3, 4$) for the interphase are imaginary for some Q_y values (for example, $Q_y = 5$); these values of Q_y correspond to interphases for which the displacement fields cannot be expressed in the form of Equation (53). Furthermore, it is interesting to note that the roots for the fiber and matrix ($Q_y = 0$) domains can also be found from this plot. The symbolic software package MATHEMATICA [26] was used for drawing the plots.

Results and Discussion

E-glass IMHS epoxy, carbon IMHS epoxy and Kevlar 49 IMHS epoxy are considered in this discussion; typical material property values are given in Table 1 [3]. Parametric studies were performed by varying the parameter ξ_y and the fiber volume fraction (V_f) and the results are presented.

Figures 5, 6, and 7 present the constituent stresses under different loading conditions as follows:

- Figure 5 — carbon IMHS epoxy — uniform temperature change of 1 °C.
- Figure 6 — E-glass IMHS epoxy — longitudinal shear load of 1 MPa.
- Figure 7 — Kevlar 49 IMHS epoxy — transverse shear load of 1 MPa.

Figures 6 and 7 show the distribution of stresses as a function of radial distance only, for the purpose of clarity. As can be seen, the Mori-Tanaka analyses provide a simple way to calculate the approximate stress state in composites with interphasial regions.

Figures 8, 9, and 10 show the distribution of shear stresses in carbon IMHS epoxy as a function of ξ_y under longitudinal and transverse shear loading conditions. It is clearly seen that changing the interphase stiffness changes the stress distribution in all the constituents. Hence, optimizing the

interphasial stiffness is an attractive option for optimizing composite materials for specific mechanical requirements.

Figures 11 and 12 show the constituent stresses in a Kevlar 49/IMHS epoxy composite under a uniform temperature change of 1 °C for volume fractions 0.4 and 0.6, respectively. Comparisons are made between the results of concentric cylinder assemblage (CCA) analysis [3] and the results of Mori-Tanaka analysis. It is seen that the Mori-Tanaka analysis takes into account fiber-fiber interaction through the average matrix stresses.

Conclusions

- The *non-dilute* local stresses in the constituents (fiber, interphase, and matrix) of a fiber-reinforced epoxy have been predicted using a Mori-Tanaka analysis. The interphase has been treated as a region with Young's modulus and coefficient of thermal expansion gradients — a direct consequence of the changes in the microstructure of the matrix near the fiber surface. The Navier's equations of elasticity have been solved in "closed-form" for each loading condition.

- A parametric study is used to demonstrate the fact that changes in the interphase properties can drastically alter the stress state in the interphase; this is important to the structural properties and performance of a composite since constituent stresses affect fiber/matrix adhesion and interaction.

- The ideas behind the interphase model reported in this study can be
  - used to provide guidance for controlling local failures in a composite with interphasial property gradients, and for the design of such material systems,
  - used to assess the influence of
    - ▲ fiber surface coatings,
    - ▲ fiber-matrix chemical interactions, and
    - ▲ morphological variations in regions of the matrix material

    on the local stress state and global properties, and

- extended to metal matrix and ceramic matrix composites with suitable modifications to the input properties.

References

1. K. Jayaraman, K. L. Reifsnider and R. E. Swain, "The Interphase in Unidirectional Fiber-Reinforced Composites: I. A Review of Characterization Methods," submitted to *Journal of Composites Technology & Research*, Oct. 1991.

2. K. Jayaraman, K. L. Reifsnider and R. E. Swain, "The Interphase in Unidirectional Fiber-Reinforced Composites: II. A Review of Modeling Studies," submitted to *Journal of Composites Technology & Research*, Oct. 1991.

3. K. Jayaraman and K. L. Reifsnider, "The Interphase in Unidirectional Fiber-Reinforced Epoxies: Effect on Residual Thermal Stresses," submitted to *Composites Science and Technology*, Oct. 1991.

4. Y. Mikata and M. Taya, "Stress field in a Coated Continuous Fiber Composite Subjected to Thermo-mechanical Loadings," *Journal of Composite Materials*, Vol. 19, 1985, pp. 554-578.

5. G. P. Tandon and N. J. Pagano, "A Study of Fiber-Matrix Interfacial Modeling," *Proceedings of the Fourth Japan-U.S. Conference on Composite Materials*, 1988, pp. 191-200.

6. N. J. Pagano and G. P. Tandon, "Elastic Response of Multidirectional Coated-fiber Composites," *Composites Science and Technology*, Vol. 31, 1988, pp. 273-293.

7. N. J. Pagano and G. P. Tandon, "Thermo-elastic Model for Multidirectional Coated-Fiber Composites: Traction Formulation," *Composites Science and Technology*, Vol. 38, 1991, pp. 247-269.

8. Y. Benveniste, G. J. Dvorak and T. Chen, "Stress Fields in Composites with Coated Inclusions," *Mechanics of Materials*, Vol. 7, 1989, pp. 305-317.

9. W. Zhang, "Computation of Stress Fields in Unidirectional n-Phase Fibrous Composites under Longitudinal and Transverse Loads," *Computers and Structures*, Vol. 34, 1990, pp. 647-653.

10. K. H. Lo, R. W. Schmitz and W. G. Gottenberg, "Determination of Flexible Interlayer Thickness for Fiber Reinforced Composites," *Proceedings of the Materials Research Society Symposium*, Vol. 170, 1990, pp. 55-58.

11. A. Dasgupta and J. S. Sirkis, "The Importance of Coatings to Structurally Embedded Optical Fiber Sensors in Smart Structures," *AIAA Journal*, in press, 1991.

12. J. D. Eshelby, "The Determination of the Elastic Field of an Ellipsoidal Inclusion, and Related Problems," *Proceedings of the Royal Society of London*, Vol. A241, 1957, pp. 376-396.

13. J. D. Eshelby, "The Elastic Field Outside an Ellipsoidal Inclusion," *Proceedings of the Royal Society of London*, Vol. A252, 1959, pp. 561-569.

14. T. Mori and K. Tanaka, "Average Stress in Matrix and Average Elastic Energy of Materials with Misfitting Inclusions," *Acta Metallurgica*, Vol. 21, 1973, pp. 571-574.

15. Y. Benveniste, "A New Approach to the Application of Mori-Tanaka's Theory in Composite Materials," *Mechanics of Materials*, Vol. 6, 1987, pp. 147-157.

16. S. G. Lekhnitskii, *Theory of Elasticity of an Anisotropic Body*, Mir Publishers, Moscow, 1981, Chapter 5.

17. G. Subbaraman and K. L. Reifsnider, Mechanical Response of a Fuel Clad with Radial Property Variations, *Proceedings of the Twelfth Annual Meeting of the Society of Engineering Science*, 1975, pp. 1235-1243.

18. G. Subbaraman and K. L. Reifsnider, The Effect of Liquid Sodium Thermo-chemical Reactions with Stainless Steels on Mechanical Response, *Proceedings of the International Conference on Liquid Metal Technology in Energy Production*, 1976, pp. 324-330.

19. G. A. Van Fo Fy, "A Study of the Effect of Fiber Treatment on Stress Distribution in Glass-Reinforced Plastic Structures," *Prikladnaya Mekhanika*, Vol. 3, 1967, pp. 106-112.

20. T. Mura, *Micromechanics of Defects in Solids*, Martinus-Nijhoff Publishers, The Hague, 1982.

21. Z. Hashin and B. W. Rosen, "The Elastic Moduli of Fiber-Reinforced Materials," *Journal of Applied Mechanics*, Vol. 31, 1964, pp. 223-232; Errata, Vol. 32, 1965, p. 219.

22. N. J. Pagano, "The Stress Field in a Cylindrically Anisotropic Body under Two-Dimensional Surface Tractions," *Journal of Applied Mechanics*, Vol. 39, 1972, pp. 791-796.

23. R. M. Christensen and K. H. Lo, "Solutions for Effective Shear Properties in Three Phase Sphere and Cylinder Models," *Journal of the Mechanics and Physics of Solids*, Vol. 27, 1979, pp. 315-330.

24. P. S. Theocaris and A. G. Varias, "Accurate Evaluation of the Transverse Shear Modulus in Unidirectional Fibrous Composites," *Rheologica Acta*, Vol. 26, 1987, pp. 182-192.

25. S. L. Ross, *Differential Equations*, Blaisdell Publishing Company, New York, 1964.

26. MATHEMATICA, *A System for Doing Mathematics by Computer*, Wolfram Research, Inc., Champaign, IL, 1988.

27. MACSYMA, *A Computer Algebra System and Programming Environment*, Symbolics, Inc., Burlington, MA, 1988.

Table 1. Material properties.

Property	E-glass	carbon	Kevlar 49	IMHS epoxy
E_{11} (GPa)	76.00	214.00	124.00	3.50
E_{22} (GPa)	76.00	14.00	6.90	3.50
G_{12} (GPa)	31.15	14.00	2.80	1.30
α_{11} (ppm/ $^\circ$C)	4.90	-1.00	-5.20	65.00
α_{22} (ppm/ $^\circ$C)	4.90	10.10	41.50	65.00
ν_{12}	0.22	0.20	0.36	0.35
ν_{23}	0.22	0.25	0.30	0.35
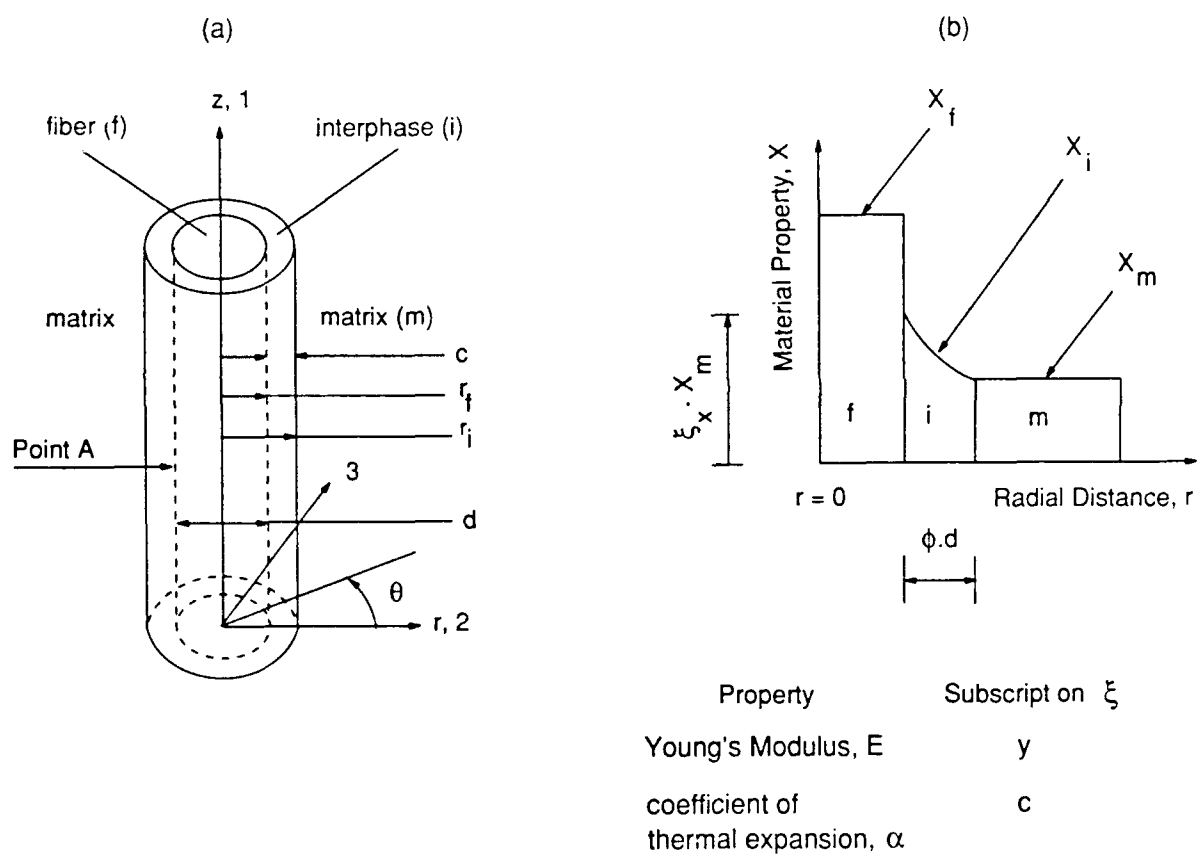
Figure 1. Schematic of the interphase: (a) Location, and (b) Property Variation.
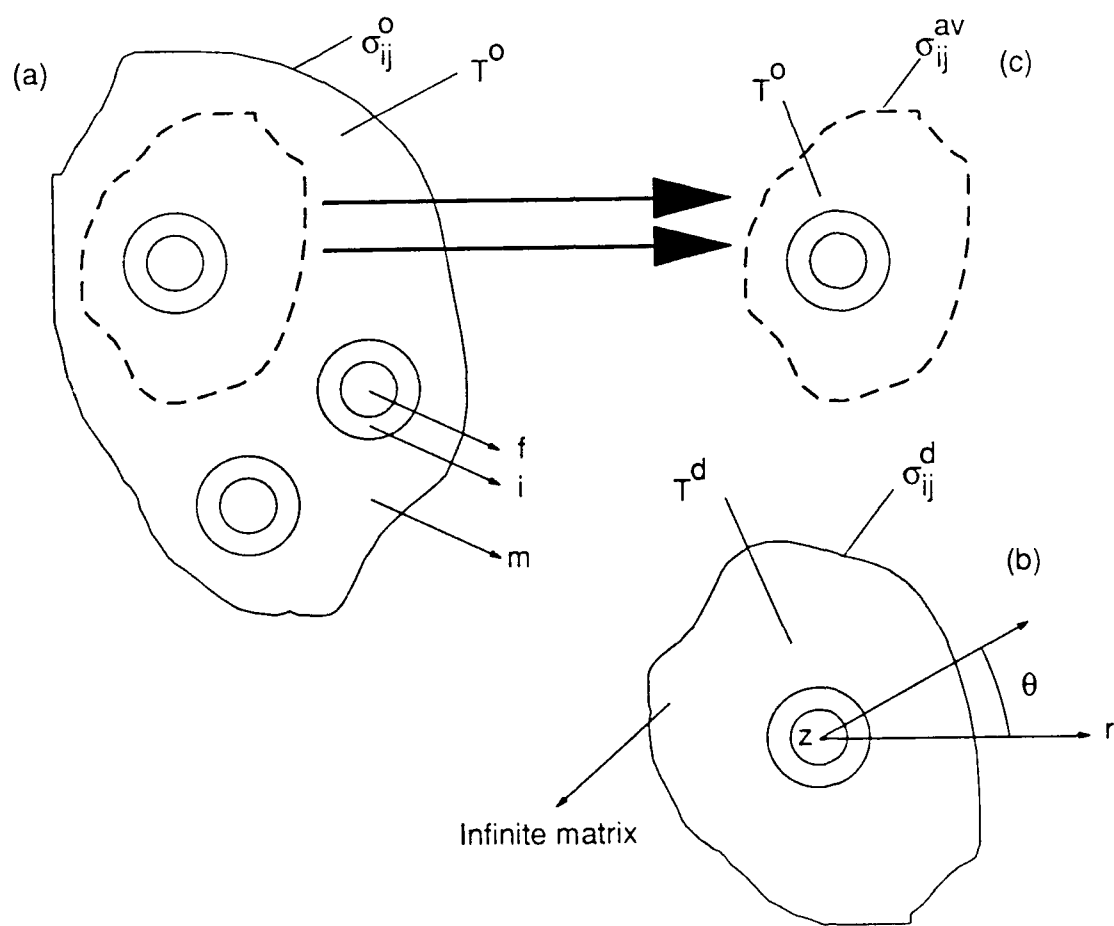
Figure 2. Schematic representations of a composite depicting the idea behind the Mori-Tanaka analysis.
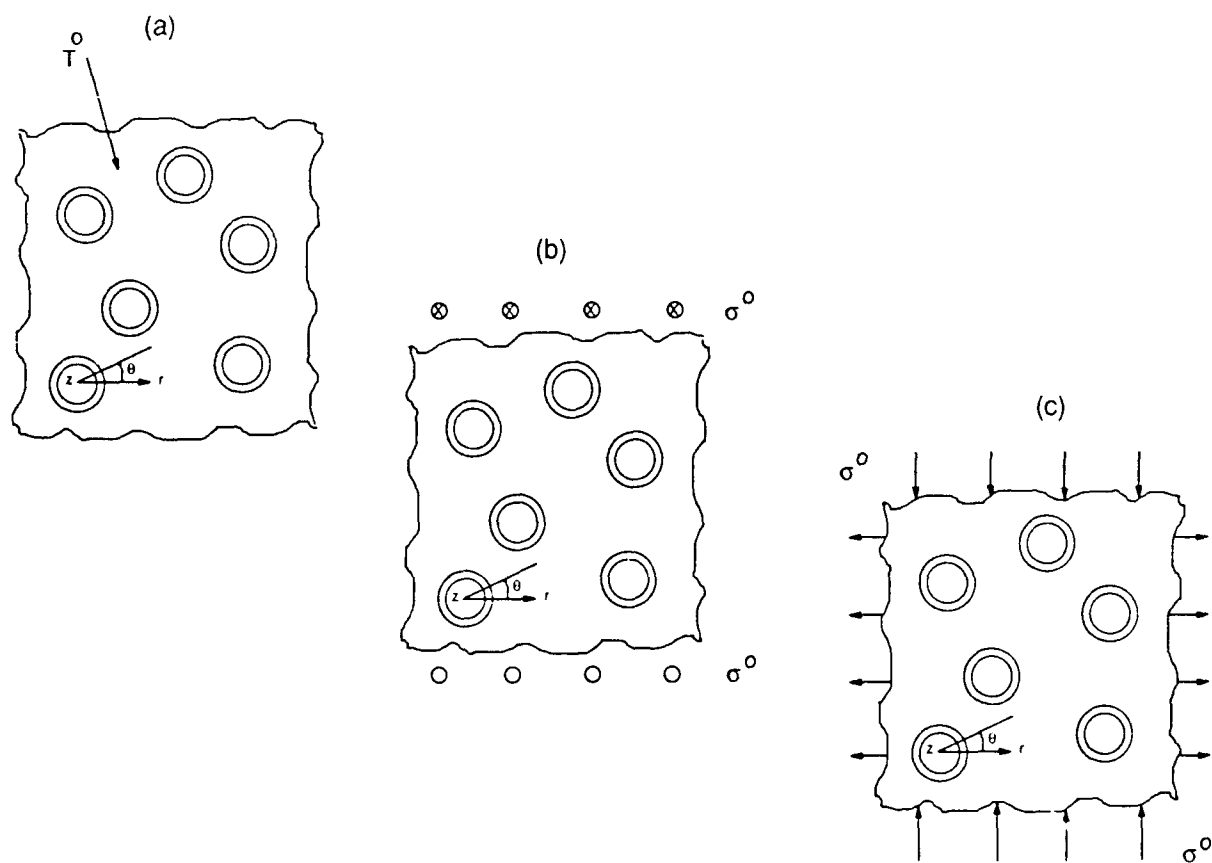
Figure 3. Loading configurations under consideration: (a) Uniform temperature change, (b) Applied longitudinal shear, and (c) Applied transverse shear.

(a)   (b)
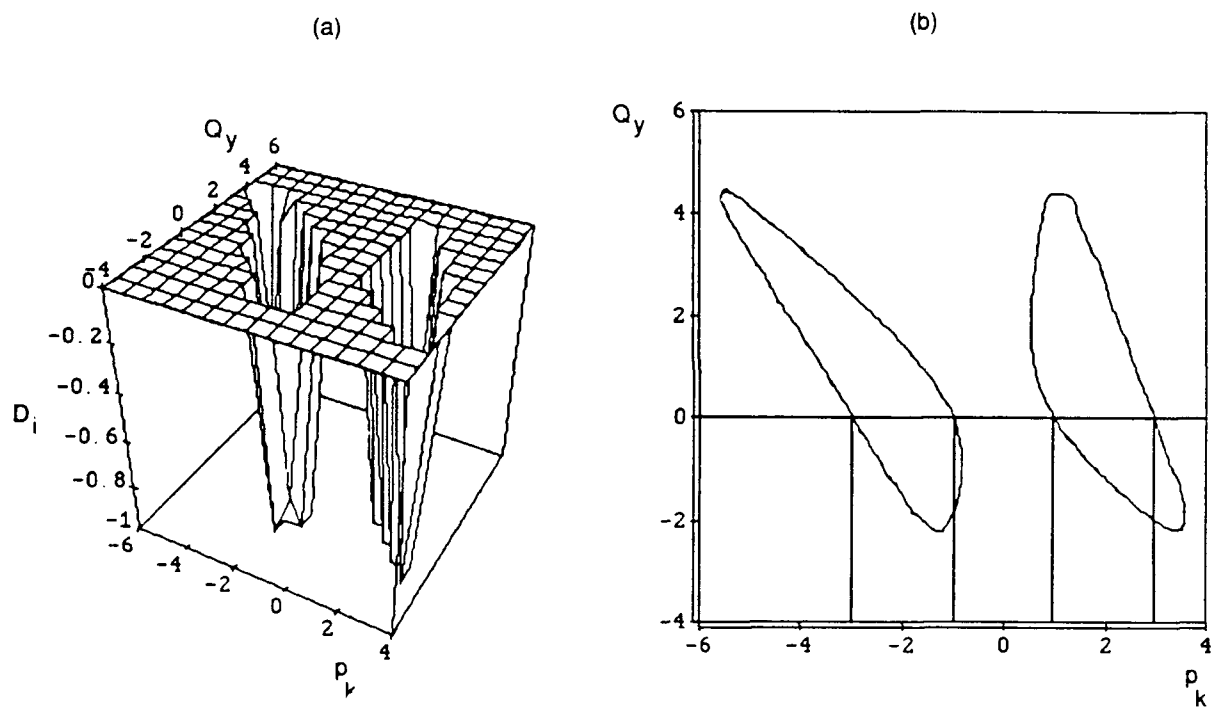
Figure 4. A three-dimensional plot and a contour plot showing the roots of the characteristic equation encountered in the solution of the transverse shear problem.
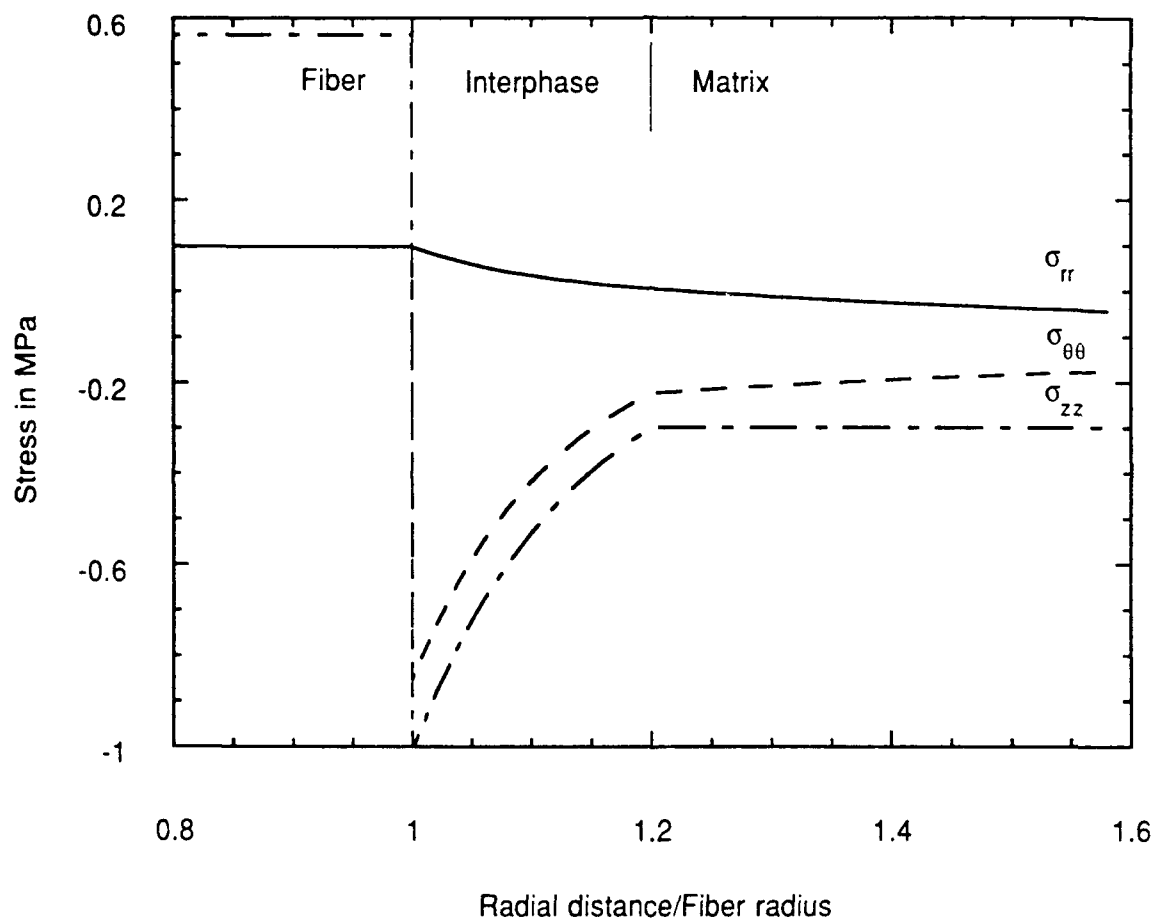
Figure 5. Constituent stresses in a carbon/IMHS epoxy composite under a uniform temperature change of 1 °C ($V_f = 0.4$; $\phi = 0.1$; $\xi_y = 4.5$; $\xi_c = 0.75$).
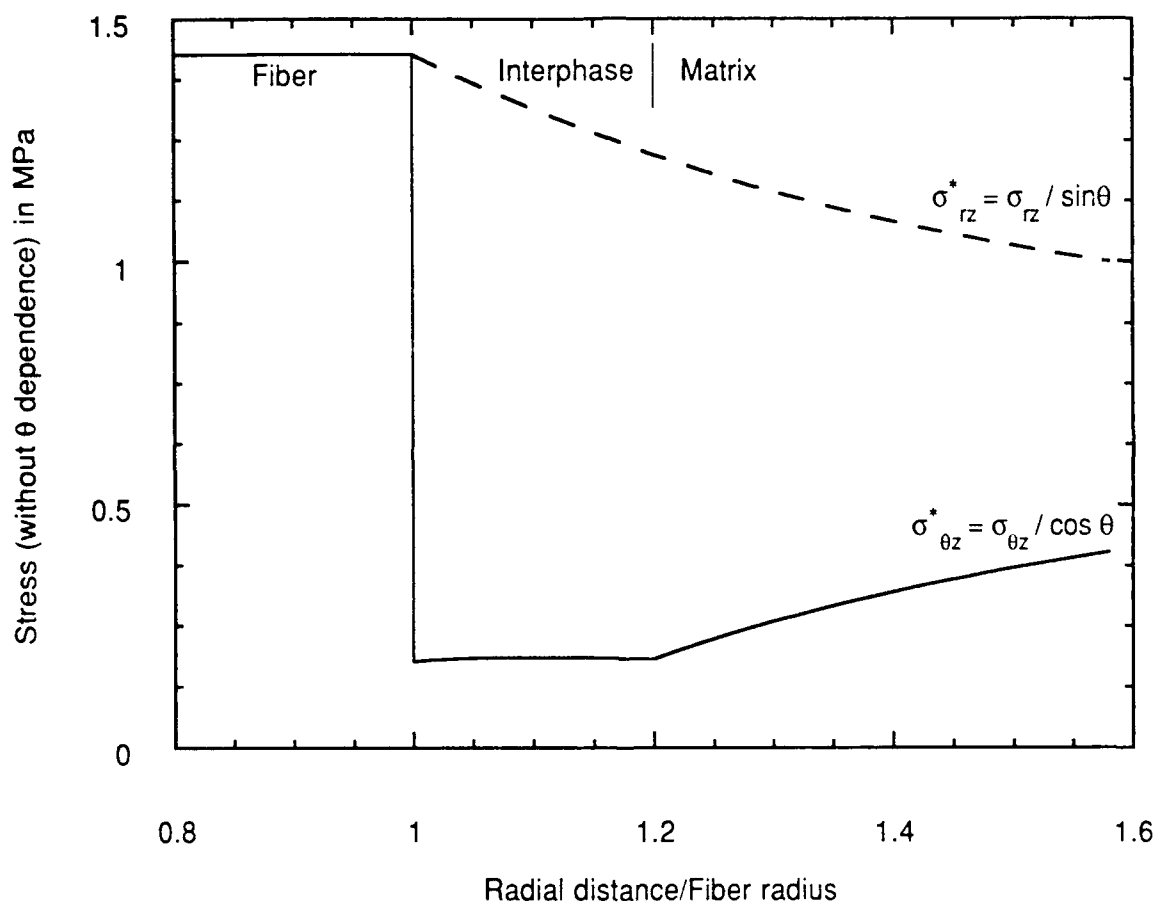
Figure 6. Constituent stresses in a E-glass/IMHS epoxy composite under a longitudinal shear load of 1 MPa ($V_f = 0.4$; $\phi = 0.1$; $\xi_v = 3$).
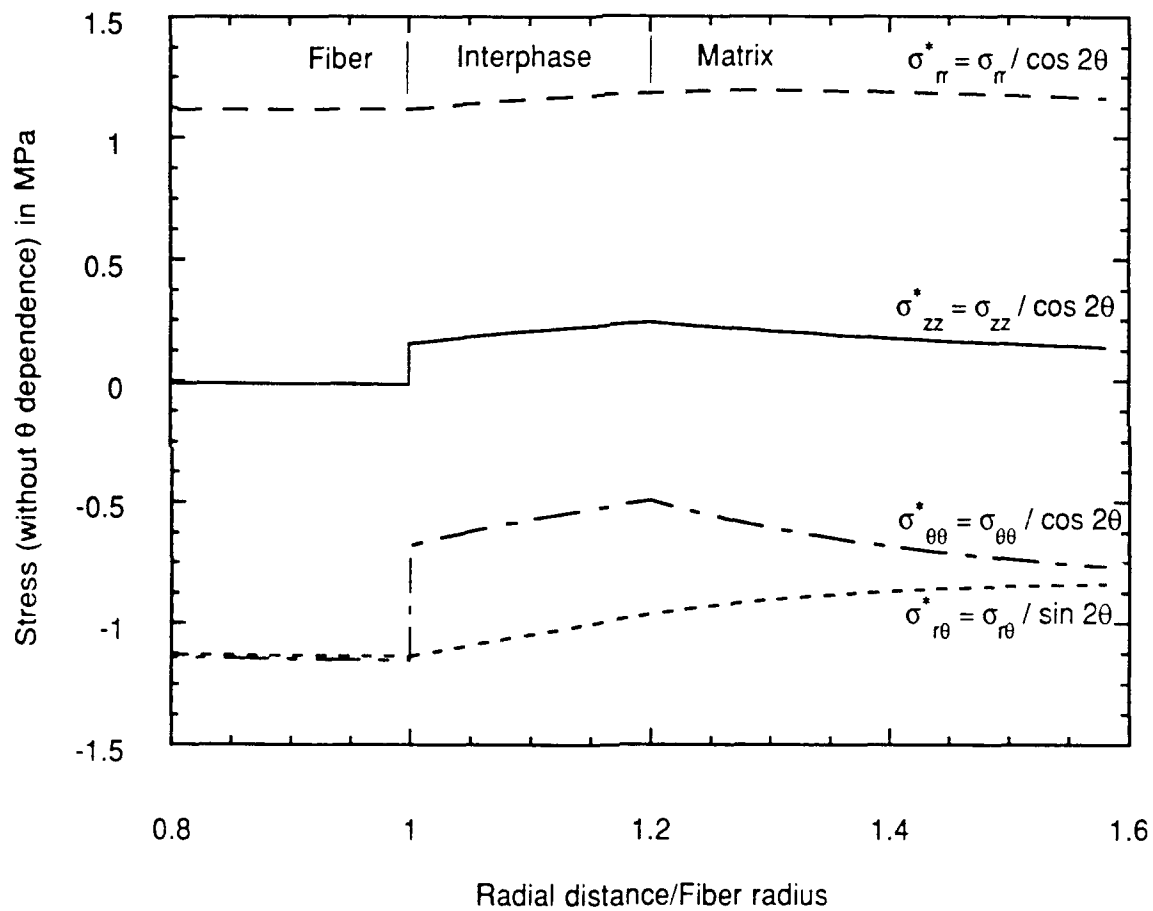
Figure 7. Constituent stresses in a Kevlar 49/IMHS epoxy composite under a transverse shear load of 1 MPa ($V_f = 0.4$; $\phi = 0.1$; $\xi_y = 1.49$).
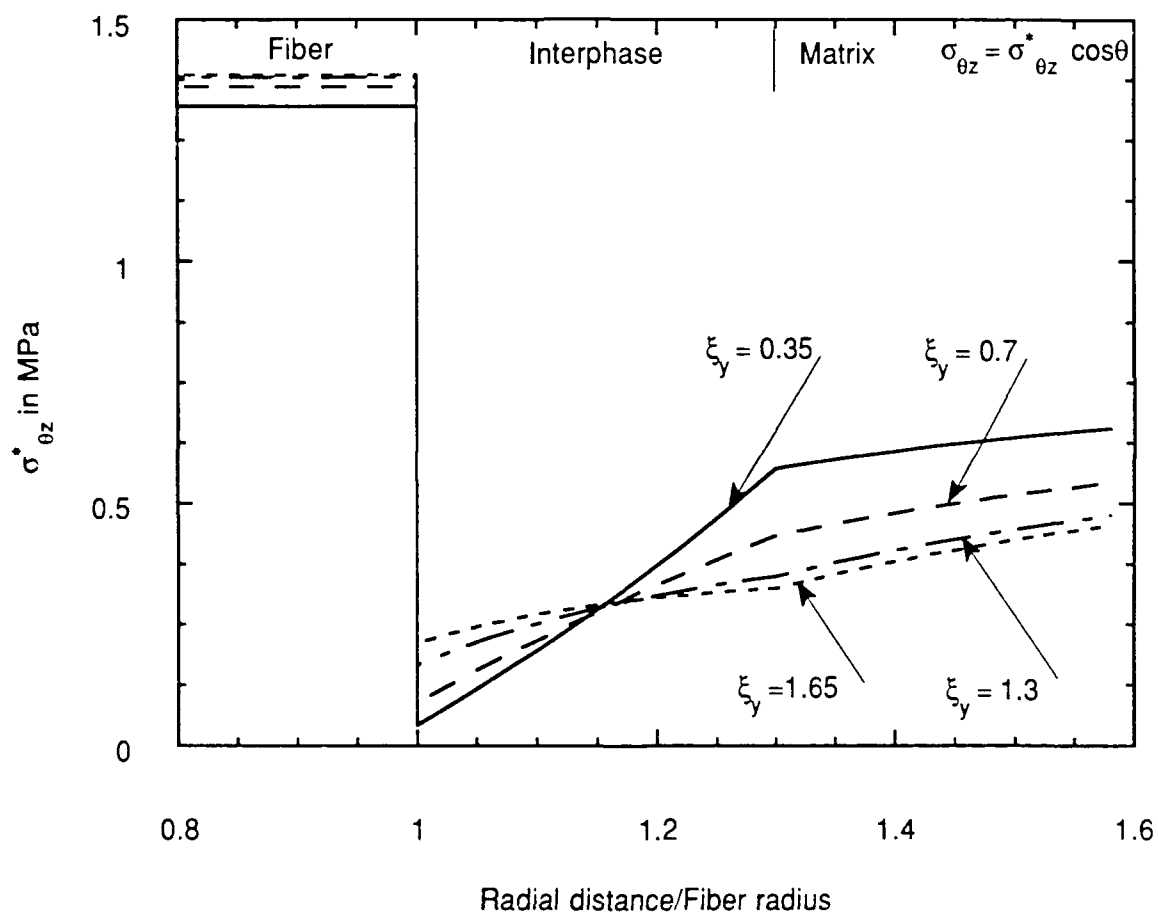
Figure 8. Shear stress $\sigma^*_{\theta z}$ as a function of ξ_y in a carbon/IMHS epoxy composite under a longitudinal shear load of 1 MPa ($V_f = 0.4$; $\phi = 0.15$).
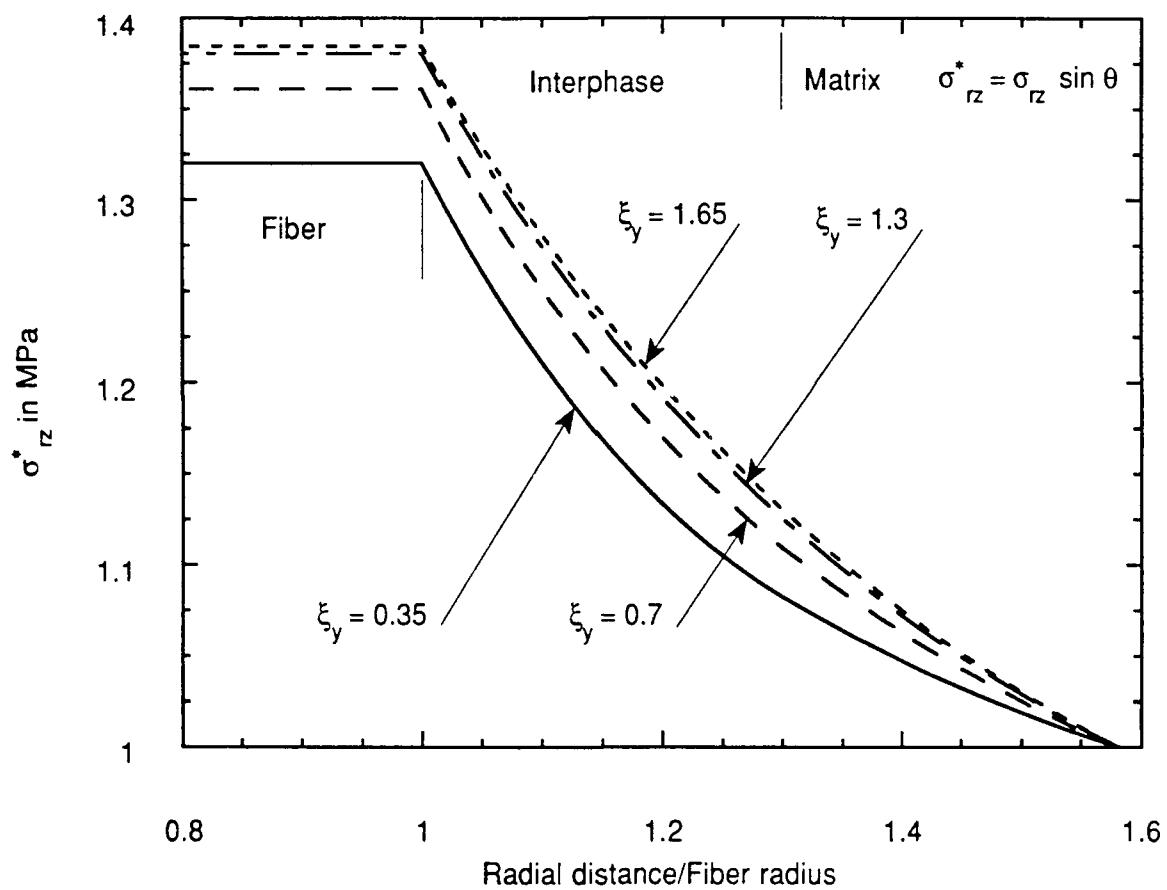
Figure 9. Shear stress σ^{*}_{rz} as a function of ξ_y in a carbon/IMHS epoxy composite under a longitudinal shear load of 1 MPa ($V_f = 0.4$; $\phi = 0.15$).
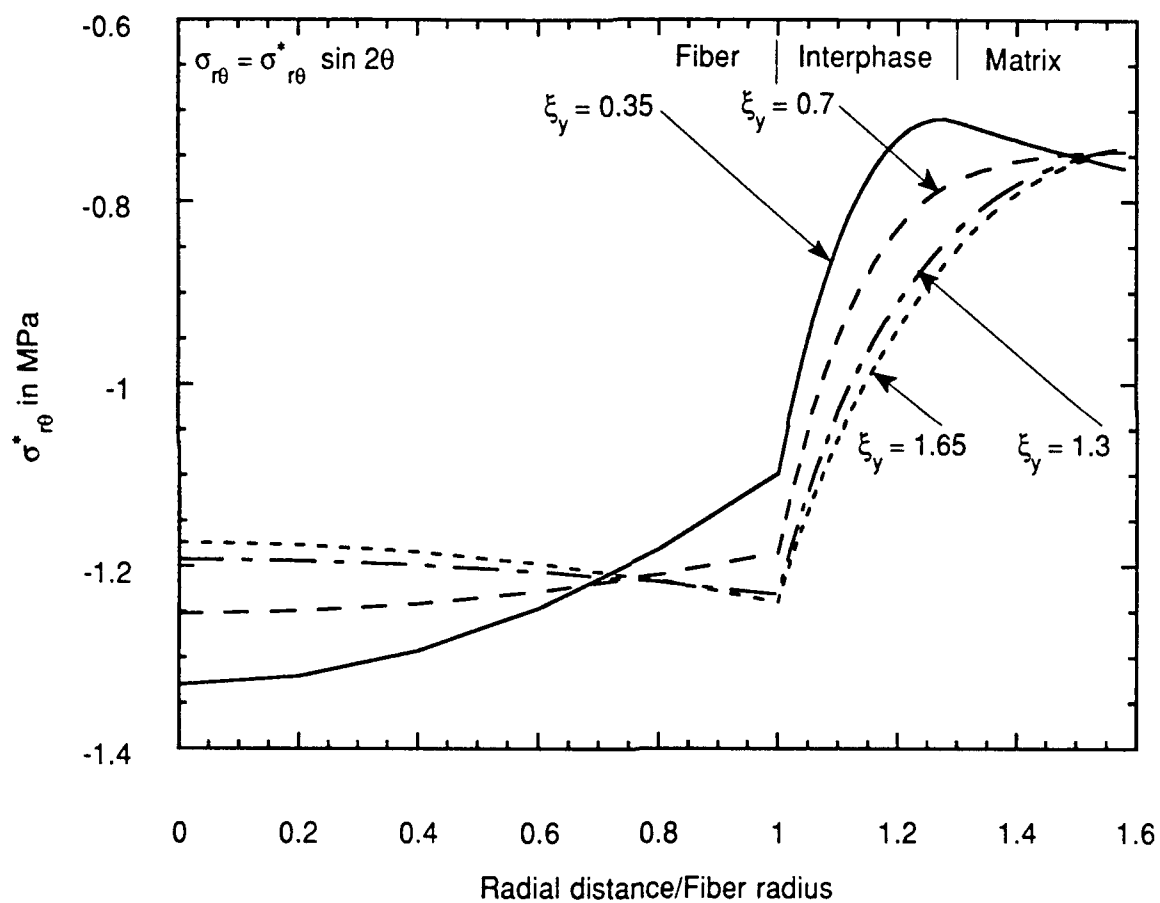
Figure 10. Shear stress $\sigma^*_{r\theta}$ as a function of ξ_y in a carbon/IMHS epoxy composite under a transverse shear load of 1 MPa ($V_f = 0.4$; $\phi = 0.15$).

3. The Interphase in Unidirectional Fiber-Reinforced Epoxies: Mori-Tanaka Analysis of the Effect on Local Stress Fields
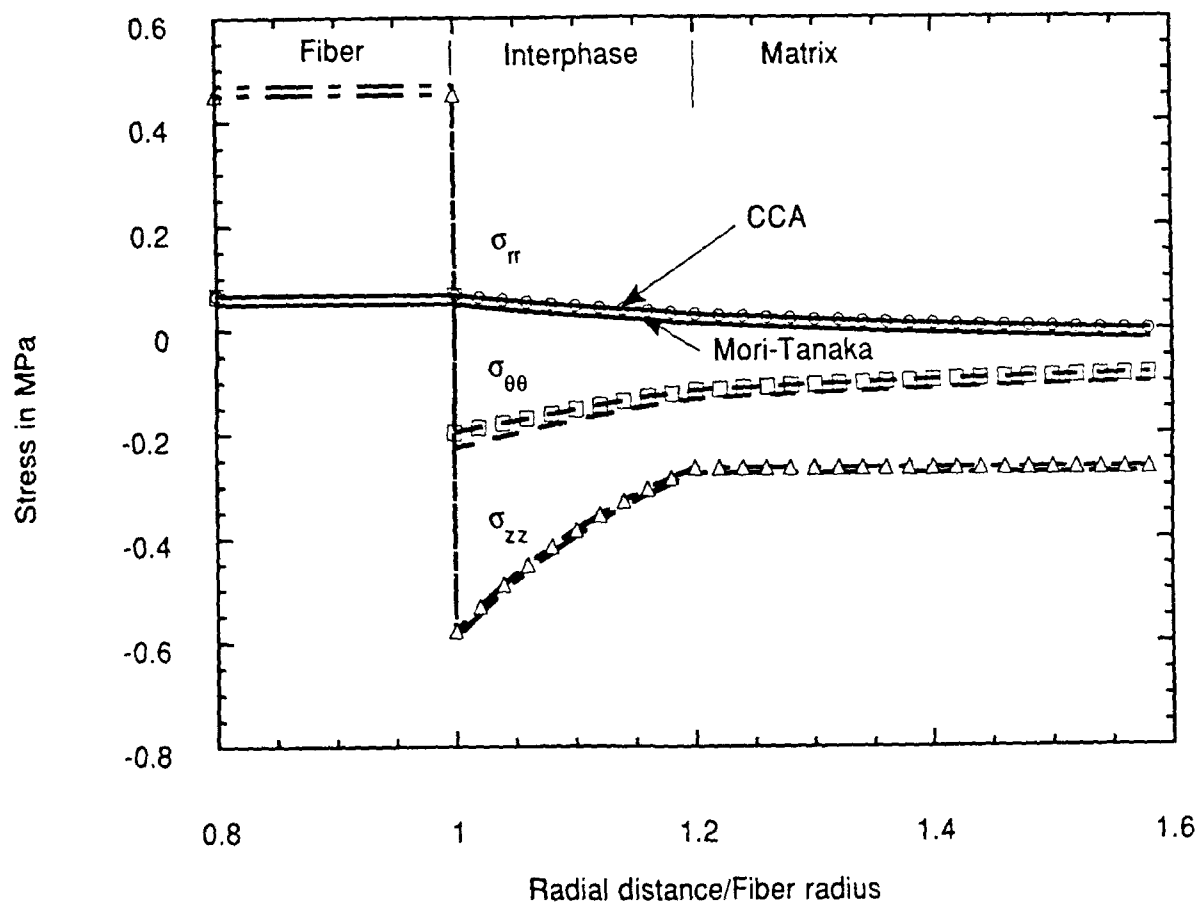
Figure 11. Constituent stress comparison between concentric cylinder assemblage (CCA) and Mori-Tanaka analyses in a Kevlar 49/IMHS epoxy composite under a uniform temperature change of 1 °C ($V_f = 0.4$; $\phi = 0.1$; $\xi_y = 3$; $\xi_c = 0.75$).
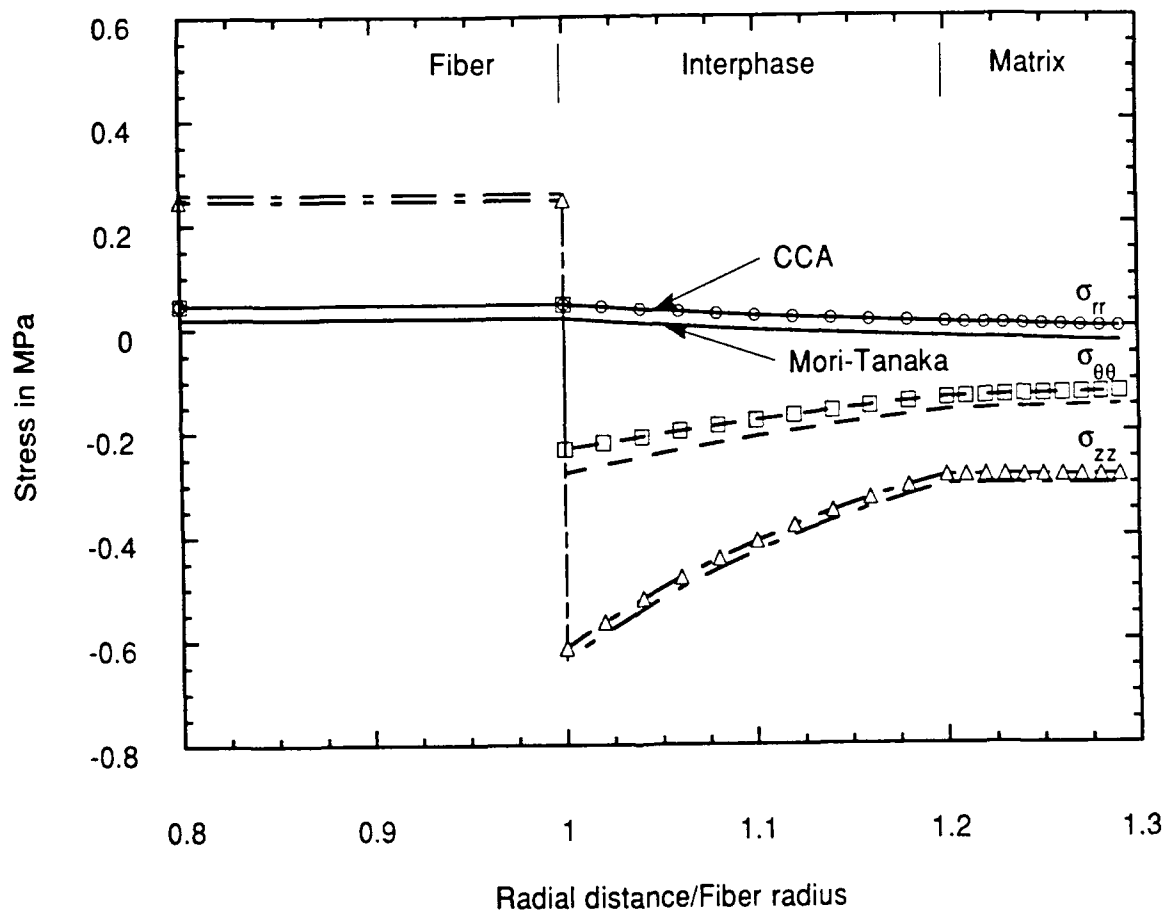
Figure 12. Constituent stress comparison between concentric cylinder assemblage (CCA) and Mori-Tanaka analyses in a Kevlar 49/LMHS epoxy composite under a uniform temperature change of 1 °C ($V_f = 0.6$; $\phi = 0.1$; $\xi_y = 3$; $\xi_c = 0.75$).

4. The Effect of the Interphase/Interface Region on Creep and Creep Rupture of Thermoplastic Composites

Yeou Shin Chang and David A. Dillard

Technical Progress

The past year has seen a number of our VIMS funded activities come to fruition. After long delays, three new lots of materials were received with the same fibers and matrix, but different surface treatments and interphase regions. These materials have been carefully tested in various ways to allow us to put together three of the first papers which deal with the effect of the interphase on static and time dependent mechanical properties of a thermoplastic composite material system. Although new questions have arisen through these activities, insights have been gained into the role which the interphase region may play in thermoplastic composite performance. These results are the culmination of our prior VIMS activities, and are expected to be completed this summer with the graduation of Y. S. Chang.

In the preliminary creep rupture tests reported in prior VIMS reports, we had observed that the creep rupture strength of AS4(1)/J2 composite laminates ($[\pm 45/90_2]_s$) degraded about 19% within four decades of time period. This rate is twice that observed for T300/934 laminates in earlier studies conducted at VPI. Several possibilities were considered to explain this discrepancy. First, the thermoplastic matrix lacks the crosslink structure present in thermosetting systems. Secondly, the testing temperatures of the creep rupture studies differ for the two composite systems. Thirdly, the interphase properties of fiber/matrix differ in the thermoset and thermoplastic composites. Finally, the thermoplastic composite may exhibit a greater degree of nonlinear behavior than a thermoset composite. Within the past year, we have ruled out the first two concerns, and seem left with the conclusion that either differences in interphase region or differences in polymer ductility or constitutive properties must have accounted for the anomalous results seen in the AS4(1)/J2 system.

Creep rupture data collected on the three most recent batches of material have indicated that the strength degradation rate in creep is not significantly different from that observed earlier in thermoset composites. This has forced us to focus a great deal of attention on the differences between the initial (AS4(1)) and more recent (AU4, AS4(2), and AS4CGP) material lots. DuPont

claims that both lots of material should have been identical, but XPS results suggested that the chemistry of the fiber surfaces were different. Specifically, the initial lot of AS4 fibers contained less oxygen and slightly more nitrogen than the AS4(2) fibers, as indicated in Table 1. There also seemed to be different constitutive properties for the initial and final lots of materials. The aging behavior was different, suggesting that the resin systems may also have been dissimilar. Much more delamination was observed in the initial lot of material; this may have directly affected the creep rupture strengths. In spite of these observed differences, it has been difficult to pinpoint the exact reasons why the initial lot of material behaved so differently than the subsequent batches received.

IGC tests were performed on the AS4CGP fibers in order to compare fiber surface energy with values obtained by Bolvari and Ward [1] for AU4 and AS4 fiber systems. Results suggested that the bonding to the AS4CGP fiber should be quite good. The T_g of the epoxy sizing on the AS4CGP fibers was found to be -10°C by DSC. It should be noted that the epoxy on the AS4CGP fiber surfaces does not contain curing agent. As a result, the epoxy may not totally crosslink during the sample preparation step and/or consolidation process. Thus, the epoxy may be in a rubbery or viscous state at room temperature. Evidence also exists that the epoxy sizing may be able to diffuse into the surrounding polymer matrix, and perhaps alter the properties of this interphase.

The mechanical properties of J2 composites are summarized in Table 2, including results from the meso-indentation test. When comparing the maximum mean hardness pressure (MMHP), the AU4 composite possesses the weakest interface by approximately 22% relative to the surface treated fibers. The AS4CGP and AS4(2) are essentially indistinguishable. However, the AS4(1) appears to have a greatest bond strength by roughly 31% over the AS4CGP and AS4(2) composites. This may be explained, in part, by the differences in fiber lot and/or processing conditions for the AS4 systems (1) and (2). Due to the limitations on the micromechanics model and what was observed in the tests, only approximate Interfacial Shear Strength (ISS) values were obtainable for three (highlighted by star) of the four systems. The ISS of the AS4(1)/J2 composite is the highest resulting the highest transverse tensile strength. Thus, as expected, the lowest ISS results in the lowest transverse tensile strength for the AU4/J2 composite. Although the ISS's of the AS4(2)/J2 and AS4CGP/J2 composites are approximately the same, the transverse tensile strength of the AS4(2)/J2 composite is larger than the AS4CGP/J2 composite. This may be due to a compliant interphase in the AS4CGP/J2 composite.

Figure 1 shows the Log[E' and E'' (Pa)] vs. temperature (°C) plot for J2 composites, including unannealed AS4(1)/J2, as well as annealed AS4(1)/J2, AU4/J2, AS4(2)/J2, and AS4CGP/J2 specimens. The transition temperatures (at the peak of E'' not tan(δ)) of unannealed AS4(1)/J2, annealed AS4(1)/J2, AU4/J2, AS4(2)/J2, and AS4CGP/J2 specimens are 168°C, 172.3°C, 168.8°C, 168.8°C, and 165.6°C, respectively. Three specimens were tested for each composite system and the T_g values of each individual system are all very close, deviating only ±0.5 °C difference from sample to sample. Also, the specimens used for the DMA tests are [90]$_{12}$ lamina, i.e., the testing direction is matrix dominated. Therefore, although the T_g values of the tested composite systems do not deviate substantially, the high and low values encountered on the annealed AS4(1)/J2 and AS4CGP/J2 systems become important. The low T_g value of the AS4CGP/J2 system may be because of the epoxy sizing. This may also explain why the storage modulus of AS4CGP/J2 composite is lower than that of both AU4/J2 and AS4(2)/J2 composites.

4. The Effect of the Interphase/Interface Region on Creep and Creep Rupture of Thermoplastic Composites

Short term creep and recovery tests were conducted at low stress levels. The stress levels, according to the DMA results, were all in the range between 10 and 20 MPa. Thus the creep and recovery tests were performed in the linear viscoelastic range. A typical plot for the creep compliance curves of AS4(1) J2 composites at elevated temperatures is shown in Figure 2. Based on the time-temperature superposition principle (TTSP), a master curve can be formed by shifting creep compliance curves to either the right or the left with respect to the selected creep compliance curve (reference curve). Several master curves are formed and shown in Figure 3. As expected, the annealed specimens become stiffer and require large shift factors to shift the creep compliance curves. As a result, the master curves of the annealed specimens are flatter than the unannealed specimens.

A one-week creep test was also conducted at 108.7°C for an unannealed AS4(1) J2 $[90]_{12}$ lamina by using the DMA. This was done to investigate annealing effects on the creep behavior of the composites. The creep curve for the one-week creep test is also shown in Figure 3. This curve almost overlaps with the master curve of the annealed AS4(1)/J2 composites. The correspondence indicates that the unannealed specimen was aged and became brittle during the creep test.

Figure 4 shows the creep rupture results of AU4/J2, AS4(2) J2, and AS4CGP J2 laminates ($[\pm 45 \ 90_2]_s$). The creep rupture strength of these laminates degrades approximately 9% within five decades of time period, which is less than half of the values for the AS4(1)/J2 laminates. Aging effects, differences in polymer constitutive behavior, fiber surface variations, and delamination have all been implicated in explaining this confusing behavior.

Figure 5 and 6 show the fracture surfaces of the specimens failed at an intermediate and long creep rupture life for AS4(1) J2, AU4/J2, AS4(2)/J2, and AS4CGP/J2 laminates. Figure 5(a) shows that matrix was smeared at the -45/90 interface. It also shows good adhesion is obtained in AS4(1) J2 system, which confirms the ISS results. Figure 5(b) shows clean fiber surfaces (at 45 -45 plies) in AU4 J2 laminates. Figure 5(c) shows that matrix was pulled up at the 45/-45 interface in the AS4(2) J2 laminates. River patterns were observed in Figure 5(d) for the AS4CGP J2 laminates at the 45 -45 interface.

Figure 6(a) have shown flake-shape hackles in AS4(1)/J2 composites. Two possible factors may explain the brittle failure of the AS4(1) J2 composites. They are (a) the aging process proceeds during the creep rupture tests; (b) a rigid interphase is formed in AS4(1) J2 composites. For long creep rupture life, severe plastic deformation was observed in the other three composite systems, see Figure 6(b), 6(c), and 6(d). Nonetheless, clean fiber surfaces were still observed in AU4 J2 composites.

Conclusion

We have demonstrated that the mechanical properties of the J2 composites are affected by the level of fiber-matrix adhesion and by the properties of the interphase region. Both the AS4(2) J2 and AS4CGP J2 composites have good fiber-matrix adhesion; and yield higher strength values than those of the AU4 J2 composites in the static and creep rupture tests. The interphase region also plays an important role in determining the creep rupture strength, e.g., the creep rupture strength

of the AS4CGP/J2 laminates is greater than that of the AS4(2)/J2 laminates. In other words, composites that possess good static mechanical properties may not necessarily dictate good long term mechanical performance.

From the interphase interface effect point of view, it is difficult to compare the creep rupture results of the AS4(1) J2 composites with those of the other composite systems. It is because the AS4(1) fibers may be different from the other fiber systems, according to the XPS results. The aging effect on the composites may also play an important role in determining the creep rupture strength. However, more efforts are needed to demonstrate the aging effect on the creep rupture strength of the composites.

References

1. Bolvari, A. E. and Ward, T. C. "Determination of Fiber-Matrix Adhesion and Acid-Base Interactions," in Inverse Gas Chromatography: Characterization of Polymers and Other Materials Ed. Lloyd, D. R., Ward, T. C. and Screiber, H. P., ACS Symposium Series 391, 1989.

Table 1. XPS Results of Carbon Fibers

	AU4/J2*	AS4(2)/J2*	AS4CGP/J2*	AS4(1)/J2*	AU4	AS4(2)	AS4CGP
C	94.8%	87.5%	83.8%	89.2%	95.6%	85.9%	83.3%
O	2.0%	9.9%	14.4%	5.6%	2.7%	11.6%	16.1%
N	3.2%	2.6%	1.8%	4.2%	1.7%	2.5%	0.6%

* Fibers were taken from prepregs.

Table 2. Mechanical Properties of J2 Composites

	AU4/J2	AS4(2)/J2	AS4CGP/J2	AS4(1)/J2
MMHP/ISS* [MPa]	473/77.2	575.7/~96.5	582.6/~96.5	758.5/~124.1
σ^f_{22} [MPa]	34.2±3.4 (5)+	54.2±1.7 (4)	48.7±2.2 (5)	70.0±3.3 (4)
E_{22} [GPa]	8.9±0.2	8.5±0.4	8.3±0.3	8.8±0.6
V_f [%]	57.4%	55.7%	53.6%	54.4%
σ^f [MPa] $[\pm45/90_2]_s$	196.0/181.9	316.0/302.7	316.0/309.1	279.5±19.9 (4)

* Meso-indentation tests.   MMHP: Maximum Mean Hardness Pressure.   ISS: Interfacial Shear Strength
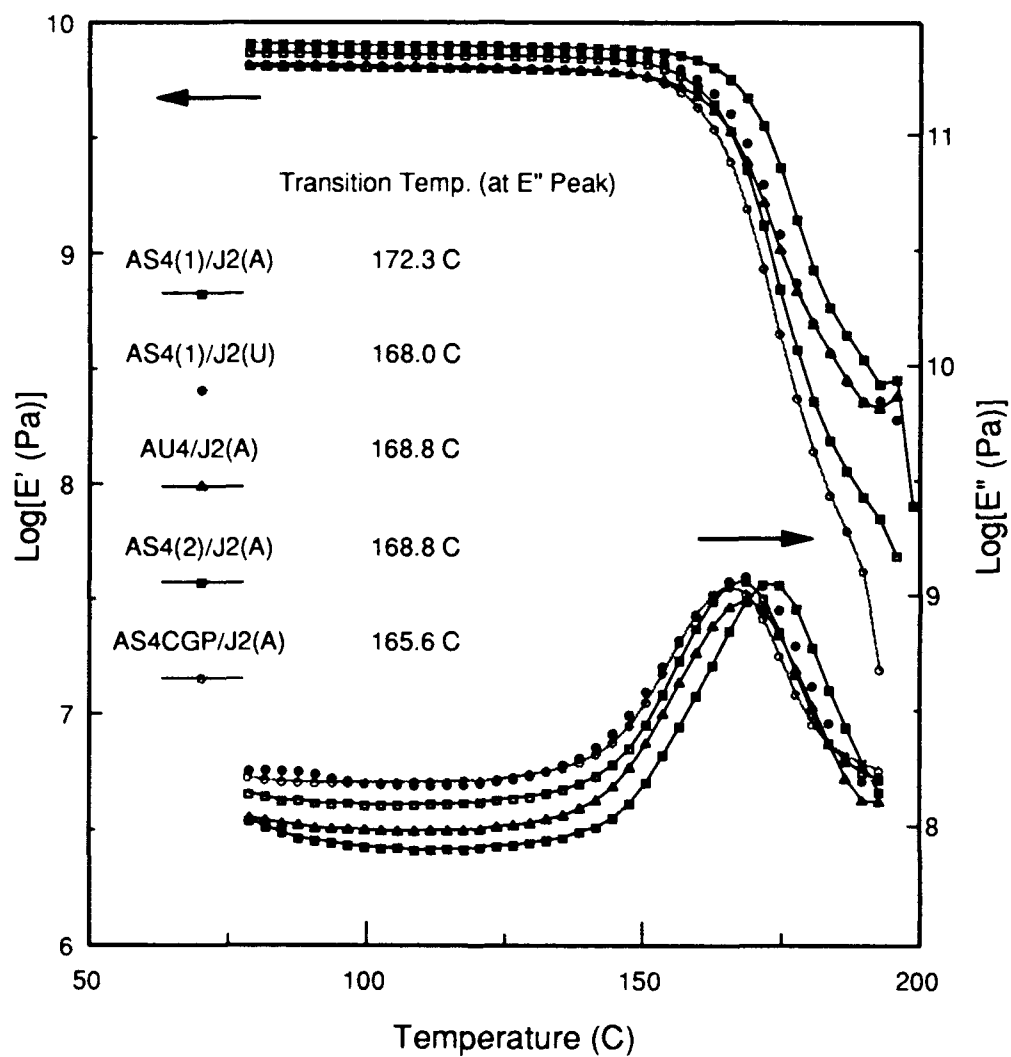+ Numbers in the parentheses denote the number of tested specimens.

4. The Effect of the Interphase/Interface Region on Creep and Creep Rupture of Thermoplastic Composites
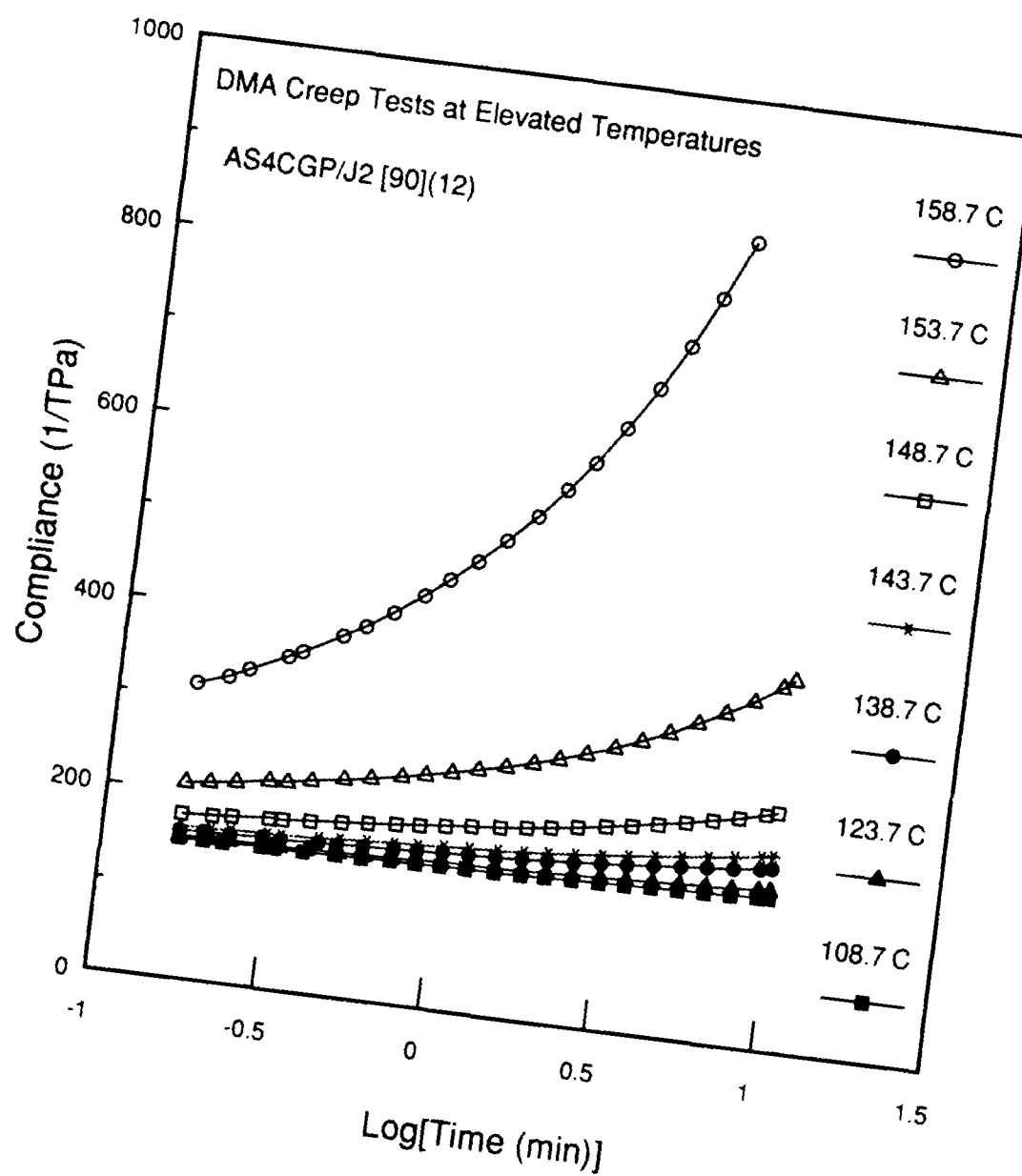
Figure 1. DMA results for J2 composite lamina [90]₁₂.

Figure 2. Typical creep compliance curves at elevated temperatures ranging from 108.7°C to 160°C for AS4CGP J2 composite lamina [90]₁₂.

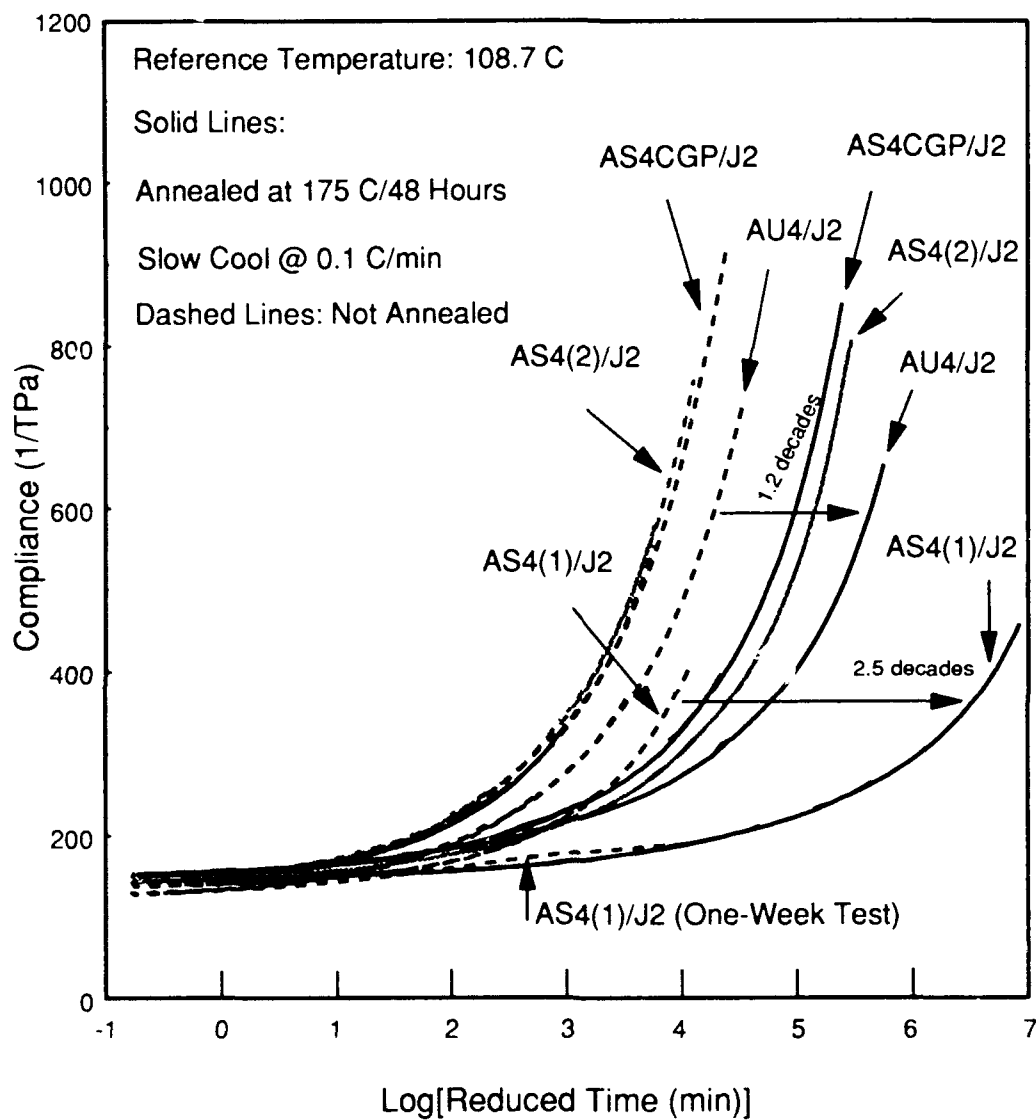4. The Effect of the Interphase/Interface Region on Creep and Creep Rupture of Thermoplastic Composites

Figure 3. Master curves for annealed (solid line) and unannealed (dashed line) J2 composites, reference temperature: 108.7°C. Also shown, a one-week creep test for unannealed AS4(1) J2 composite.
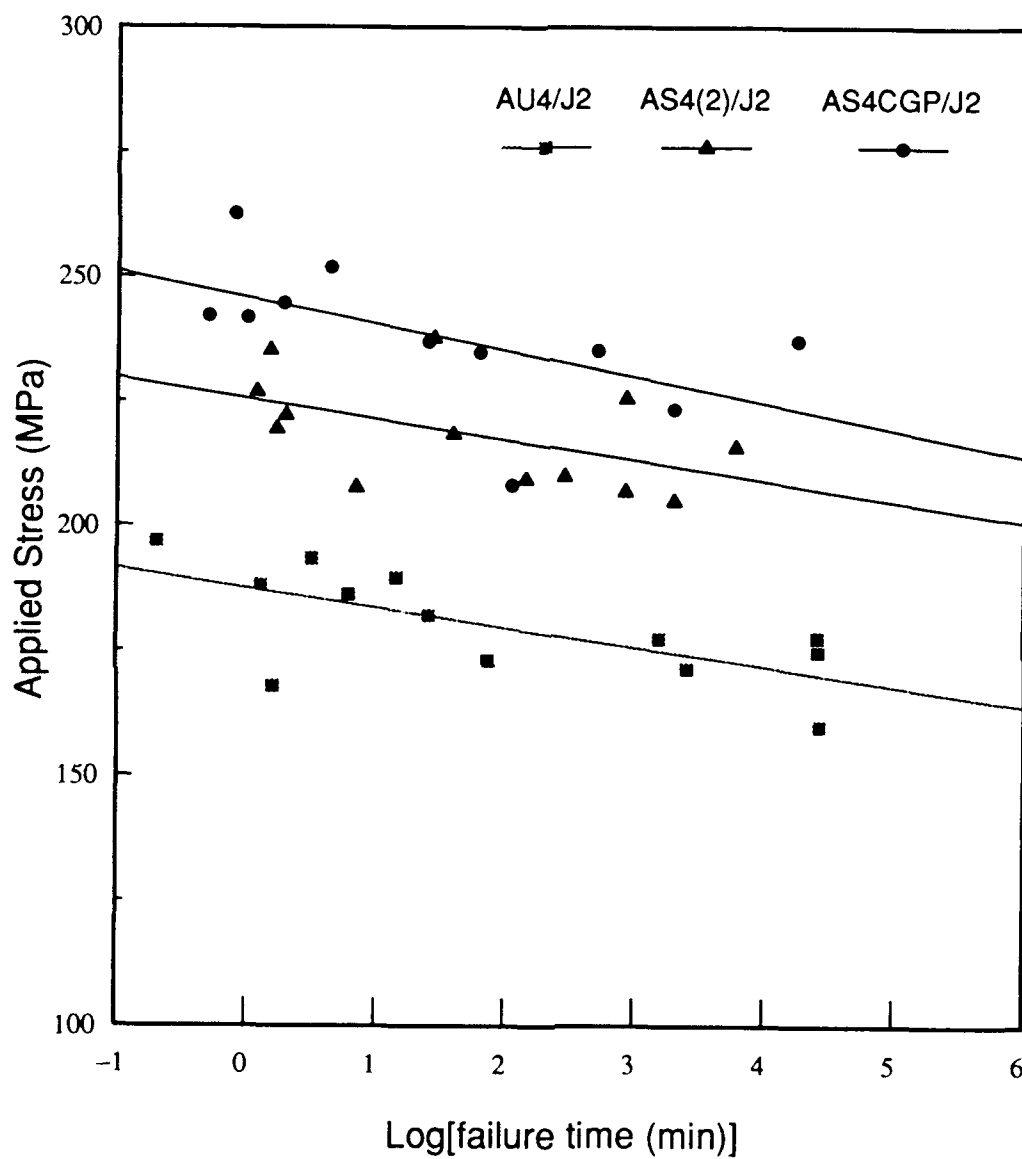
Figure 4. Creep rupture results and least square fit lines for AU4/J2, AS4(2)/J2, and AS4CGP/J2 laminates ([± 45 90₂]ₛ), at 120°C.
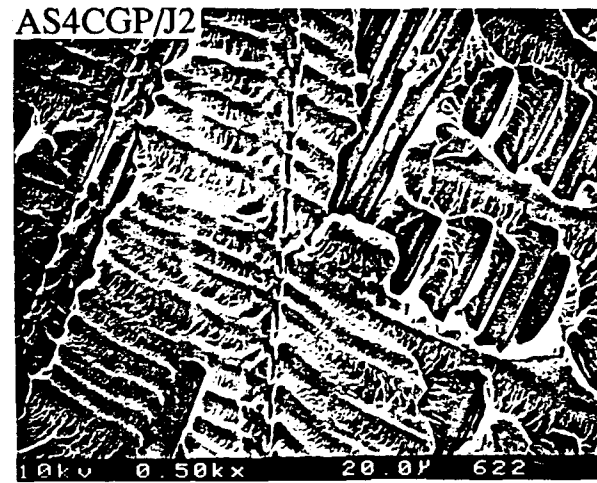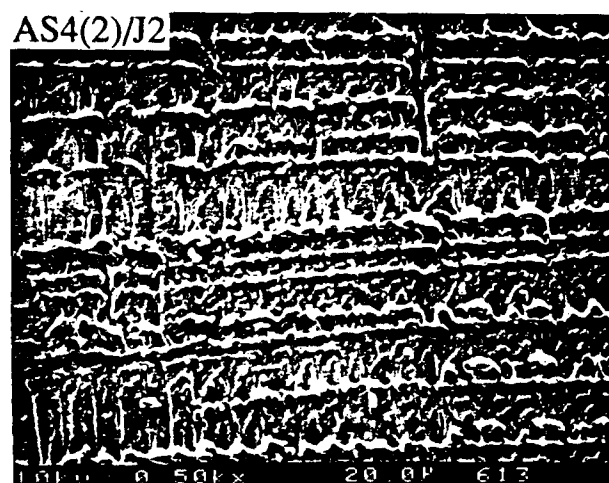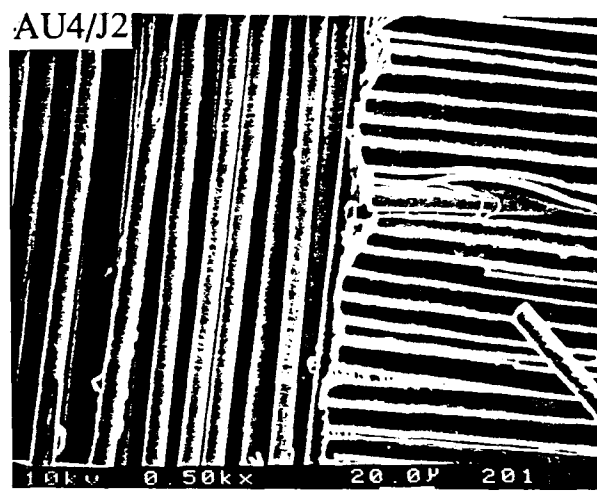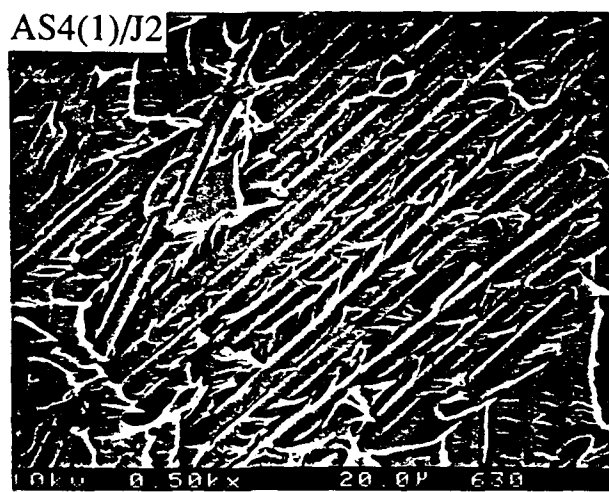
Figure 5. SEM photomicrographs for the fractured specimens with intermediate creep rupture life.

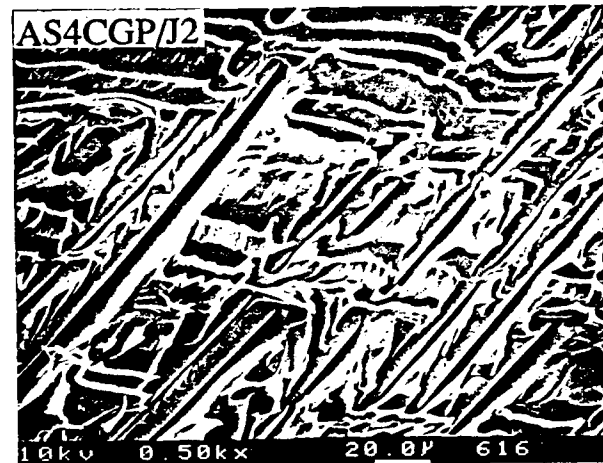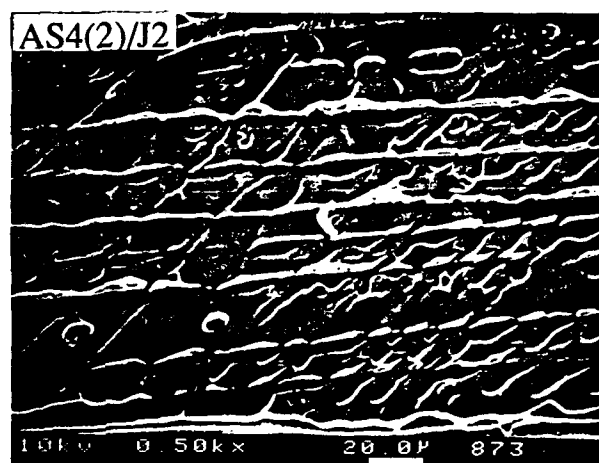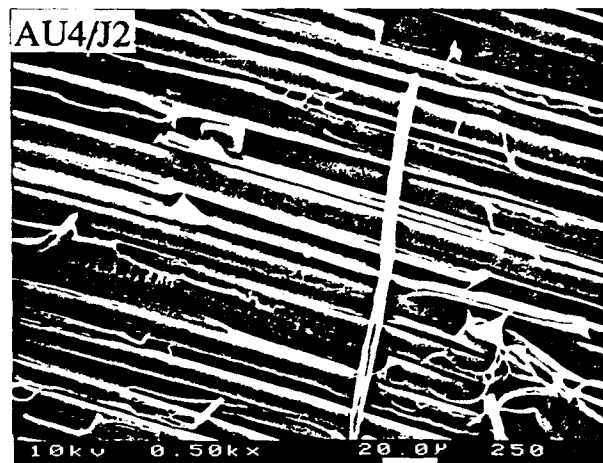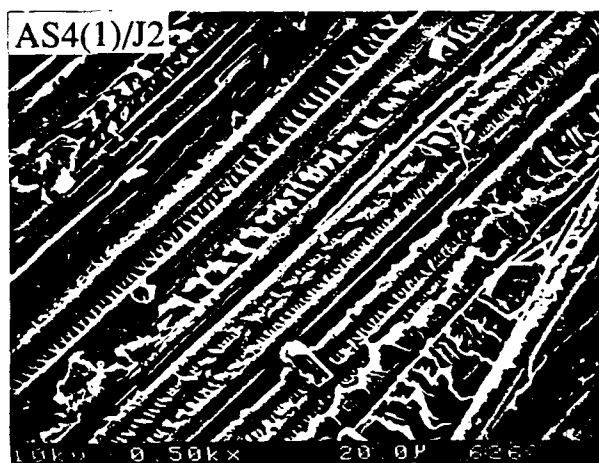4. The Effect of the Interphase/Interface Region on Creep and Creep Rupture of Thermoplastic Composites

120

Figure 6. SEM photomicrographs for the fractured specimens with long creep rupture life.

4. The Effect of the Interphase/Interface Region on Creep and Creep Rupture of Thermoplastic Composites

5. The Meso-Indentation Technique

John J. Lesko, Kenneth L. Reifsnider and David A. Dillard

Introduction

Meso-indentation testing of composite materials has proven to be sensitive to the fiber/matrix interfacial quality of continuous fiber composites [1]. These indentations differ from the single fiber micro-indentation technique in that a Vickers or 1.58 mm ball penetrator is used to contact a relatively large region of fiber and matrix as shown in Figure 1. The indentations are produced by pressing the penetrator into the surface of a composite with fibers oriented along the axis of punching. Both the Vickers diamond pyramid and ball indenter geometries show good sensitivity to the interfacial quality [2]. Likewise, the fixed load technique (Vickers) and the Continuous Ball Indentation Test (CBIT) are capable of generating reproducible measures of relative bond quality, at the very least.

The CBIT has shown great promise for quantitative assessment. In this technique, the load and indenter penetration depth are recorded during the course of the indentation. Thus, an elastic, and/or elastic-plastic responses can be measured. This allows for the detection of the onset of damage (i.e. nonlinear response). A residual impression resulting from the ball contact in the weak interface composite of AU-4/Epon 828 mPDA is shown in Figure 2. Such indentations contact many fibers and their surrounding matrix over a region roughly 300 to 600 microns across. The residual depth is $\simeq 10$ microns. Figure 2 clearly reveals the interfacial failure in the form of rings. The central ring of failure was observed following an initially elastic response. The onset of this nonlinearity is believed to be the result of interfacial failure. Other experimental and analytical studies suggests this to be the case [1]. It is at this elastic limit that a maximum applied indenter pressure is achieved. Having not reached this Maximum Mean Hardness Pressure (MMHP), the composite responds elastically and no residual damage to the surface is observed.

A study was undertaken of a graphite/Epon 828 mPDA composites which possessed the same fiber and matrix, with a systematic alteration to the fiber surface chemistry. The composite systems were provided by the Composite Materials & Structures Center of Michigan State University and were characterized by Madhukar and Drzal [3-5]. The meso-indentation studies revealed that the maximum applied indenter pressure, i.e. MMHP, correlated with the interfacial shear strength (ISS) obtained from a single fiber fragmentation test (SFFT). As the strength of the interface significantly affects the laminate strength under virtually all states of stress, preliminary CBIT results also suggest correlations to laminate performance in shear and compression. (The compressive failure mechanics of composites are highly dependent on the shear transfer characteristics at the fiber-matrix

interface.) For instance, the compression strength from IITRI is found to be 150 to 200% of the MMHP. The laminate shear strength is observed to be roughly 10 to 20% of the MMHP. Recent investigations of subsurface damage reveal repeatable and characteristic deformation modes directly related to shearing at the interface/interphase, as shown if Figure 3. The scanning electron micrograph reveals the formation of a kink band in the zone of maximum shear predicted by the elastic contact analysis. Within this band, the fiber-matrix bond is failed. The phenomena depicted in Figure 3 is repeatable and is independent of the contact diameter and penetrator size used. This leads the author to believe that the kinking situation is an initiation phenomena related to the observed nonlinearity in the indentation response, i.e. MMHP.

The "representative strain to failure," (i.e. the contact strain at MMHP) recorded by the CBIT also appears to provide an indication of the ductility of the fiber/matrix bond. This value appears to closely reflect the state of the interface as affected by surface treatments and sizings. For instance, the unreacted epoxy "C" sizing of the AS-4C/Epon 828 mPDA composite was reported, particularly for the single fiber fragmentation test and laminate shear tests, to embrittle the interphase region [4]. The representative strain response reflects this finding; the AS-4 composite is found to be $\simeq 20\%$ more ductile than the AS-4C composite.

In summary, the author believes that the MMHP can provide a meaningful quantitative representation of the interfacial condition. This assertion is based on the following observations:

1. The representative stress-strain response from the CBIT data is a quantitative representation of the material response under penetration possessing the ability to discern nonlinearities.

2. Characteristic deformation is observed as a result of interfacial failure initiated below the surface at the MMHP.

3. There is evidence that the MMHP correlates to the shearing characteristics reported for the three systems [4].

Thus, with the ability to quantitatively measure the applied stresses and displacements, with the knowledge of when failures/nonlinearities are occurring and the knowledge of what type of failures occur, a quantitative assessments of strength may be made through this technique given an accurate analytical analysis. The analysis in this case must understand how the constituents interact to produce interface failure. Thus, a micromechanical analysis is employed to investigate the interface stress state due to ball penetration.

A Micromechanical Analysis of the Interface Response Under Meso-Indentation

The micromechanics model which describes the response of the interface under an applied ball indenter pressure has been formulated [6]. This "cellular" analysis yields a unique understanding of the state of stress at the interface based on a measurable set of applied conditions. The model provides interface stresses resulting from the ball contact of a composite with the noted orientation for systems which respond elastically. The models' predictions of maximum stresses corroborate the experimental evidence of subsurface (the location is $\simeq 65\%$ of the contact diameter below the surface) interface failure initiated in shear.

The micromechanical analysis of the AU-4 composite's CBIT response returns a maximum interface shear stress of 71.8 MPa/10.4 ksi. We have assumed that the composite responds elastically up to this point. This implies that the fiber-matrix bond remains intact up to this point and no other damage (e.g. plasticity) occurs in the fiber or matrix. This predicted maximum interfacial shear stress is $\simeq 90\%$ higher than the reported value of ISS from the single fiber fragmentation test (SFFT) of (37.2 MPa 5.4 ksi). Herrera-Franco et. al. [7] also reported a value for ISS of 23.44 MPa 3.4 ksi for a micro-bead debond test (MBDT) test on AU-4/Epon 828 mPDA, which is roughly a third of the CBIT assessment. However, when comparing the interface shear stress from CBIT to that obtained from the single fiber micro-indentation test (SFMI) on an actual composite (AU-4/Epon 828 mPDA: ISS = 55.8 MPa 8.1 ksi) [7], the CBIT prediction is only 28% greater. The latter comparison is possibly the most significant in that both are performed on an actual composite and obtain their measure through a micromechanical analysis for the point of maximum elastic interface shear stress. A summarized comparison of this data is presented in Figure 4. We conclude that the single fiber (modeled) system tests provide a somewhat lower assessment of the ISS. Verpoest [8] suggests that with an improved shear lag analysis, the ISS measured from the SFFT based on Kelly's shear lag model (used for the values reported here [6]) is low. Correcting this value based on this assertion would provide better agreement with the interface measurements obtained by the composite interface test techniques (i.e. SFMI and CBIT).

Nonetheless, we see that different tests provide different values of ISS due to differences in specimen construction, method of load introduction, as well as understanding and interpretation of the interface stress state. Thus, no direct comparison can be made. However, the one distinction that can be made is through the interpretation of the value and how it can be used. The CBIT test provides an average measurement of numerous interfaces within an as-manufactured composite containing the representative fiber arrangement, morphology, etc. This may be quite important in that the surface treatments and sizings applied to carbon fibers are not uniform along their length, or possibly, about their diameter [9]. Therefore, we suggest that the CBIT may reflect a more representative measure of the interface properties in an actual composite.

Comparison of Meso- & Micro-Indentation Techniques

Preliminary comparisons of micro- and meso-indentation techniques on material cut from close proximity (within a 50mm square laminate) reveals a discrepancy. In Figure 5, the normalized bond strength from the two techniques are plotted against the laminate's performance in shear for comparison purposes. We clearly see that the meso-indentation technique is capable of sensing the differences in fiber surface conditions introduced on the graphite Epon 828 mPDA systems. However, the SFMI technique shows limited sensitivity and a reversal in the relative bond quality between AU-4 and AS-4 composites. These discrepancies may be related to the differences in location of failure and the criteria set for determination of interfacial failure during the course of indentation. This investigation is however not exhaustive and continues. Regardless, we see the possible advantages of the meso-technique: simplicity and the sampling of many interfaces over a relatively short period of time. Nonetheless, both techniques maintain particular value in the understanding of how interfacial conditions manifest themselves in as-processed laminated composites.

Summary & Remarks

This introductory investigation into composite indentation testing reveals results which are very promising for future applications of these and similar techniques. Meso-indentation testing could potentially provide an inexpensive and efficient means of performing, at the very least, comparative studies of interfacial quality. Experimental and analytical work suggests that the ball indentation testing is most sensitive to the shearing characteristics of composites. The CBIT possess the greatest potential for making quantitative measures of interfacial bond strength. This method possesses the advantage of simplicity and the capability of probing many interfaces in an as-fabricated laminated composite from one indentation. Further work is underway to explore the application of the meso-indentation technique to measuring interfacial properties in ceramic and thermoplastic systems.

Meso-Indentation Studies on Various Materials

The Interface and Creep Rupture of Thermoplastic Composites

Yeou-Shin Chang of the Materials Engineering Science Program has initiated a study of the effect that the interfacial quality has on the creep rupture properties of carbon fiber/thermoplastic laminates [10]. J2, an amorphous thermoplastic, was film prepreged onto AU-4, AS-4 and AS-4CGP carbon fiber by DuPont and formed into laminates at the VA Tech fabrication laboratory. (The AS-4CGP fiber is the AS-4 surface treated fiber with a waterborne unreacted unknown epoxy sizing deposited on its surface.) Mr. Chang relied on the meso-indentation technique to quantify the quality of the interface. A summary of the meso-indentation results and laminate test performed by Mr. Chang are summarized in Table 1. It was found that the surface treated fiber provided an increase in the MMIIP of about 25% over the untreated AU-4 fiber. The addition of a the CGP sizing appeared to provide no improvement in shear or transverse static strength properties. It is the opinion of the author that due to the inert nature of the thermoplastic-epoxy sizing interface, no advantage in shear transfer properties are gained. This sizing may, however, produce a boundary which can blunt cracks or relieve stress concentrations as evidenced by the significant increase in tensile strength for the AS-4CGP composite. The electrochemical surface treatment strips off the weak boundary layer present on the AU-4 fiber, thus producing a surface which readily bonds (mechanically and possible chemically) to the carbon fiber. This interface allows for a notable improvement in off axis strength, laminate level properties.

From the above results Mr. Chang was able to show that with these distinctly different interfaces, the creep rupture rate was not affected. However, the creep rupture strength was affected and shown to be consistent with the static tensile strength results.

Powder Prepreging Process and its Affects on Graphite/LaRC TPI Interfaces

The greatest obstacle to the use of high performance thermoplastics in composites is the processing difficulties experienced with higher T_g matrix systems. Although these composites would eliminate

the need for the hazardous chemicals used in epoxies and present solvent-based thermoplastic prepreging processes, the present hotmelt techniques are too costly. Thus, Dr. Rick Davis and student Ta-Hua Yu of the Chemical Engineering department have begun a unique investigation into powder pregreging of thermoplastics by a aqueous suspension process. However, one of the primary concerns is the state of the interface for such systems produced in the presence of water. Thus, it was through an interdisciplinary effort that the meso-indentation test sought to study the interfacial quality of these composites.

Initial studies were undertaken on five systems whose prepreg and laminate fabrication processes were carefully monitored. The panels produced by Mr. Yu were manufactured via the conditions tabulated [11] in Table 2. The panels were found to possess good fiber distribution, fiber volume fractions of about 60% and relatively low void content. All five composites were supplied to the author blind and meso-indented. Reviewing the MMHP's measured (see lower portion of Table 2), the repeatability of the technique was demonstrated in comparing panels 2 and 3. Notice that these two panels are essentially identical and yield MMHP's which are very close. This finding is significant in that we are beginning to see the accuracy and precision which this technique allows.

The question of interface quality was answered in this study through both the meso-indentation results and scanning electron microscopy. The indentation responses showed a significant portion of nonlinear behavior prior to failure of the interface, suggesting good bonding (i.e. enough bond strength so as to yield the matrix). Likewise the MMHP's for all five systems were high and considered typical of composites with significant fiber-matrix bonding. It has been the experience of the author that MMHP below 60 ksi normally indicate weak bond quality. The SEM's of residual impressions best show what was learned form the indentation responses. In Figure 6 the presence of good bonding is evidenced by the ability of the deformed fiber to hold onto the matrix and permanently deform the polymer.

These findings have allowed Dr. Davis and Mr. Yu to quantitatively evaluate their progress for future investigations. With the importance of the interface conditions and their affects on the laminate level performance a technique like this has proven useful in understanding processing conditions for powder prepreging. The meso-indentation technique has assisted their study as a simple and inexpensive means to quickly survey a number of processing conditions for the ones most appropriate for their needs. Presently, Dr. Davis and Mr. Yu have settled on the optimum conditions based these finding and supplied four additional systems for future evaluation by meso-indentation.

The Role Interfacial Quality Plays in the Fatigue Performance of Polymeric Composites

The Air Force Office of Scientific Research has undertaken a comprehensive study of fiber-matrix interfacial properties and their effects on the performance of aerospace structural materials. Over twenty systems have been assembled by the Northrop Corporation and the McDonnell-Douglas Aircraft Company (McAir) to assess the optimum fiber-matrix combinations and interfacial conditions for satisfying the demanding design requirements for both commercial and fighter aircraft structural composite materials. The fourteen graphite polymeric systems obtained by the Materials Response Group (MRG) are summarized in Table 3. These systems consist of various combina-

tions of different fibers (varying in strength and stiffness) and matrices (standard and toughened thermosets, as well as thermoplastics). More importantly, the interphase face is altered through combinations of proprietary surface treatments and sizings. Both companies have devoted nearly three years to characterizing their particular systems for static laminate level performance as well as single fiber chemical and mechanical parameters important to understanding composite micro-mechanics.

Dr. Robert Swain of the Engineering Science and Mechanics Department has undertaken a study of the above materials "to determine the influence of the fiber matrix interphase on the fatigue behavior of the host laminate" [12]. (See section 2) Swain is conducting fully reversed (tension-compression) fatigue tests on cross-ply laminates which have been notched by introducing a centered hole. In addition, further characterization of static strength performance and interface quality have been carried out. The meso-indentation technique has been enlisted to characterize the static interphase face quality. A summary of the meso-indentation data has been already been included in an earlier section of this report and comparisons made to other static laminate data. In this section however, additional comments are made on the nature of interfaces, as measured by meso-indentation, which result from surface treatments and sizings for various polymeric systems.

The effects of surface treatments, without sizing the fibers, in thermosetting composites is addressed in Figure 7. With increasing levels of surface treatment the strength of the interface is increased as indicated by the increase in the MMHP. An embrittlement of the interface is inferred from the decrease in the representative strain response with increasing levels of surface treatment. We might postulate that as the quality of the chemical bonding is increased, the stiffer and less ductile this interphase may become.

Introducing a sizing while altering the level of surface treatment for a toughened epoxy yields some very interesting results. In Figure 8 the T850-45 fiber has been treated 20, 50, 100, and 200% with an "A" sizing and an additional system consists of a 100% treatment with an "O" sizing. Focusing our attention on the "A" sized system: an opposite trend is observed for the 20, 50, and 100% systems from that displayed in Figure 7. Upon treating the fiber to 200%, we find that the interface strength is increased per our expectations. However, it appears from these results that the surface treatment affects the stress transfer characteristics of the sizing and the resulting interphase region. This has been suggested by Peters [13] working with an identical system. Thus, the inter-relationship of fiber surface property alteration and the anticipated performance may be more involved than thought. When the sizing is now changed from the "A" to the "O" on the 100% treated fiber the strength is unchanged however the relative ductility of the indentation response is increased by $\simeq 20\%$. Recall that the 810O system outlasted the 810A by two orders of magnitude in cross ply notched fatigue. This is a considerable difference and warrants further investigation. Thus, additional studies are underway using the meso-indentation technique to understand how the interface conditions change or degrade during the course of the materials fatigue life. This work will possibly lead to understanding the evolution of damage which appears to occur at the fiber-matrix interphase face.

In addition to the thermosetting composites, Radel-X systems were also explored with two surface variations. In Figure 9 the meso-indentation results from these two composites and J2 (an amorphous thermoplastic) composites (See section 4), presented for comparative purposes, are detailed. To preface these remarks, carbon fiber surface treatments were intended to enhance adhesion

to epoxy matrix systems [3]. In addition, most amorphous thermoplastics lack the ability to chemically bond to the fiber surface and must rely on mechanical interlocking to constitute bonding. Thus, chemical bonding experienced in thermoplastic composites may possibly be the result of weak forces. We however do see a significant increase in bond quality with the addition of a treatment for both composites. When the unreacted aqueous deposited thermosetting "CGP" sizing is applied to the surface treated fiber no significant increase in interface strength is observed. This is to be expected given that additional chemical bonding is not anticipated between the epoxy sizing and the thermoplastic matrix.

The static meso-indentation results and the long term performance point to some very critical yet complex relationships which exist between interface quality and laminate level performance. In addition, the data base assembled in this investigation is important, by itself, to the future understanding of polymeric composite interphases/faces. Given public access to this data, these results will be critical to designing materials from to constituents (fiber and matrix) and sub-constituents (interphases/faces and morphology) levels.

Interface Studies in Ceramic Composites

Mr. Steven Lee of the Department of Engineering Science and Mechanics has begun a study of the interfaces which exist in continuous fiber ceramics composites [14]. Mr. Lee has qualitatively shown that post processing heat treatments in atmosphere increase the bonding between fiber and matrix. Presently his studies involve understanding how the interphase evolves due to the heat treatments and what effects they have on interface strength. To assist in these efforts the meso-indentation technique is performed to discern its applicability to ceramic systems.

A tungsten carbide 1.58 mm ball indenter was required to perform the tests due to the high hardness of the ceramic fibers. Slightly different polishing procedures were needed to ensure a smooth and uniform surface upon which to indent; a suitable process was found by Mr. Lee. The load versus indenter penetration responses were similar to those for polymeric composites as shown in Figure 10. In all cases the onset of non-elastic response was identifiable (load = 8.5 lbs./18.7 kg, depth = 0.0006 in. 0.015 mm). A typical representative stress strain plot for the ceramic indent reveals this as well. The plateau at a MIIP of $\simeq$ 65 ksi 450 MPa, beginning at a d/D of 0.23, in Figure 11 shows the nonlinear response quite clearly. The damage associated with this response is interfacial failure depicted in Figure 12. However, the character of the damage is somewhat different from that of the polymeric composites. The scanning electron micrographs reveal a central region of fibers which are secured below the original level of the matrix. Also there is a ring of fiber, outside this central region, that reside above the matrix. It is also important to point out that no damage appears to have been induced to the fiber or matrix. This considerably simplifies the analytical modelling of the phenomena. The interface remains the only region to which a failure criteria must be applied. Assuming a linear elastic response of the constituents, a model may be developed which can determine the stresses which produced the failure.

This study has shown that the meso-indentation technique may also be useful in determining interface properties in ceramic systems. A future investigation is underway to determine if the CBIT is sensitive to various interface conditions. Samples will be heat treated at various temper-

atures to alter the level of fiber- matrix adhesion. These systems will subsequently be tested by meso-indentation to determine the degree of sensitivity to the interfacial quality.

References

1. J.J. Lesko, "Indentation Testing of Composite Materials: A Novel Approach to Measuring Interfacial Characteristics and Engineering Properties," Masters Thesis, Department of Engineering Science and Mechanics, College of Engineering, Virginia Polytechnic Institute and State University, March 1991.

2. J.J. Lesko, G.P. Carman, D.A. Dillard, & K.L. Reifsnider, "Indentation Testing of Composite Materials as a Tool for Measuring Interfacial Quality," Composite Materials: Fatigue and Fracture, ASTM STP 1156, in press.

3. M.S. Madhukar and L.T. Drzal, "Effect of Fiber-Matrix Adhesion on the Longitudinal Compressive Properties of Graphite/Epoxy Composites," Proceedings of the Fifth Technical Conference of the American Society for Composites, 1990, pp. 849-858.

4. M.S. Madhukar and L.T.Drzal, "Fiber-Matrix Adhesion and its Effect on Composite Mechanical Properties. I. In-plane and Interlaminar Shear Behavior of Graphite/Epoxy Composites," Journal of Composite Materials, August 1991, pp. 932-957.

5. M.S. Madhukar and L.T. Drzal, "Fiber-Matrix Adhesion and its Effects on Composite Material Properties. II. Tensile and Flexural Behavior of Graphite/Epoxy Composites," Journal of Composite Materials, August 1991, pp.958-991.

6. G.P. Carman, J.J. Lesko, K.L. Reifsnider, D.A. Dillard, "Micromechanical Model of Composite Materials Subjected to Ball Indentation," submitted to Journal of Composite Materials, October 1991.

7. P. Herrera-Franco, W.L. Wu, L.T. Drzal, and D.L. Hunston, "Comparison of Methods to Access Fiber-Matrix Interface Strength," The Adhesion Society, Proceedings, 1991, pp. 21-23.

8. I. Verpoest, M. Desaegkr, and R. Keunings, "Critical Review of Direct Micromechanical Test Methods for Interfacial Strength Measurements in Composites," Controlled Interphases in Composite Materials, H. Ishida, Ed., Elsevier Sciences Publishing Co., Inc. 1990, pp. 653-666.

9. Private Communications with D. Wilson and D. Lynn of BASF Structural Materials, Inc., Charlotte, NC, 1991.

10. Y.S. Chang, J.J. Lesko, D.A. Dillard, and K.L. Reifsnider, "The Effect of the Interphase Interface region on the Creep Rupture of Thermoplastic Composites," ASTM STP, ASTM Symposium on High Temperature and Environmental Effects on Polymeric Composites, submitted for publication, October 1991.

11. Individual communications from Dr. Rick Davis, Department of Chemical Engineering, Virginia Polytechnic Inst. & St. Univ., November 1991.

12. Robert E. Swain, "The Role of the Fiber Matrix Interphase in the Static and Fatigue Behavior of Polymeric Matrix Composite Laminates," Ph.D Dissertation, Department of Engineering Science and Mechanics, College of Engineering, Virginia Polytechnic Institute and State University, Feb., 1992.

13. P.W.M. Peters, and H. Albertsen, "The Fiber/Matrix Interphase in CFRP with a Phase-Separating Matrix System," Proceedings of Interfacial Phenomena in Composite Materials, 17-19 September 1991, pp. 101-104.

14. Individual communications from Mr. Steven Lee, Department of Engineering Science and Mechanics, Virginia Polytechnic Institute and State University, September 1991.

Table 1. Summary of meso-indentation data and selected laminate properties for the A_-4 J2 composites [10].

	AU-4/J2	AS-4/J2	AS-4CGP/J2
MMHP/ISS (MPa)	473/77.2	575.7/~96	582.6/~97
0° Tensile Strength (GPa)	1.612	1.828	1.635
90° Tensile Strength (MPa)	34.2	54.2	48.7
Shear Strength form ±45°Tension (MPa)	94.8	159.8	153.5
Shear Strength from Iosipescu Test (MPa)	44.8	81.9	72.4

Table 2. Summary of processing conditions and selected mechanical data for powder prepreged AS-4/LaRC TPI composites [11].

LARC-TPI COMPOSITES SERIES SUMMARY

panel no.	1	2	3	4	5
carriage movement %	30	55	55	55	55
tension (lb)	.2 to 2	3±.25	3±.25	3±.25	3±.25
prepreg layers	1	1	1	1	2
panel layers	8	16	16	16	8
vacuum bag	no	yes	yes	no	no
v_p% ASTM	61.8	56.4	55.9	57.2	54.4
v_p% optical	70.24	63.04	62.36	65.4	53.23
v_{void}% optical	.86	.46	.44	2.8	.97
MMHP(ksi)	92.7±14.5 82%	74.7±4.5 99%	75.5±8.5 85%	87.3±8.7 99%	83.8±8.7 81%
G_{12}(GPa) Iosipescu	2.85 (3") -------- 2.83 (2")	--------	--------- 3.36	--------	3.28 --------
S_{12}(MPa) Iosipescu	72(3") -------- 84(2")	--------	---------- 81	--------	68 --------

Table 3. List of material systems investigated in the interphase study [12].

Material Systems Obtained from McAIr

Material Type Acronym	Fiber Modulus, Msi	Fiber Strength, ksi	Percent Surface Treatment	Fiber Sizing	Matrix Type	Material Series Acronym
52U	32	550	20	Unsized	T. Epoxy	
55U	32	550	50	Unsized	T. Epoxy	5U
510U	32	550	100	Unsized	T. Epoxy	
82A	45	850	20	"A" sized	T. Epoxy	
85A	45	850	50	"A" sized	T. Epoxy	
810A	45	850	100	"A" sized	T. Epoxy	8A&O
820A	45	850	200	"A" sized	T. Epoxy	
810O	45	850	100	"O" sized	T. Epoxy	

Material Systems Obtained from Northrop

Material Type Acronym	Fiber Modulus, Msi	Fiber Strength, ksi	Percent Surface Treatment	Fiber Sizing	Matrix Type	Material Series Acronym
3NN	35	650	0	Unsized	S. Epoxy	3N
3SN	35	650	100	Unsized	S. Epoxy	
5NN	50	650	0	Unsized	S. Epoxy	5N
5SN	50	650	100	Unsized	S. Epoxy	
3RNN	35	650	0	Unsized	T-plastic	3R
3RSN	35	650	100	Unsized	T-plastic	

Figure 1. Indentation testing of unidirectional continuo̶ ̶ber composites.
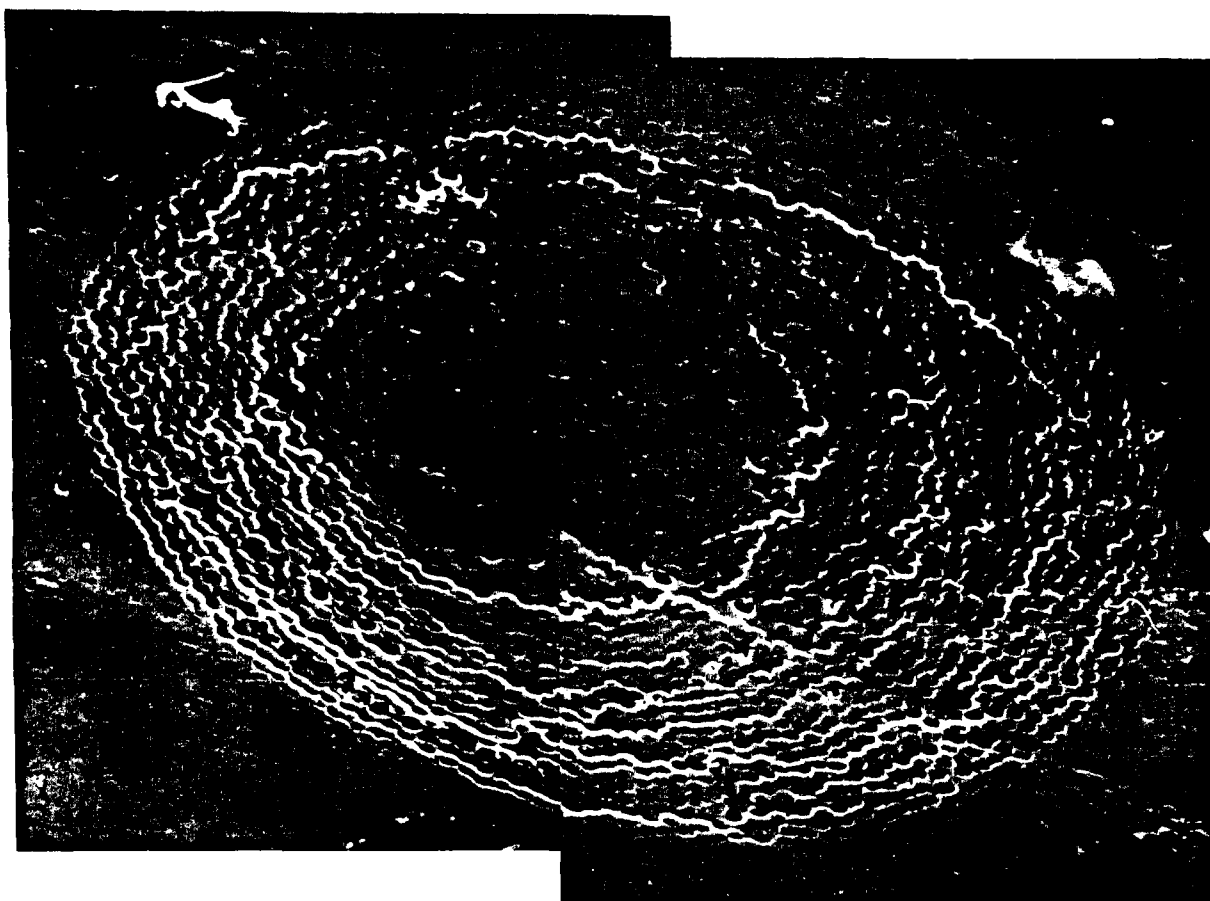
Figure 2. SEM of a residual ball impression in AU-4/Epon 828 mPDA, a weak interface system.
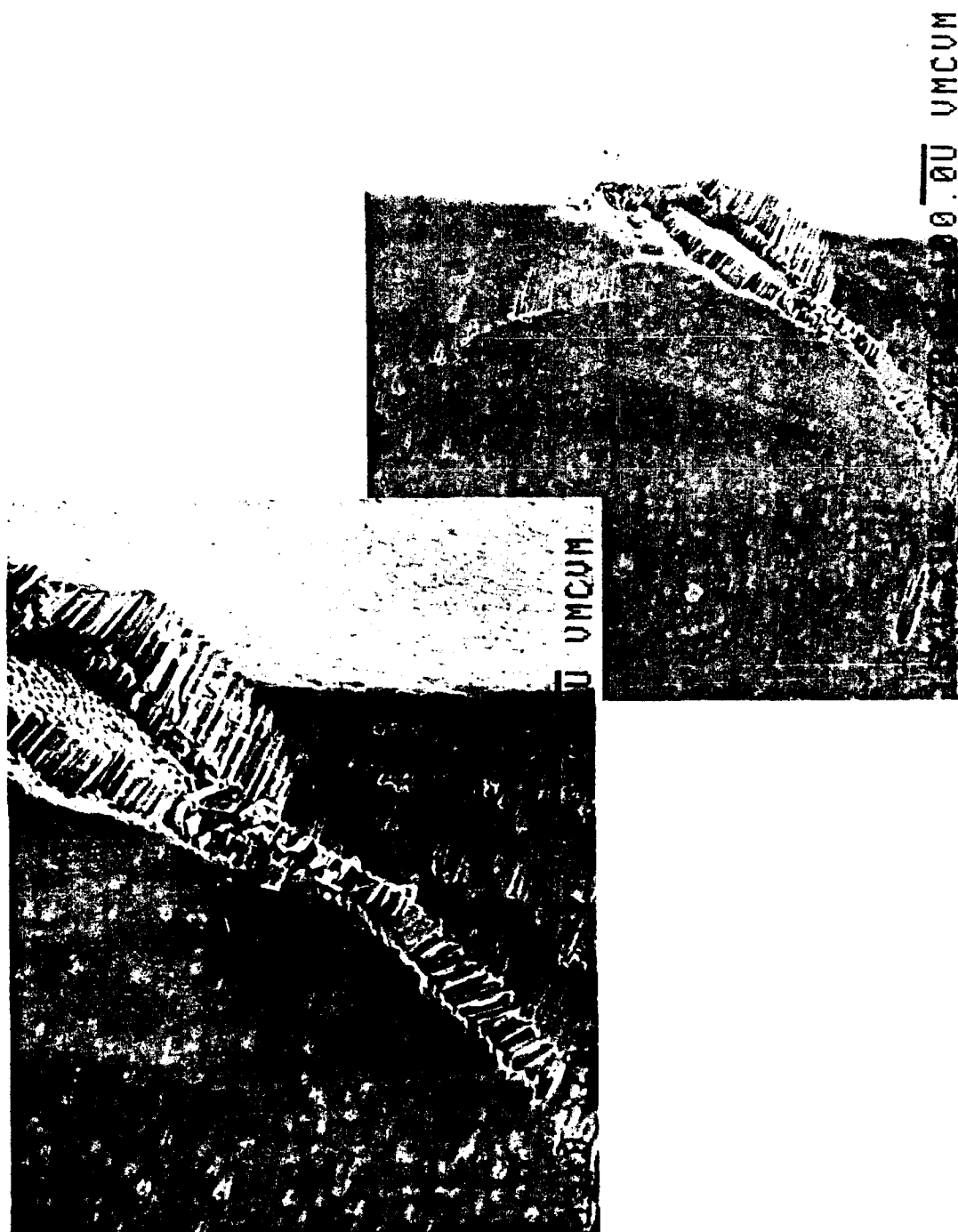
Figure 3. SEM of a subsurface kinkband initiated by ball contact of the composite.
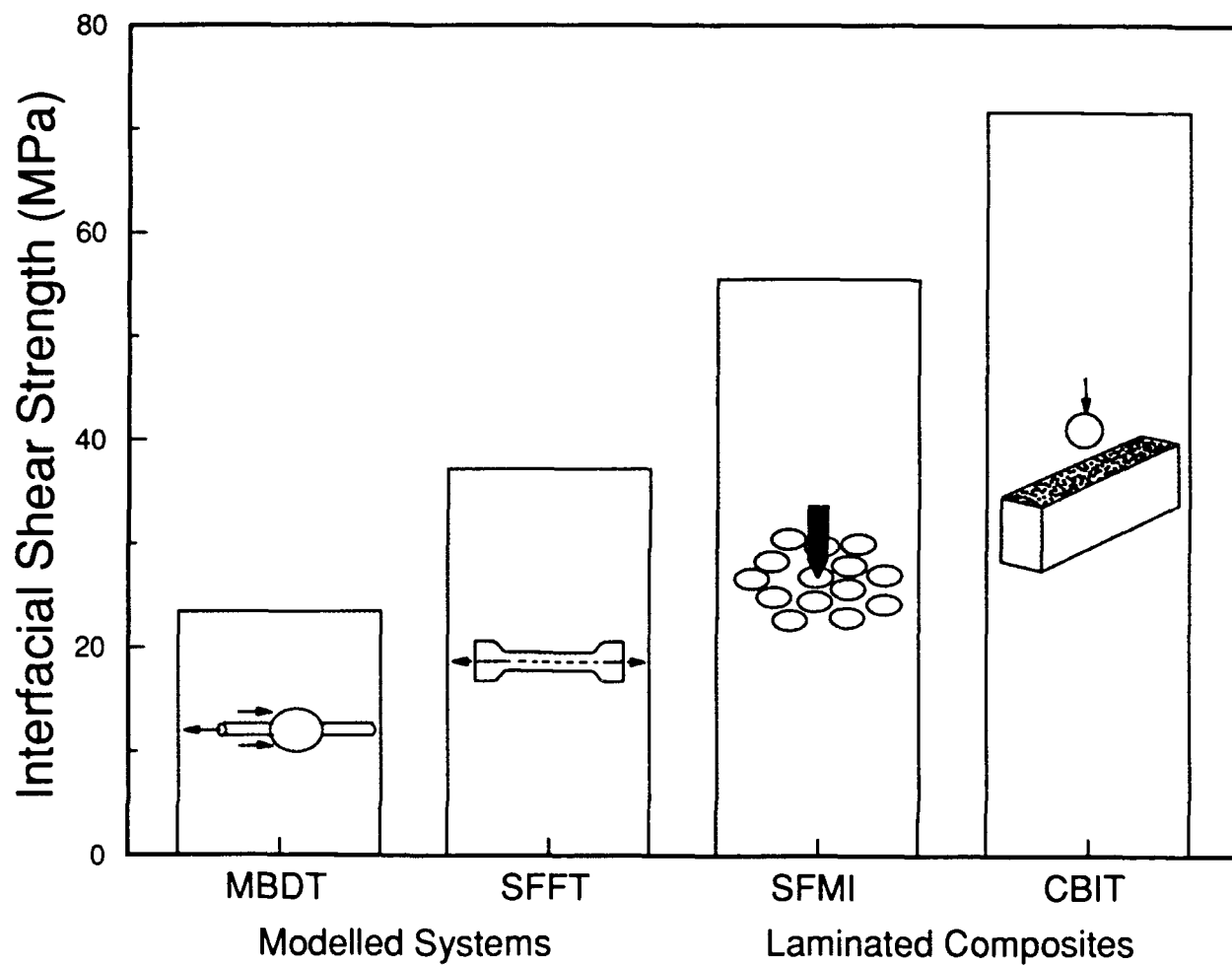
Figure 4. Comparison of ISS measured on AU-4/Epon 828 mPDA composite from four techniques; MBDT, SFFT, SFMI, and CBIT.
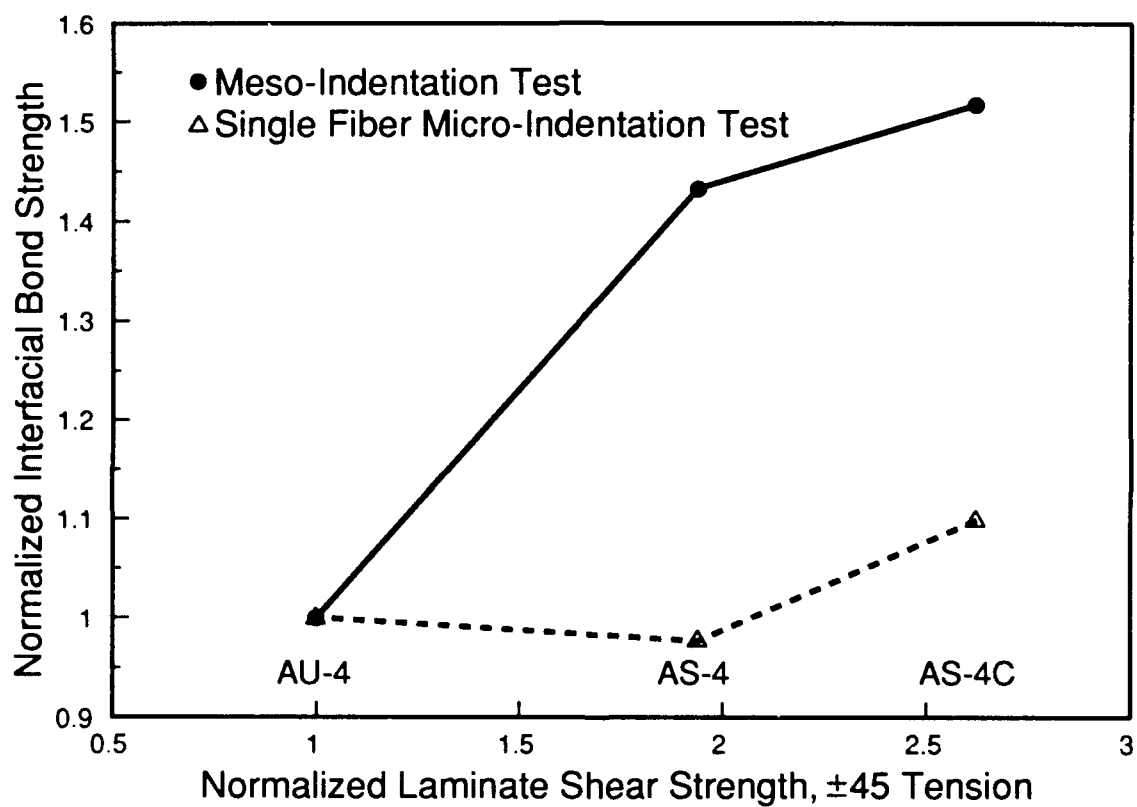
5. The Meso-Indentation Technique

Figure 5. Comparison of interfacial bond quality by micro- and meso-indentation methods on AU-4, AS-4, & AS-4C composites.
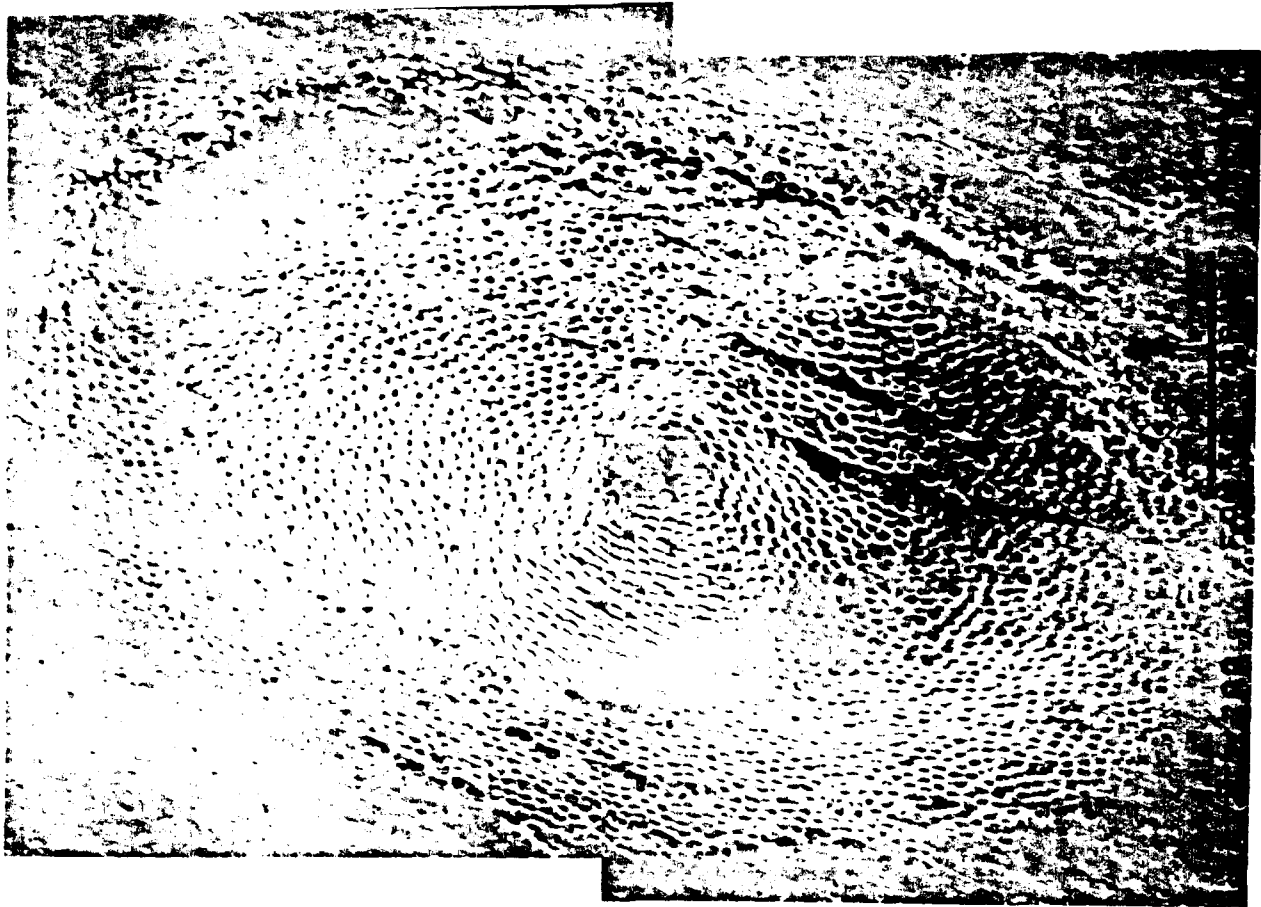
Figure 6. Scanning electron micrograph of a residual indentation typical of the AS-4 LaRC TPI composites.

Meso-Indentation of Epoxy Systems
The Effect of Fiber Surface Treatment
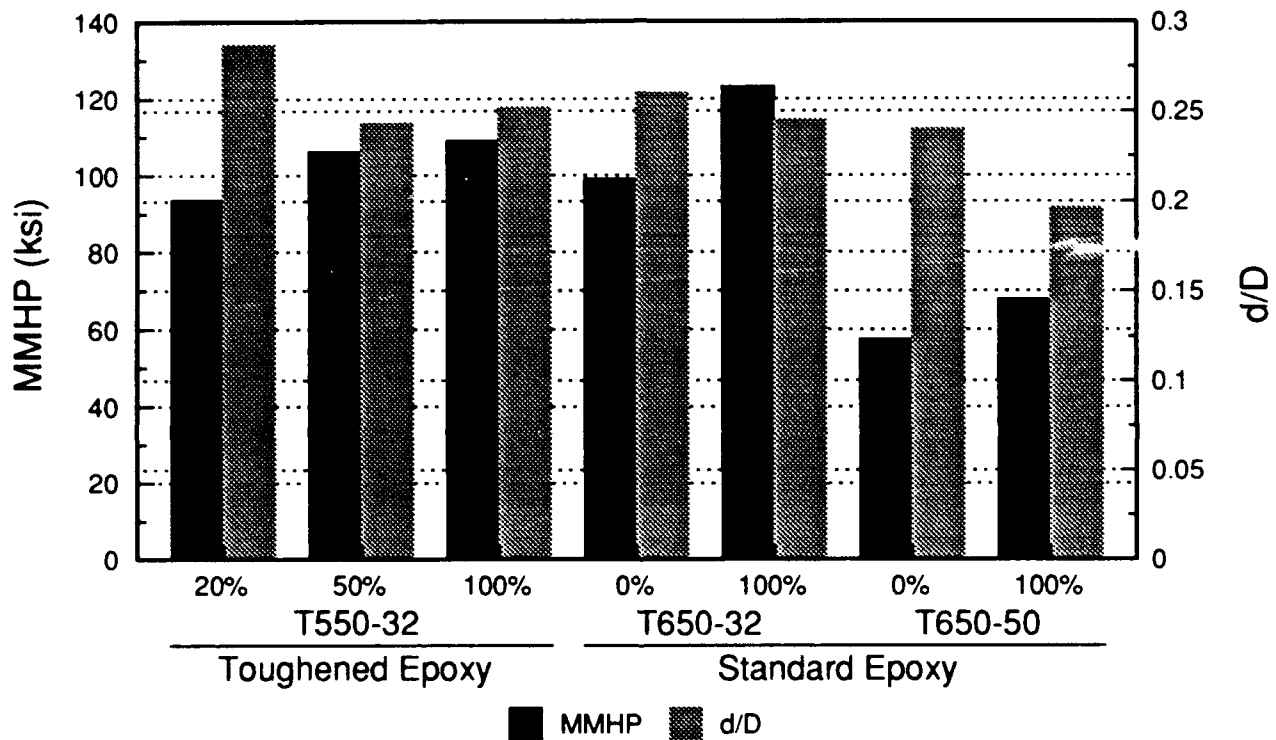
Figure 7. The effect of fiber surface treatment on interface properties of epoxy composites as measured by the meso-indentation test.

Meso-Indentation of Epoxy Systems
The Effects of Fiber Surface Treatments & Sizings
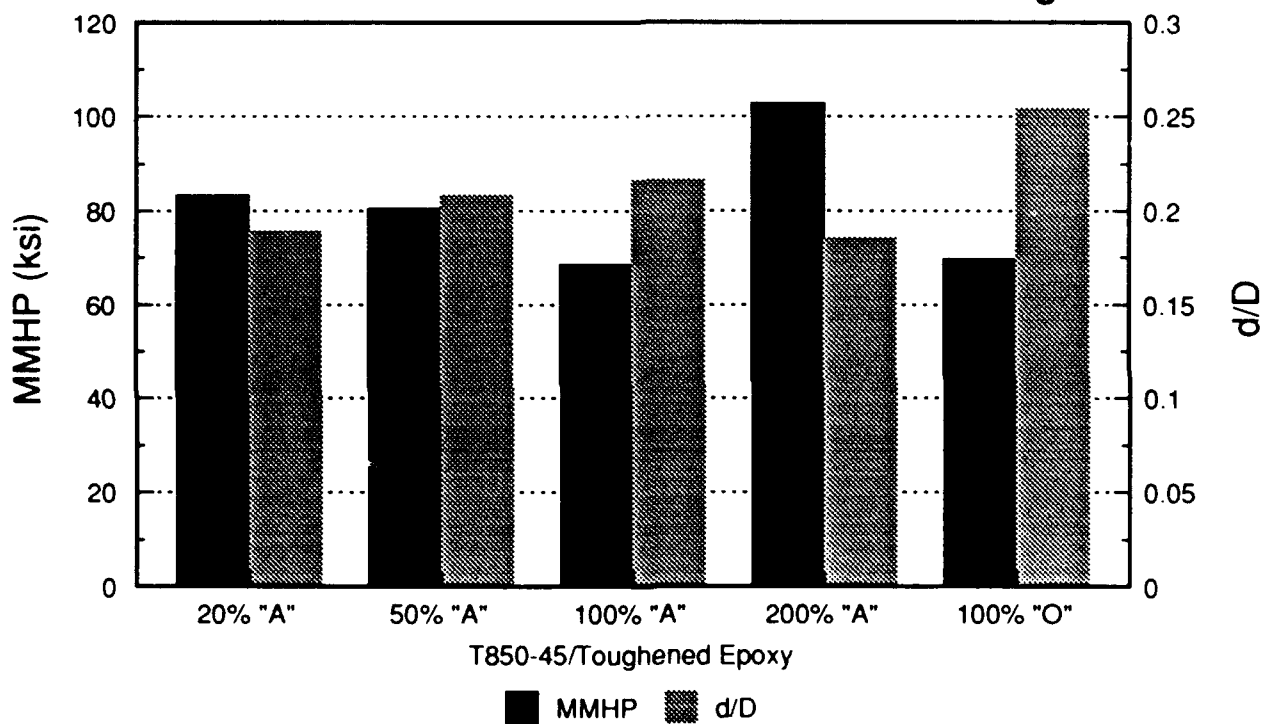
Figure 8. The effect of surface treatments and sizings on the interface properties of epoxy composites as measured by the CBIT.

Meso-Indentation of Thermoplastic Systems
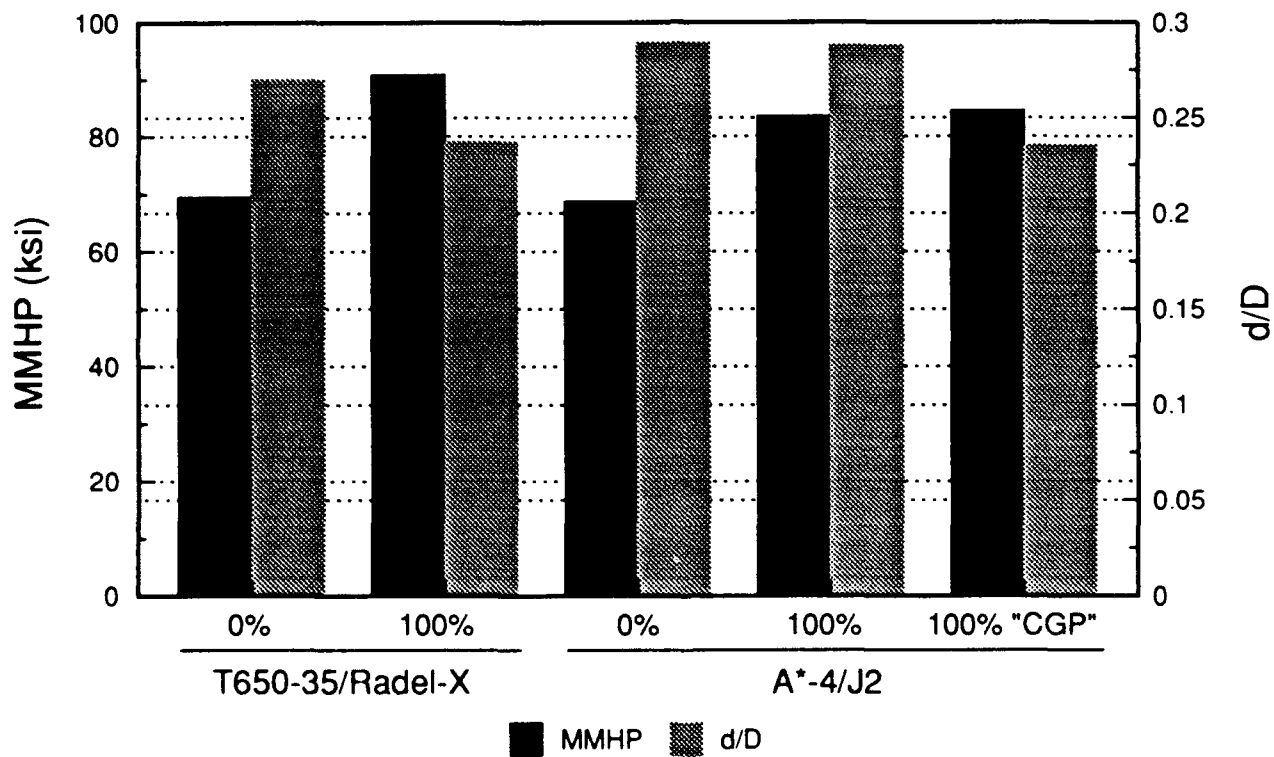
Figure 9. The effect of surface treatments and sizings on the interface properties of thermoplastic composites as measured by CBIT.
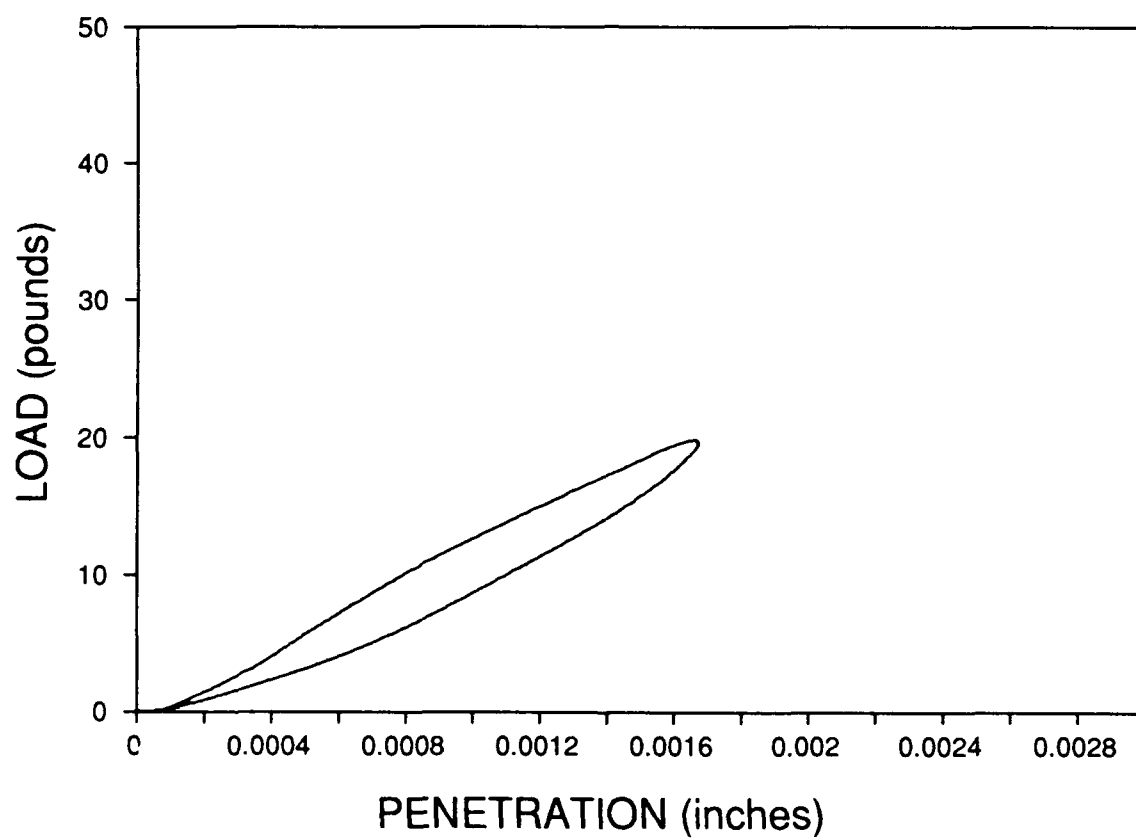
Figure 10. A typical load verses indenter penetration response for the CBIT of a continuous fiber ceramic composite.
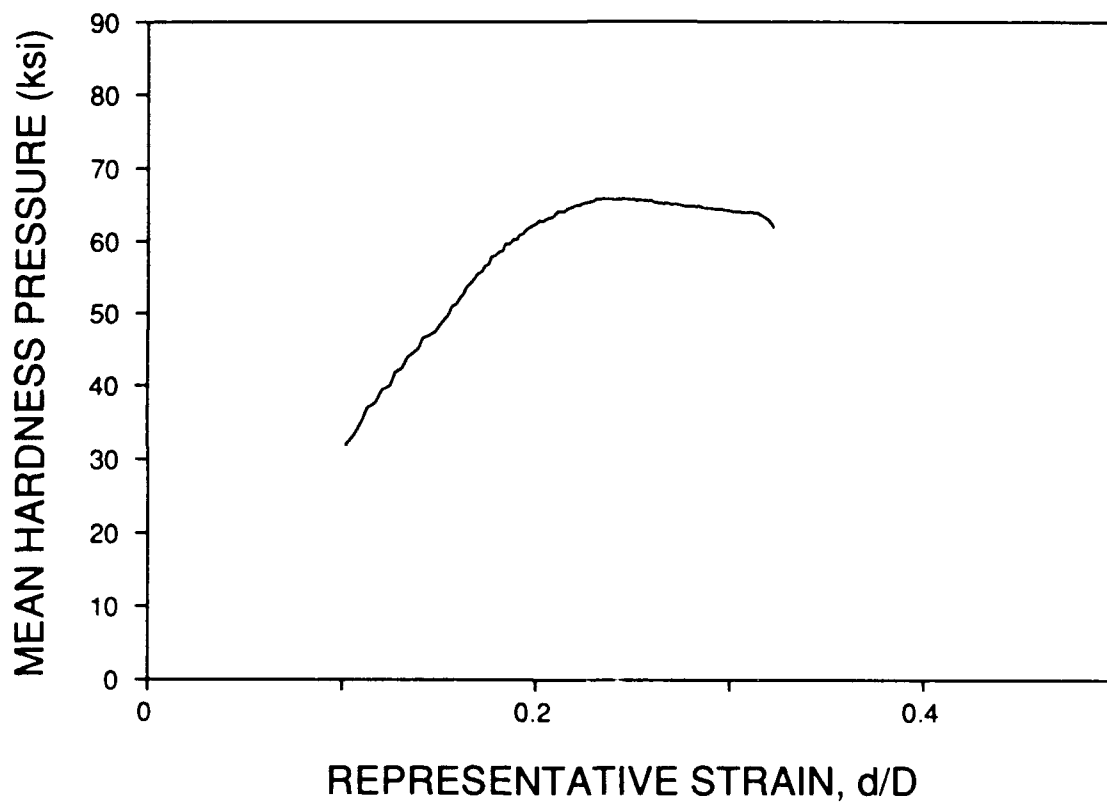
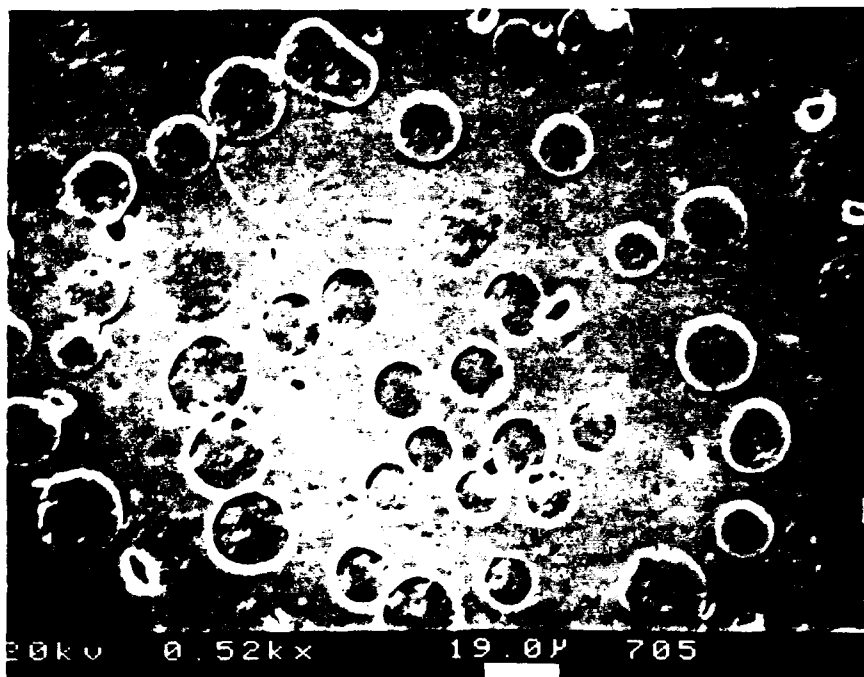Figure 11. A typical representative stress-strain response for the meso-indentation test of a ceramic composite.
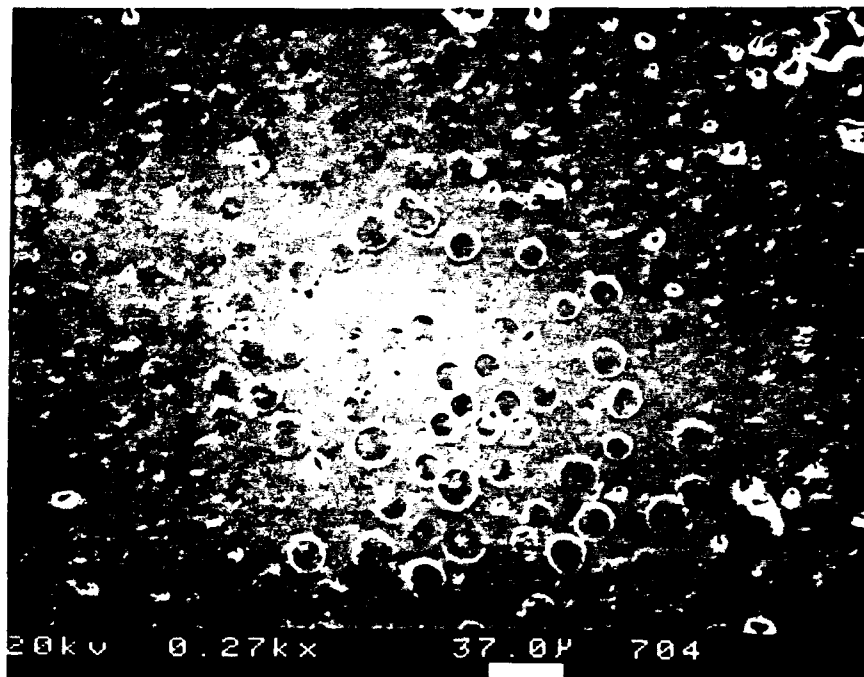
Figure 12. Scanning electron micrographs of residual impressions resulting from meso-indentation [14].

CHARACTERIZATION of COMPOSITE MATERIALS DYNAMIC RESPONSE USING LOAD/STROKE FREQUENCY RESPONSE MEASUREMENT

M. Elahi , A. Razvan, K.L. Reifsnider[1]

Materials Response Group
Department of Engineering Science and Mechanics
Virginia Polytechnic Institute and State University
Blacksburg, Virginia

ABSTRACT

A new experimental technique was developed to characterize damage development in composite materials. The technique does not require interruption of the test. It utilizes the frequency response measurement of load/stroke signals to characterize fatigue damage in terms of parameters such as phase and gain. Test frame and frequency dependency of the method was investigated. Center—notch quasi—isotropic and unidirectional specimens were fatigue cycled at various load levels. From the fatigue test results, it was found that gain is related to the total damage and phase may be related to the rate of damage in the specimen. Results also indicated that the method was sensitive to the applied load level and the material systems. This technique might be able to overcome problems involved in fatigue damage characterization of unidirectional laminates during high temperature testing of composites where extensive splitting and elevated temperatures limit the use of extensometers.

Key Words, Phase lag. gain. unidirectional laminate. quasi-isotropic. fatigue. stiffness. dynamic response.

[1] Graduate Research Assistant. graduate project assistant. Alexander Giacco professor respectively. Materials Response Group. Engineering Science and Mechanics. Virginia Polytechnic Institute and State University. Blacksburg. VA 24061-0219.

INTRODUCTION

Failure modes of composite materials are complicated and generally different from those of metals. Unlike most isotropic materials where a single crack is the dominant mode of failure, in composites fatigue damage is extensive and is spread throughout the specimen volume. In composites micro—cracks may be initiated at an early stage of loading, but the materials can sustain the load until final failure after many additional cycles of loading [1,2].

Fatigue failure can occur if the residual strength of material degrades to the level of applied load [3]. This degradation can be caused by matrix cracking [4], delamination [5], fiber fracture [6], and interfacial debonding [7]. Any combination of these may be responsible for fatigue damage, which may result in reduced fatigue strength and stiffness [1-7]. Material properties, specimen geometry, stacking sequence, waveform type, loading waveform frequency, loading mode, loading rate, time, and temperature are some of the variables critical in any fatigue study or service environment [8-12]. Variation in any of these variables could result in different damage evolution mechanisms and processes.

The state of damage is related to the three most important engineering material characteristics: stiffness, strength, and life. In general, stiffness is related to damage in a deterministic fashion. Therefore, stiffness loss, which is often large and easily measured, can often provide a basis for the characterization of fatigue damage or rate of damage development [13-15]. The most common technique for measuring stiffness change is by means of an interrupted fatigue test. Fatigue cycled specimens are typically stopped at various stages of life and loaded quasi—statically to measure their stiffness. This procedure is repeated during the life of specimen. The end result is a relationship between the static stiffness degradation and the stage of life. Due to the static nature of this measurement technique, important information is neglected using this method. Every time the test is stopped, the initial conditions to this forced vibration problem are altered [16]. In order to fully understand the fatigue behavior of materials as a function of stiffness change, it is desirable to monitor the dynamic response of the specimen continuously in real time.

Several investigators have utilized dynamic stress—strain signals in order to characterize fatigue damage development by measuring phase and stiffness where the phase values are obtained either from direct measurement at the zero—crossing po'': of signals [16], or by constructing a hysteresis loop [17-18]. This procedure requires use of an extensometer or an attached strain gage to measure strain. In high temperature or high frequency fatigue tests, there is always the possibility of extensometer slippage [16], and it is difficult to attach any strain measurement device to a specimen inside a furnace. Another shortcoming of an extensometer procedure is in the fatigue testing of unidirectional materials. These fatigue tests may cause a great deal of matrix splitting on the specimen surface which, in turn, limits the use of an extensometer by disrupting the position of the extensometer contact points.

So has developed a free—vibration technique for the measurement of material damping under periodic—chirp excitation [19]. Using an experimental arrangement similar to that of So, in the present case a new experimental technique is developed to resolve the aforementioned problems. Based on this technique, a new approach to the interpretation of fatigue behavior is proposed. This method utilizes the load and stroke signals from a servo—hydraulic test machine to measure quantities such as phase lag and gain[2], for measuring damping and compliance, respectively. Even though a thorough understanding of these dynamic parameters is not at hand, our preliminary results indicate a good correlation between stiffness degradation, phase, and gain response measured in this fashion. If this is true, this technique could be a valuable tool for the dynamic evaluation of composite parts under conditions in which a change of strength, stiffness, and life must be monitored and interpreted in terms of durability, damage tolerance, etc.

---

[2] Gain is defined as the ratio of the magnitude (amplitude) of a steady—state sinusoidal output relative to the causal input; the length of a phasor from the origin to a point of the transfer locus in a complex plane [22].

EXPERIMENTAL PROCEDURE

In order to characterize the phase and g?'n functionals, four different servo—hydraulic test frame units were used. This was in conjunction with two different material systems (described below). As listed in Table 1, units 3 and 4 have the same load frames, while having different hydraulic grips. Units 2 and 3 have the same hydraulic grips but different load frames. Unit number 1 was unique, and did not have any common features with the other units. It is believed that through such a test arrangement, the effect of griping, load frame characteristics, signal conditioning as well as amplifiers could easily be identified and determined.

Different material systems were fatigue cycled (tension—tension, $R = 0.1$) under load—controlled using MTS servo—hydraulic testing machines at a frequency of 10 Hz under a sinusoidal waveform. Notched specimens made of Hercules AS4 fiber and American Cyanamid's Cycom 985 matrix with an stacking sequence of $[0/45/90/ - 45]_{s2}$ were used. Thin adhesive interlayers measuring 12.7 μm (0.0005 in.) in thickness were placed between each layer and on one of the outside surfaces. These specimens had an average length of 139.7 mm (5.5 in.), width of 25.4 mm (1.0 in.), thickness of 2.461 mm (0.0969 in.), and a 6.35 mm (0.25 in.) diameter hole at the center [20].

Also, eight ply unidirectional coupons made of Hexcel's graphite/epoxy prepreg with a layer of release cloth (non-teflon coated) embedded at the middle ply were used in this investigation. Specimens had an average length of 152.4 mm (6 in.), width of 25.4 mm (1 in.), and thickness of 1.27 mm (0.05 in.). Glass epoxy tabs with 30 deg. tapering were used to reduce the stress concentration due to gripping of the specimen. Tabs and the tab—section surfaces of the specimen were lightly sand—blasted for cleaning as well as to increase the mechanical friction between the adjoining surfaces. Cyanamid's FM-300K adhesion film was used for binding the tabs to the specimens. The tabs were then cured at 177 deg. C (350 deg. F) for 1 hour in a hot press at 75 psi. [21].

Dynamic data acquisition was performed using an HP 9000/PC-315 computer in—line with an HP-3852A/HP-3853A data acquisition control unit as well as an HP 3562-A dynamic signal an-

alyzer (Figure 1). A software routine was developed for real time dynamic response analysis. Phase lag and gain response of the load/stroke signals from the MTS servo—hydraulic load frame were plotted in conjunction with load stroke, and temperature data. To avoid disk storage overflow, data were sampled according to their relative change with respect to the previous events.

Working in the frequency domain, all measurements were made at the system's excitation frequency in a linear resolution mode. First, by using the cross spectrum function, the fundamental frequency was determined. Then the phase lag and gain measurements were made at this frequency using a frequency response measurement function (Figures 2 and 3).

RESULTS AND DISCUSSION

The frequency response measurement, often called the "transfer function", is defined as the ratio of a system output to its input, and yields both gain and phase as a function of frequency. In the HP 3562-A, the signal on channel 1 is assumed to be the system's input (load), and the signal on channel 2 is assumed to be its output (stroke). The frequency response is calculated as the ratio of the cross spectrum to the channel 1 (load) signal power spectrum [22]:

$$H(f) = \frac{G_{xy}}{G_{xx}} \quad \text{where} \quad G_{xy} = \text{cross spectrum}$$

$$G_{xx} = \text{channel 1 power spectrum}$$

where:

$$G_{xy} = F_x F_y^{\Box} \quad \text{where} \quad F_y^{\Box} = \text{channel 2 linear spectrum's complex conjugate}$$

$$F_x = \text{channel 1 linear spectrum}$$

where:

$$G_{xx} = F_x F_x^{\Box}$$

The dependency of gain and phase on parameters such as hydraulic test frame, excitation frequency, and the applied load level were investigated. To obtain the effect of test frame and frequency on phase and gain, a steel specimen w~s cycled at 40% of its tensile yield strength with a fatigue ratio of 0.1. It is observed that gain is not influenced by frequency but its base level is somewhat influenced by the test frame (Figure 4). As is illustrated in Figure 4, units with identical grip assembly (units 2 and 3) have identical gain response. This is in comparison with the units 1 and 4 which have different grip assembly.

Figure 5 shows the effect of excitation frequency on the phase lag response as a function of test frame. As it can be seen, phase lag is influenced linearly by the test frequency for test frame number two. This linear dependency was no longer observed by removal of the load conditioning filter from the circuitary of the controller unit. The information on the circuitary of the unit is not available to the authors at this moment but it is believed this problem is due to the inherent nonlinear nature of filters. This filter was removed on all the test frames except test frame number one; the filter could not be accessed on that unit. It can be seen that the phase lag response for test frame number one stands apart from the others. This could be a filter problem for this unit. The variation between the results obtained for test frame number 2,3, and 4 could be related to having different unsupported length in the specimen. It should be noted that the negative value of the phase is due to the fact that in the hydraulic test frame the displacement signal leads the load signal, where (theoretically) the displacement signal is generally assumed to be lagging the load signal. The phase values were normalized by a normalization factor of -1.

Using a 100 KN (22 Kips) servo—hydraulic load frame (MTS # 3), an interlayered center—notched specimen was cycled (tension—tension) to failure at 78% of its ultimate tensile strength (UTS). Using the experimental set up in Figure 1, the gain and phase lag response versus normalized life were plotted (Figures 6 and 7). Also, using a contact thermocouple, the temperature variation was recorded as a function of cycles (Figure 8).

Gain and temperature curves (Figures 6, and 8) show three distinct regions resembling the stiffness degradation in this material system as discussed by others [23-25]. The first region

occurs during the early life of the specimen where rapid increases in gain and temperature are seen. It is observed that this region is associated with matrix cracking in the 0 deg. direction, and with the start of delamination around the notch. This, in turn, created friction surfaces which gave rise to temperature increases. The second region occurs during the middle portion of the life of the specimen. It indicates a slow rate of increase in gain and temperature. This region is observed to be related to greater delamination and 0 deg. matrix cracking around the notch. This stage is also the start of delamination on the specimen edges due to the edge effect. These also create more friction surfaces which result in temperature increase. The third region occurs during the late life of the specimen. It shows a very rapid rate of increase in gain and temperature. It was observed that during this period of life, the delaminations on either side of the notch start to grow until they finally meet. There is also a great amount of fiber fracture during the final periods all the way to failure. The temperature fluctuations in that region may be due to disrupted contact between the specimen and thermocouple tip.

Normalized stiffness and *1/gain* are plotted against normalized life in Figure 9. Similarity of these two curves indicates that gain is related to the total damage. Comparison of *Gain/cycle* and *Phase/cycle* curves (Figures 6, and 7), suggest that the phase might be related to the rate of change of gain. To test this hypothesis, the *gain/cycle* curve was differentiated with respect to cycles. Figure 10 shows a plot of the slope of the gain versus cycles. This figure is very similar to the *phase/cycle* curve in Figure 7. This observation suggests that phase lag may be related to the damage rate in this case, an important parameter which is otherwise difficult to measure.

Operating at 90% of the UTS, another interlayered specimen was fatigue cycled to obtain phase, gain and temperature response. To investigate the effect of load level, these values were plotted versus cycles along with data obtained from the 78% UTS load level test (Figures 11,12). These figures indicate that load level has distinct effect on the these damage parameters such that the magnitude as well as shape of phase and gain versus cycle curves are altered, but the basic features of the curves remain unchanged. Next, the unidirectional laminates were fatigued at 60%, 65%, and 70% UTS. The gain and phase were plotted versus

cycles (Figures 13,14). These plots show the laminate response under various applied load levels. The fluctuations as well as various jumps illustrated in the Figures are due to the longitudinal matrix splittings and fiber fractur . This was verified visually where the audible sound of matrix splitting was followed by suuden jumps in the real time plots. The nature of damage in unidirectional laminates makes it difficult to obtain any quantitative measurement of damage parameters such as residual strength and stiffness. It is believed th¬t this problem could be solved using the present technique.

Even though the results might suggest an order in relative magnitude of gain and phase lag response in these material systems, no comments as to the exact nature for this behavior is available at the present time. Further analysis of this technique is currently under way and will be reported at a later date.

CONCLUSION

It has been shown that the dynamic load and stroke signals from the controllers of standard servo—hydraulic test frames can be interpreted with a waveform analysis device during the cyclic loading of composite materials, in a manner that provides information about dynamic compliance and phase lag that is directly related to the damage development processes in those materials. It is further shown that the measured parameters can provide quantitative information about the level of damage and the rate of damage development during such tests, a particularly valuable result since the quantitative measurement of damage rate during test-ing is otherwise very difficult. Major advantages of the method include the use of standard, easily obtained test equipment and test information (from standard servo—hydraulic test sys-tem controller signals), the elimination of need for contact methods for strain measurement (which are difficult to use in high temperature tests). and the ease of automated data retrieval devices to recover the test information.

Continuing efforts include the study of specific relationships between damage events and measured parameter changes. study of the damage—rate measurement capabilities of the

method, and use of the device for high temperature dynamic characterization of composite material systems.

ACKNOWLEDGEMENTS

REFERENCES

1. Lorenzo, L., Hahn, H.T., "Fatigue Failure Mechanisms in Unidirectional Composites", Composite Materials: Fatigue and Fracture, ASTM STP 907, American Society for Testing and Materials, Philadelphia, 1986, pp. 210-232.

2. Rotem, A., "Fatigue and Residual Strength of Composite Laminates", Engineering Fracture Mechanics, 25, 516, 1986, pp. 819-827.

3. Tsai, S.W., and Hahn, H.T., Introduction to Composite Materials, Technomic, 1980.

4. Talreja, R., Fatigue of Composite Materials, Technomic publishing Co. Inc., 1987, Chapter 5.

5. Herakovich, C.T., "On the Relationship Between Engineering Properties and Delamination of Composite Materials", J. Composite Materials, Vol. 15, July 1981, pp. 338-348.

6. Razvan, A., and Reifsnider, K.L., "Fiber Fracture & Strength Relationship in Unidirectional Graphite/Epoxy Composite Materials", Theoretical and Applied Fracture Mechanics. (Accepted for Publication)

7. Piggott, M.R., "The interface—An overview", 36th International SAMPE Symposium, April 15-18, 1991, pp. 1773-1786.

8. Herakovich, C.T., "Influence of Layer Thickness on the Strength of Angle—ply Laminates", J. Composite Materials, Vol. 16, May 1982, pp. 216-227.

9. Pagano, N.J., and Pipes, R.B., "The influence of Stacking Sequence on Laminate Strength", J. Composite Materials, Vol. 5, Jan. 1971, pp. 55-57.

10. Razvan, A., Bakis, C.E., Wagnecz, L., Reifsnider, K.L., "Influence of Cyclic Load Amplitude on Damage Accumulation and Fracture of Composite Laminates", J. Composite Technology & Research, Vol. 10, No. 1, Spring 1988, pp. 3-10.

11. Dan—Jumbo, E., Zhou, S.G., and Sun, C.T., "Load—Frequency Effect on Fatigue Life of IMP6/APC-2 Thermoplastic Composite Laminates", Advances in Thermoplastic Matrix Composite Materials, ASTM STP 1044, G.M. Newaz, Ed., American Society for Testing and Materials, Philadelphia, 1989, pp. 113-132.

12. Curtis, D.C., Moore, D.R., Slater, B., and Zahlan, N., "Fatigue Testing of Multi-angle Laminates of CF/Peek", Composites, Vol. 19, No. 6, November 1988.

13. O'Brian, T.K., Reifsnider, K.L., "Fatigue Damage: Stiffness/Strength Comparisons for Composite Materials", J. of Testing and Evaluation, Vol. 5, No. 5, 1977, pp. 384-393.

14. Camponeschi, E.T., and Stinchcomb, W.W., "Stiffness Reduction as an Indicator of Damage in Graphite/Epoxy Laminates", Composite Materials: Testing and Design (Sixth Conference), ASTM STP 787, I.M. Daniel, Ed., American Society for Testing and Materials, 1982, pp. 225-246.

15. Hahn, M.T., "Fatigue Behavior and Life Prediction of Composite Laminates", Composite Materials: Testing and Design, ASTM STP 674, S.W. Tsai, Ed., pp. 383-417.

16. Lifshitz, J.M., "Deformational Behavior of Unidirectional Graphite Epoxy Composite Under Compressive Fatigue", J. of Composite Technology & Research, Vol. 11, No. 3, Fall 1989, pp. 99-105.

17. Sims, G.D., and Bascombe, D., "Continuous Monitoring of Fatigue Degradation in Composites by Dynamic Mechanical Analysis", Sixth International Conference on Composite

Materials, ICCM & ECCM, Second European Conference on Composite Materials, Matthews, F.L., Buskell, N.C.R., Hodgkinson, J.M., Morton J., Vol. 4, pp. 4.161-4.171.

18. Renz, R., Altstadt, V., and Ehrenstein, G.W., 'Hysteresis Measurement for Characterizing the Dynamic Fatigue of x-SMC", J. of Reinforced Plastics and Composites, Vol. 7, Sep. 1988, pp. 413-433.

19. So, C.K., Lai, T.C., and Tse, P.C., "The Measurement of Material Damping by Free-Vibration Technique with Periodic Excitation", Experimental Techniques, May/June 1990, pp. 41-42.

20. Swain, R.E., Bakis, C.E., and Reifsnider, K.L., "Effect of Interleaves on the Damage Mechanisms and Residual Strength of Notched Composite Laminates", Presented at the Fourth Symposium on Composite Materials: Fatigue and Fracture, Indianapolis, Indiana, May 6-7, 1991.

21. Razvan, A., Reifsnider, K.L., "Fiber Fracture & Strength Degradation in Unidirectional Graphite/Epoxy Composite Materials", Theoretical and Applied Fracture Mechanics, Vol. 16, No. 1.

22. "The Fundamentals of Signal Analysis", Application note 243, Hewlett Packard Co. 1989.

23. Bakis, C.E., and Stinchcomb, W.W., "Response of Thick, Notched Laminates Subjected to Tension-Compression Cyclic Loads," Composites Materials: Fatigue and Fracture, ASTM STP 907, H.T. Hahn, Ed., American Society for Testing and Materials, Philadelphia, 1986, pp. 314-334.

24. Reifsnider, K.L., and Stinchcomb, W.W., "A Critical-Element Model of the Residual Strength and Life of Fatigue-Loaded Composite Coupons," Composite Materials: Fatigue and Fracture, ASTM STP 907, H.T. Hahn, Ed., American Society for Testing and Materials, Philadelphia, 1982, pp. 50-62.

25. Bakis, C.E., "A Test Method to Measure the Response of Composite Materials Under Re-versed Cyclic Loads," Presented at the ASTM Second Symposium on Test Methods and Design Allowables for Fiber Composites, 3-4 Nov. 1986, Phoenix, AZ.

Table 1.   MTS servo—hydraulic test frames used in the study.

Load Frame unit	Controller (Model no.)	Load frame (Model no.)	Grip assembly (Model no.)	Load Capacity (KN/Kips)
MTS # 1	458	309.21	641.36	250/55
MTS # 2	413	312.21	647	100/22
MTS # 3	448.82	380.10	647	100/22
MTS # 4	436	380.10	641.35	100/22
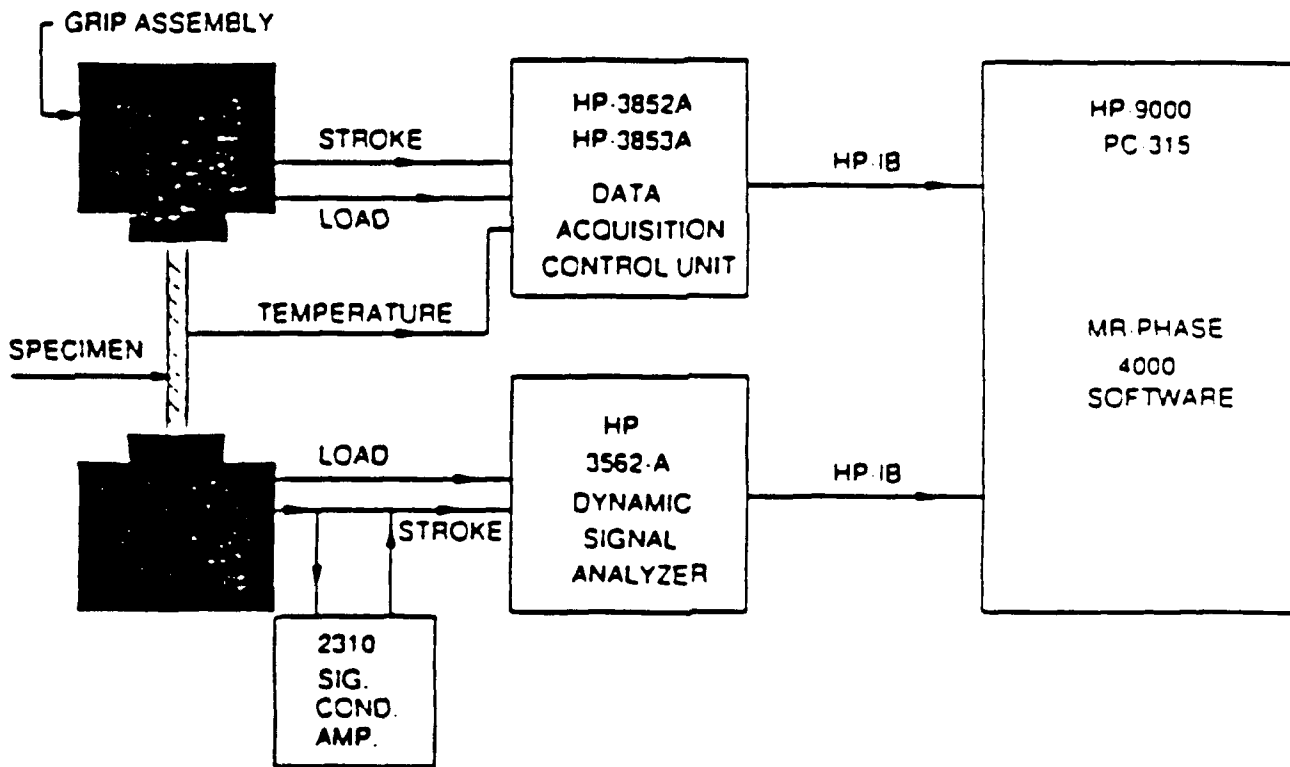
Figure 1.   :   Schematic diagram of the experimental setup.
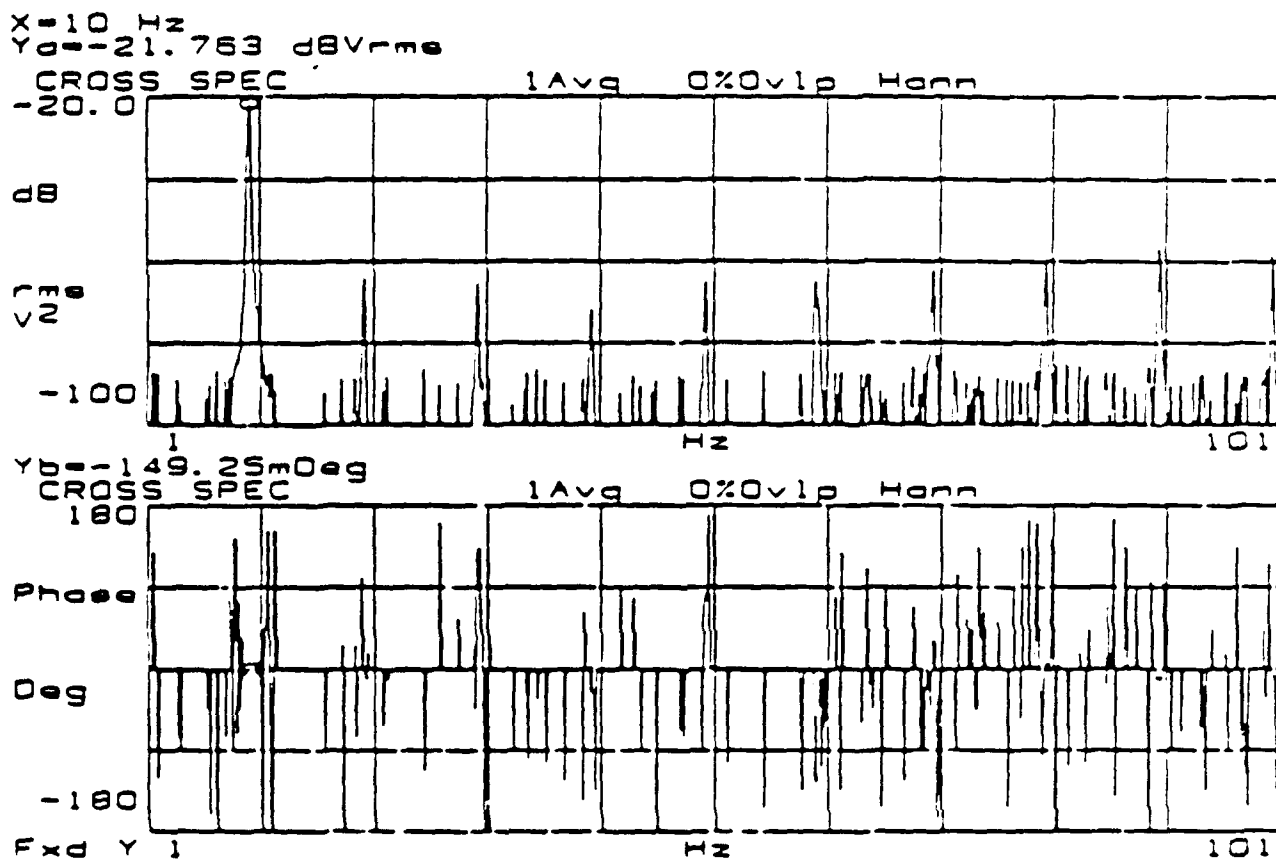
X=10 Hz
Yo=-21.763 dBVrms
 CROSS SPEC   1Avg   0%Ovlp Hann
-20.0

dB

rms
V2

-100

              1   Hz   101
Yb=-149.25mDeg
 CROSS SPEC   1Avg   0%Ovlp Hann
 180

Phase

Deg

-180

Fxd Y 1   Hz   101

Figure 2. : Cross specturm measurement of an Aluminum specimen fatigued at a frequency of
            10 Hz, and 40% σ_{yt}.

X = 10 Hz
Ya = 46.1827µ
FREQ RESP   SAvg   0%Ovlp   Hann
80.0
m

Mag

0.0
     1   Hz   101
Yb = -1.064 Deg
FREQ RESP   SAvg   0%Ovlp   Hann
180

Phase

Deg

-180
Fxd Y 1   Hz   101
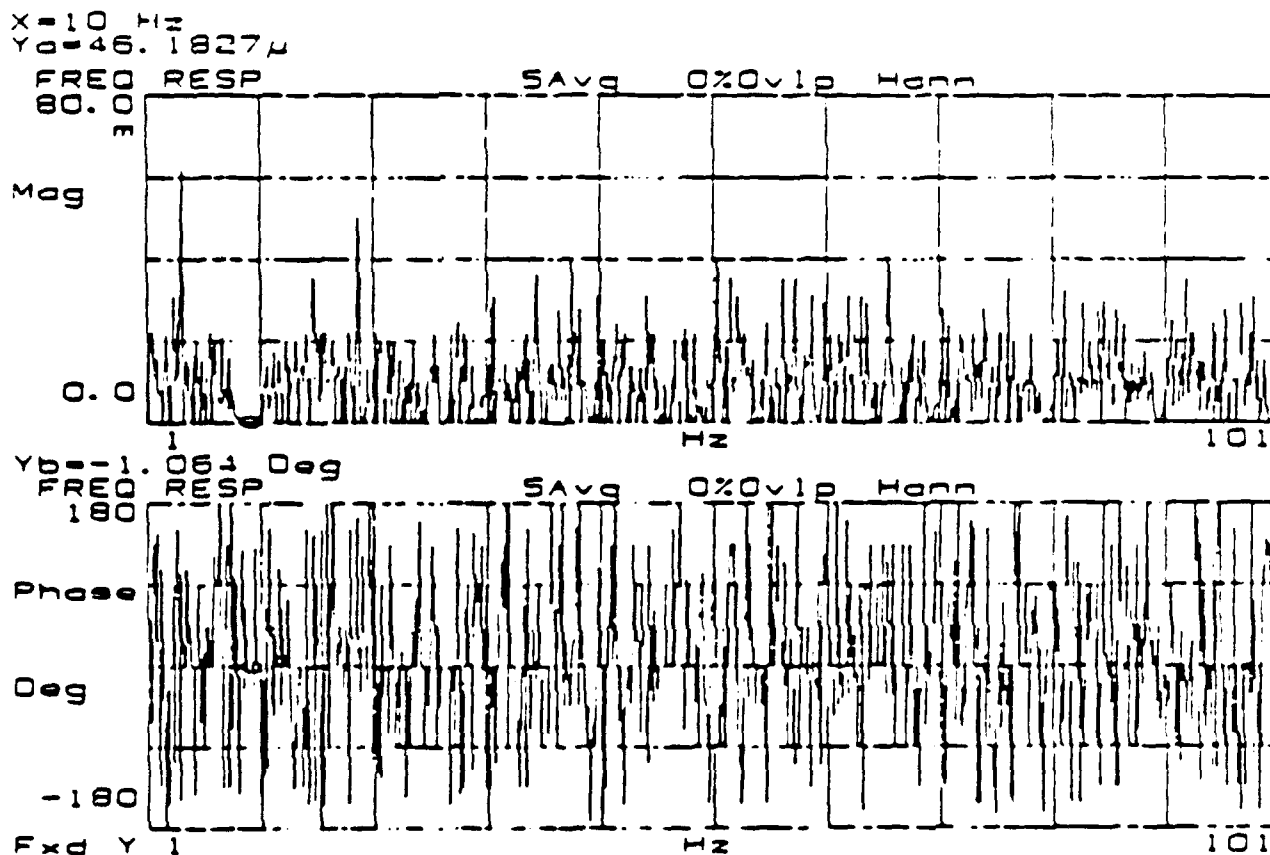
Figure 3. : frequency response measurement of an Aluminum specimen fatigued at a frequency of 10 Hz, and 40% σ_{yit}.

6. Characterization of Composite Materials Dynamic Response Using Load/Stroke Frequency Response Measurement

158
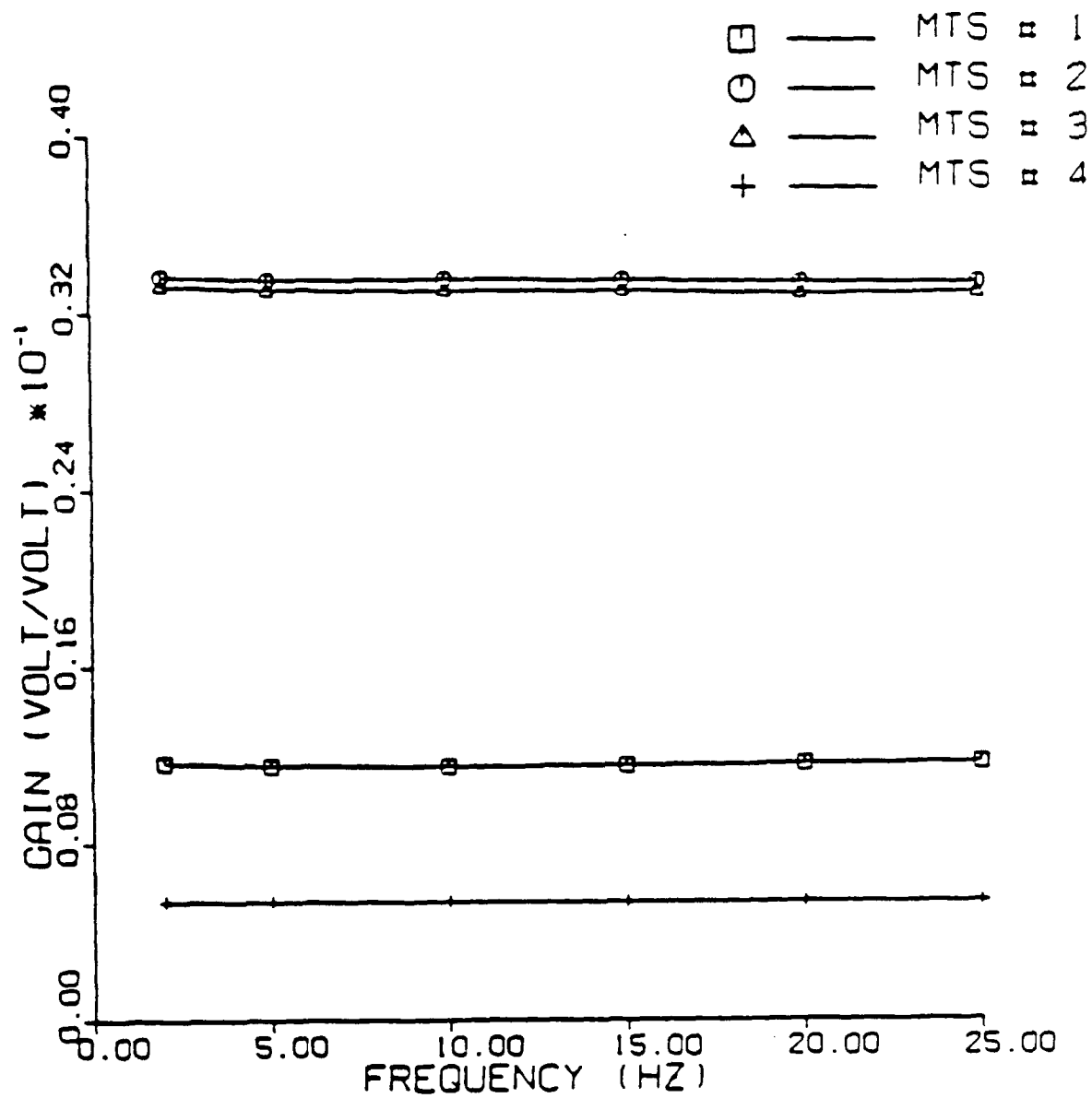
Figure 4. : Influence of test frame and freq. on gain based on fatigue test of a steel specimen cycled at 40% σ_{yr}
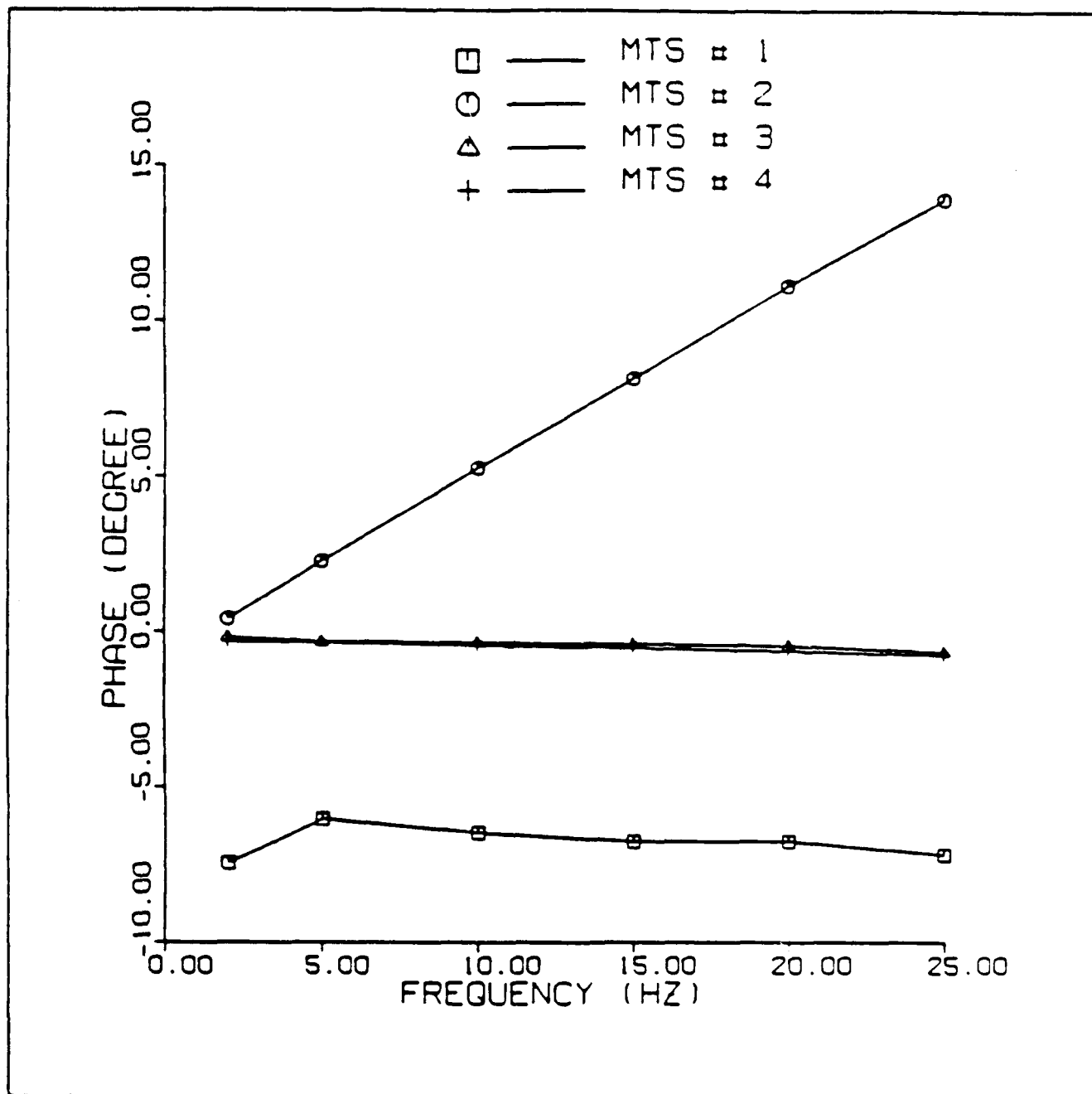
Figure 5. : Influence of test frame and freq. on phase based on fatigue test of a steel specimen cycled at 40% σ_{yt}.
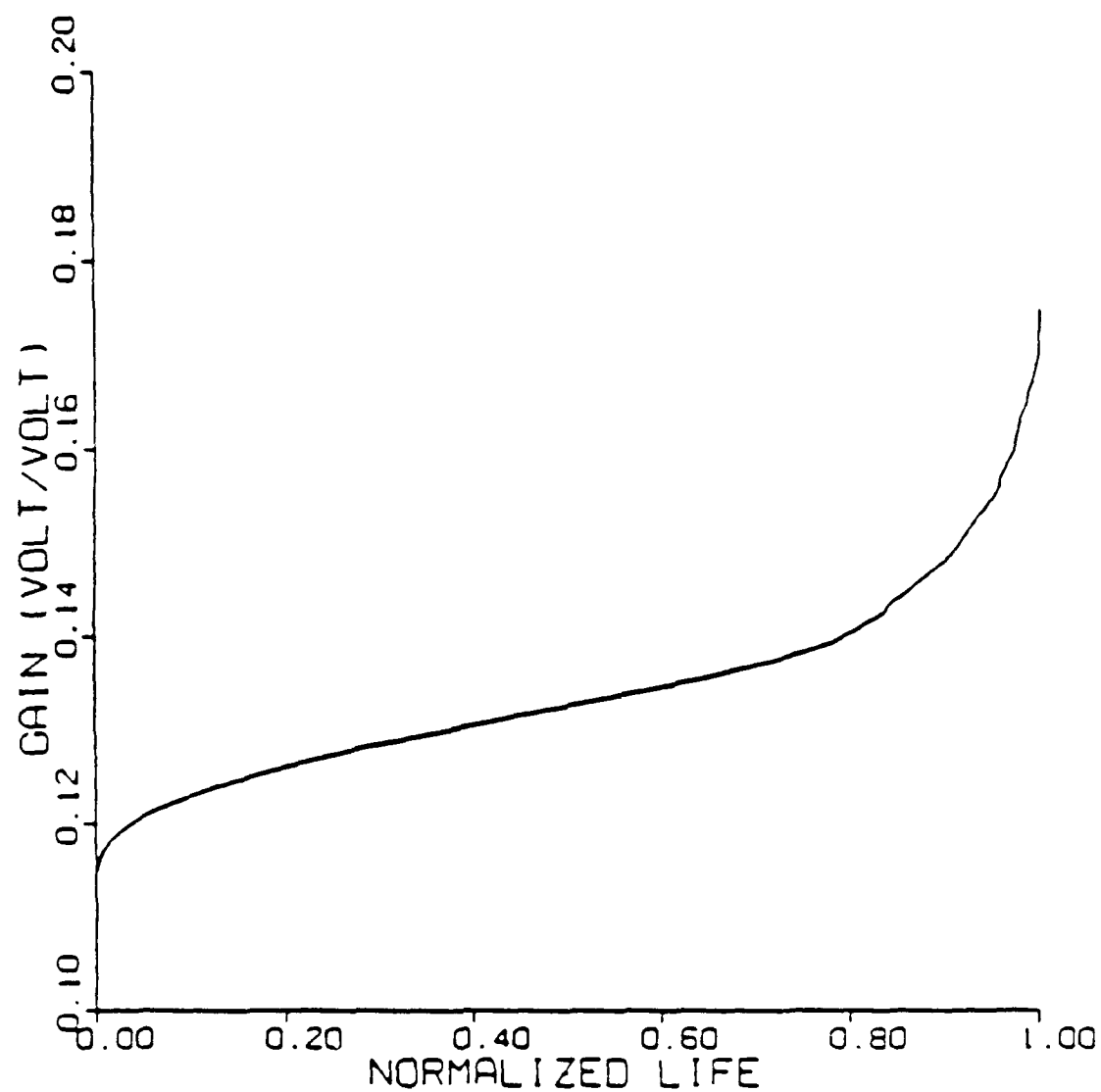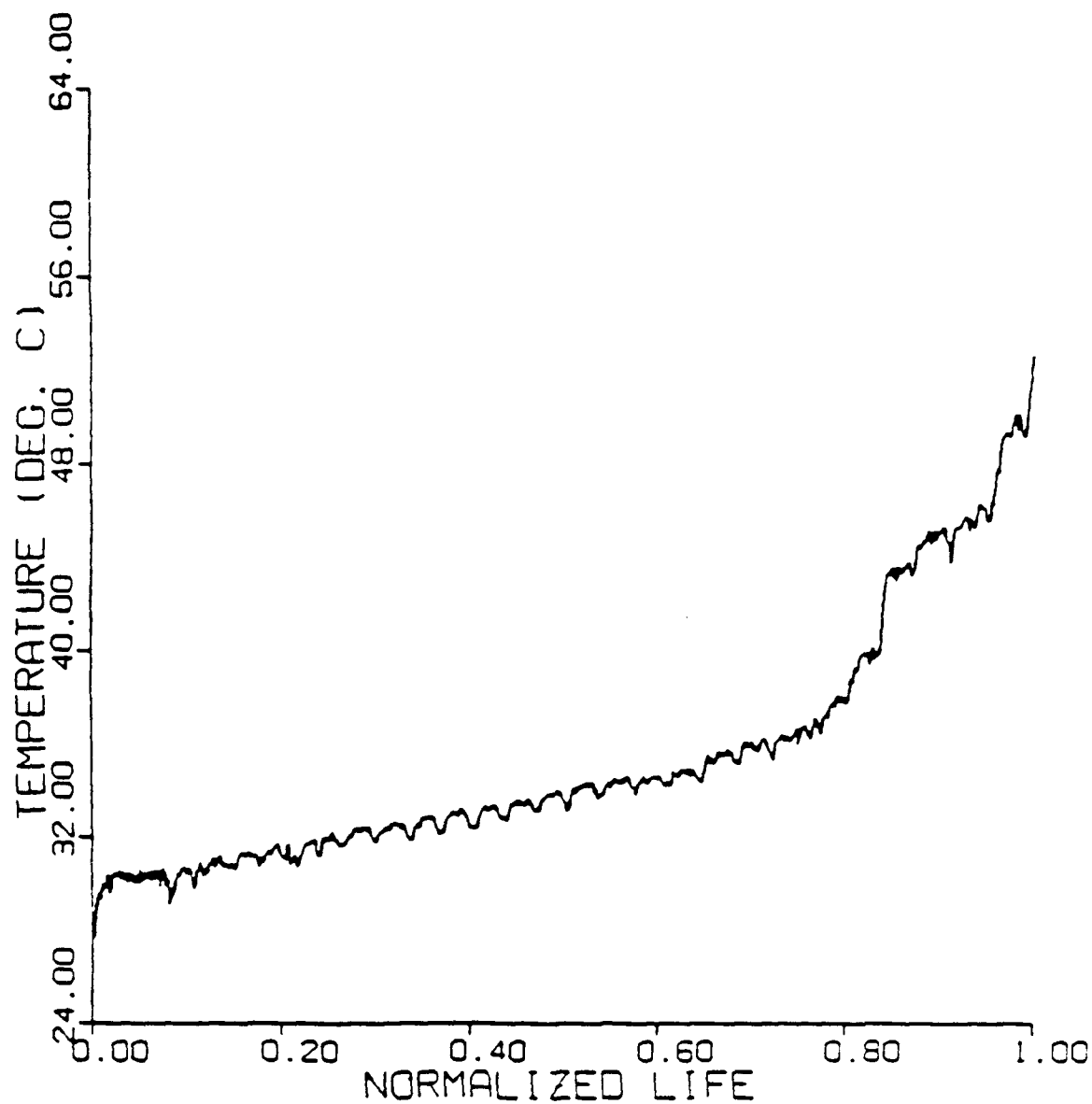
Figure 6. : Gain response vs. normalized life of AS4/985 [0/45/90/ — 45]$_{s2}$ interlayered laminate at 78% σ_u and frequency of 10 Hz.
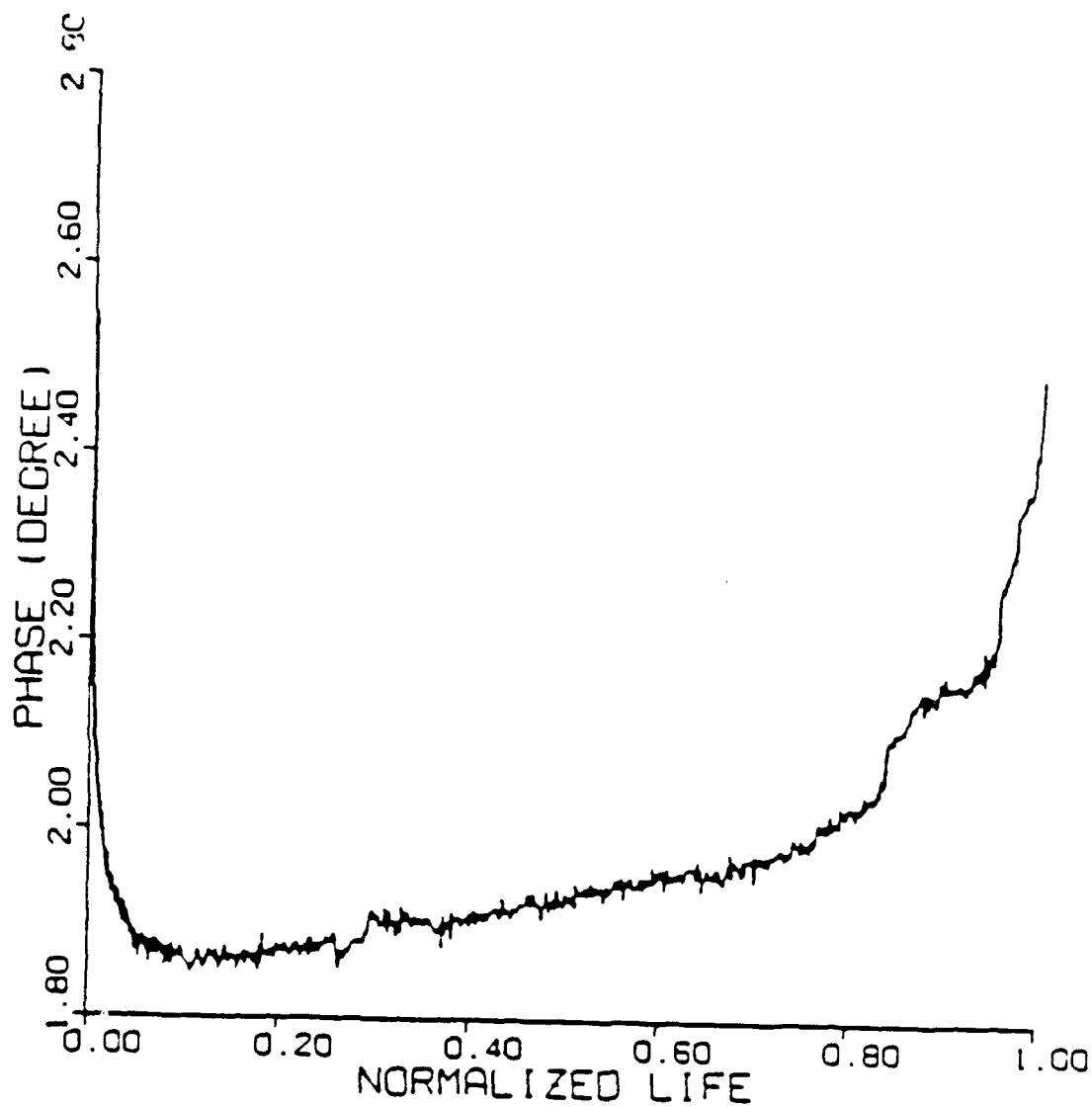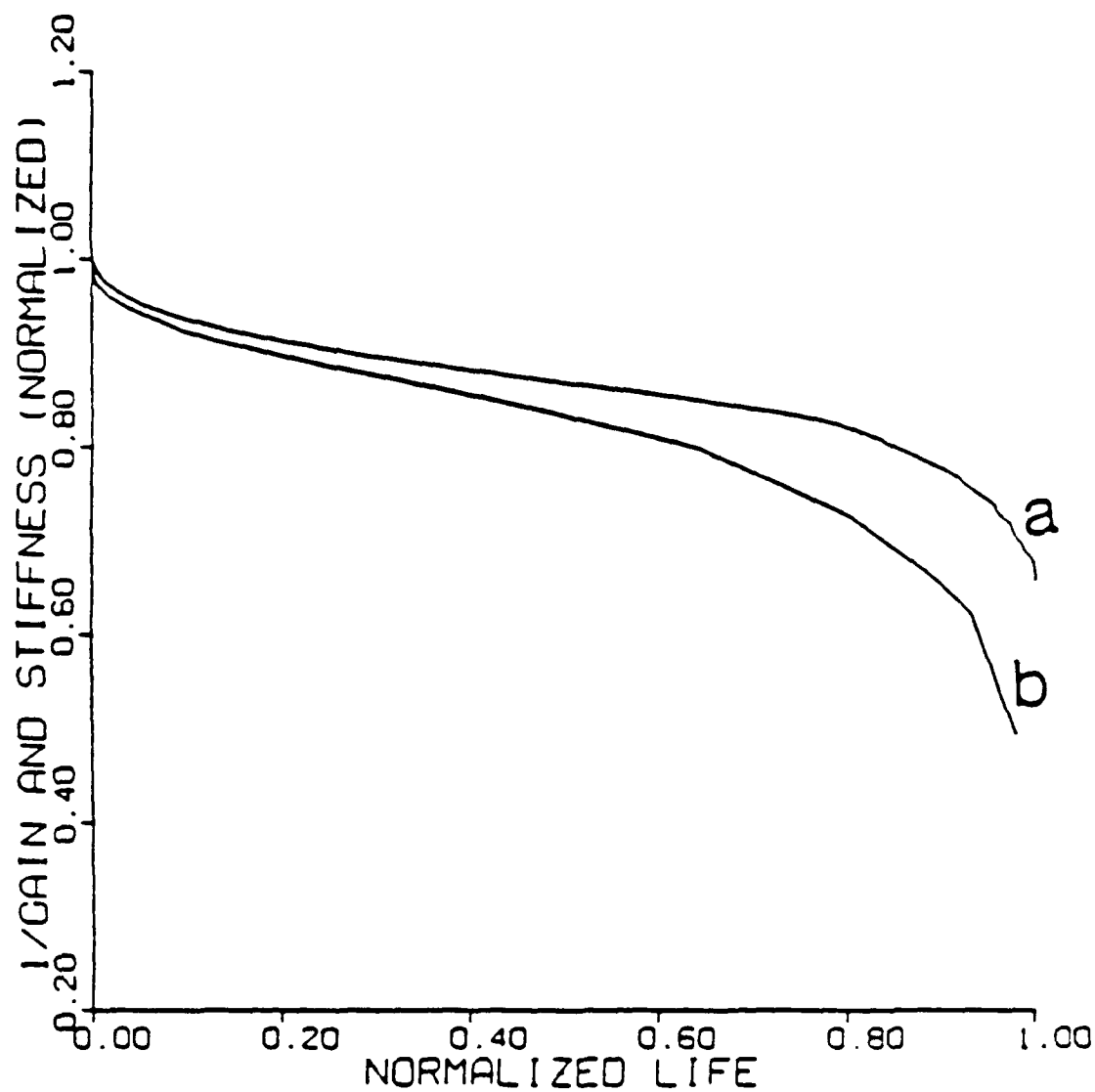
Figure 7. : phase response vs. normalized life of AS4/985 [0/45/90/ − 45]$_{s2}$ interlayered laminate at 78% σ_u and frequency of 10 Hz.

Figure 8. : Temp. response vs. normalized life of AS4/985 [0/45/90/ − 45]$_{s2}$ interlayered lami-
nate at 78% σ_u and frequency of 10 Hz.

Figure 9. : AS4/985 [0/45/90/ − 45]$_{s2}$ laminate a) normalized 1/gain, and b) normalized stiffness versus normalized life.
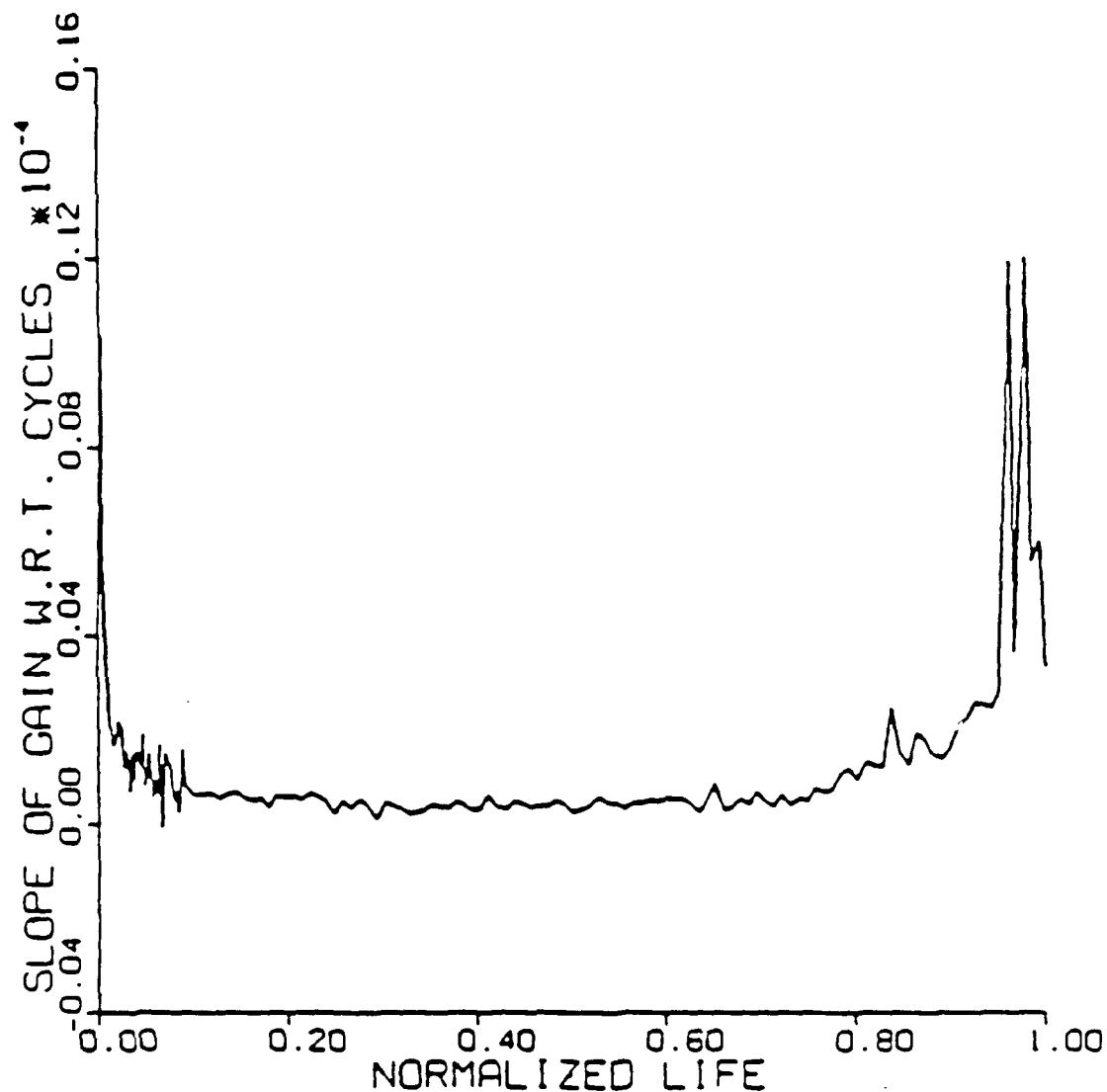
Figure 10. : slope of gain w/r to cycles vs. normalized life of AS4/985 $[0/45/90/-45]_{s2}$ laminate at 78% σ_u and frequency of 10 Hz.
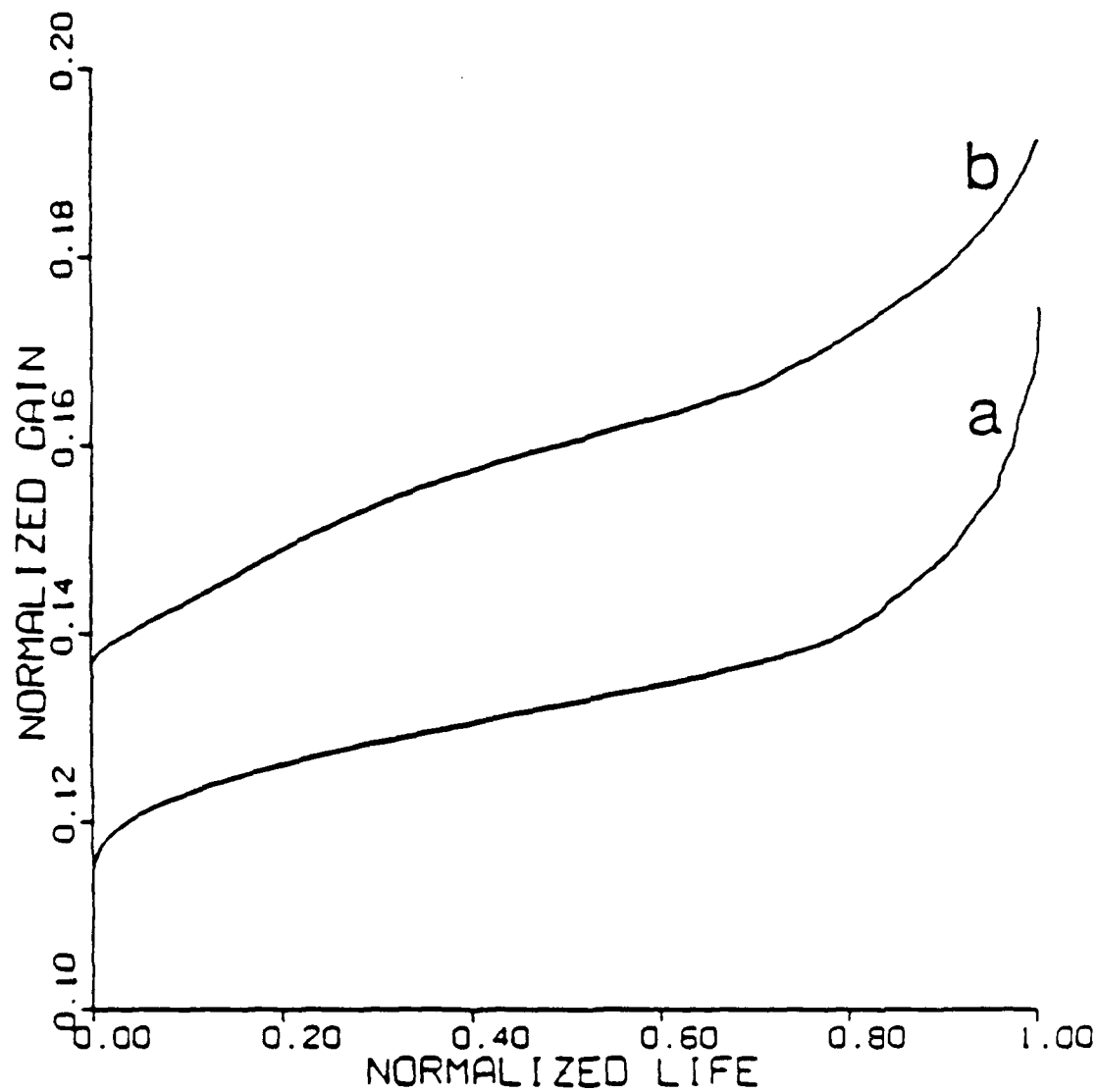
Figure 11. : Normalized gain vs. normalized life of AS4/985 $[0/45/90/-45]_{s2}$ laminate at a) 78% σ_u and b) 90% σ_u
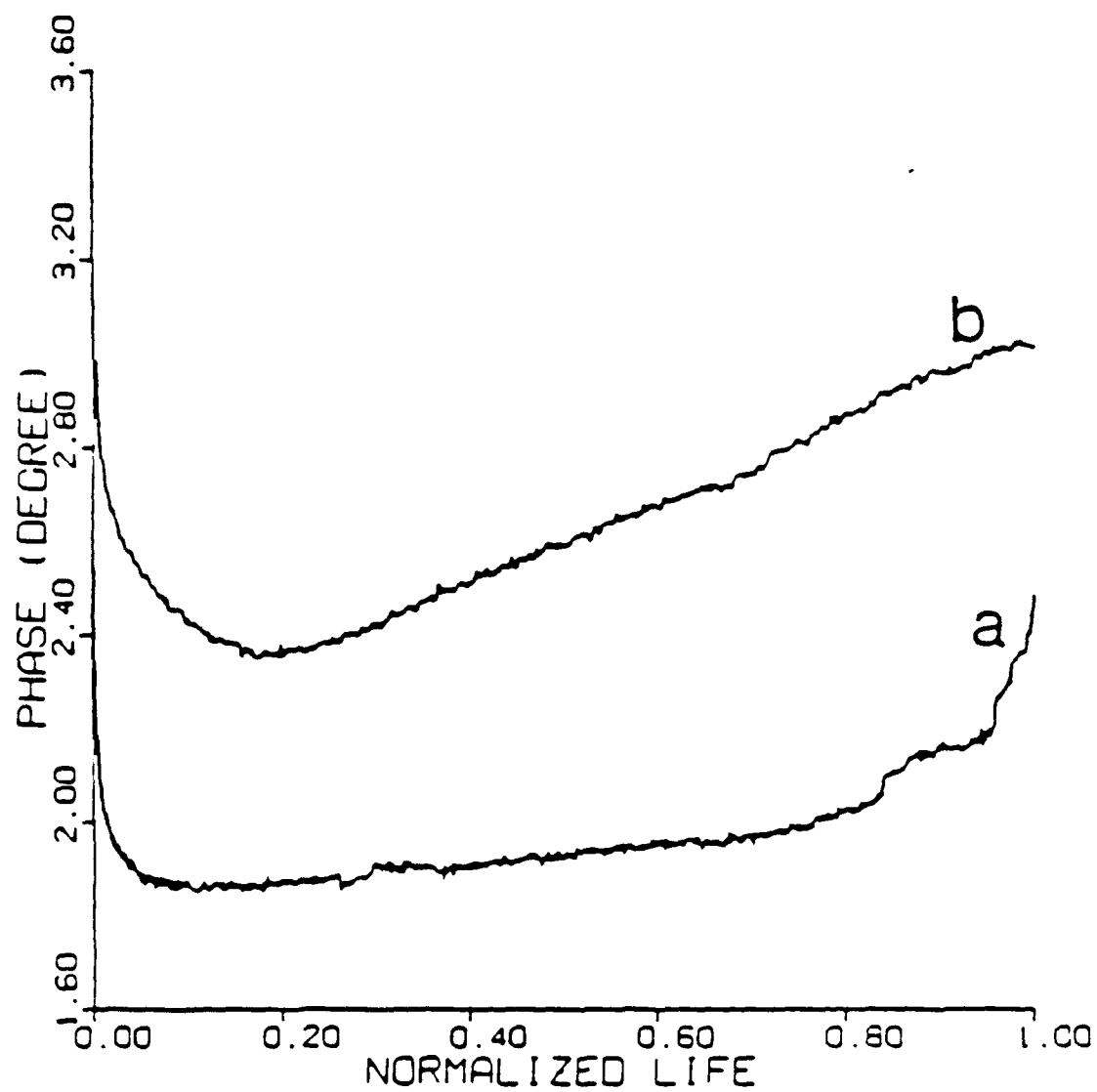
Figure 12. : Phase vs. normalized life of AS4/985 [0/45/90/ − 45]$_{s2}$ laminate at a) 78% σ_u and b) 90% σ_u
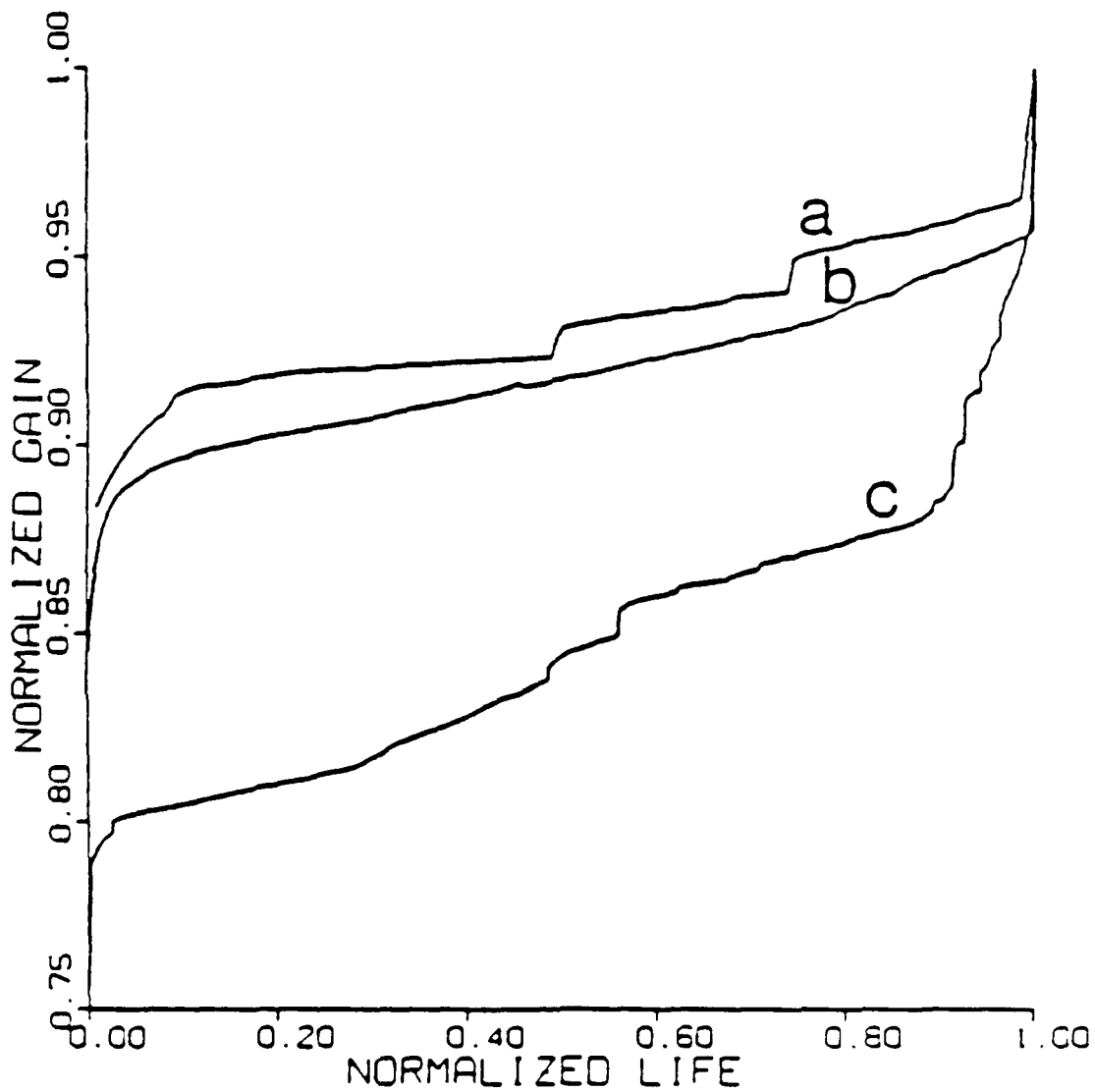
Figure 13. : Normalized gain vs. normalized life of unidirectional laminate at a) 60%, b)65%, and c) 70% σ_u
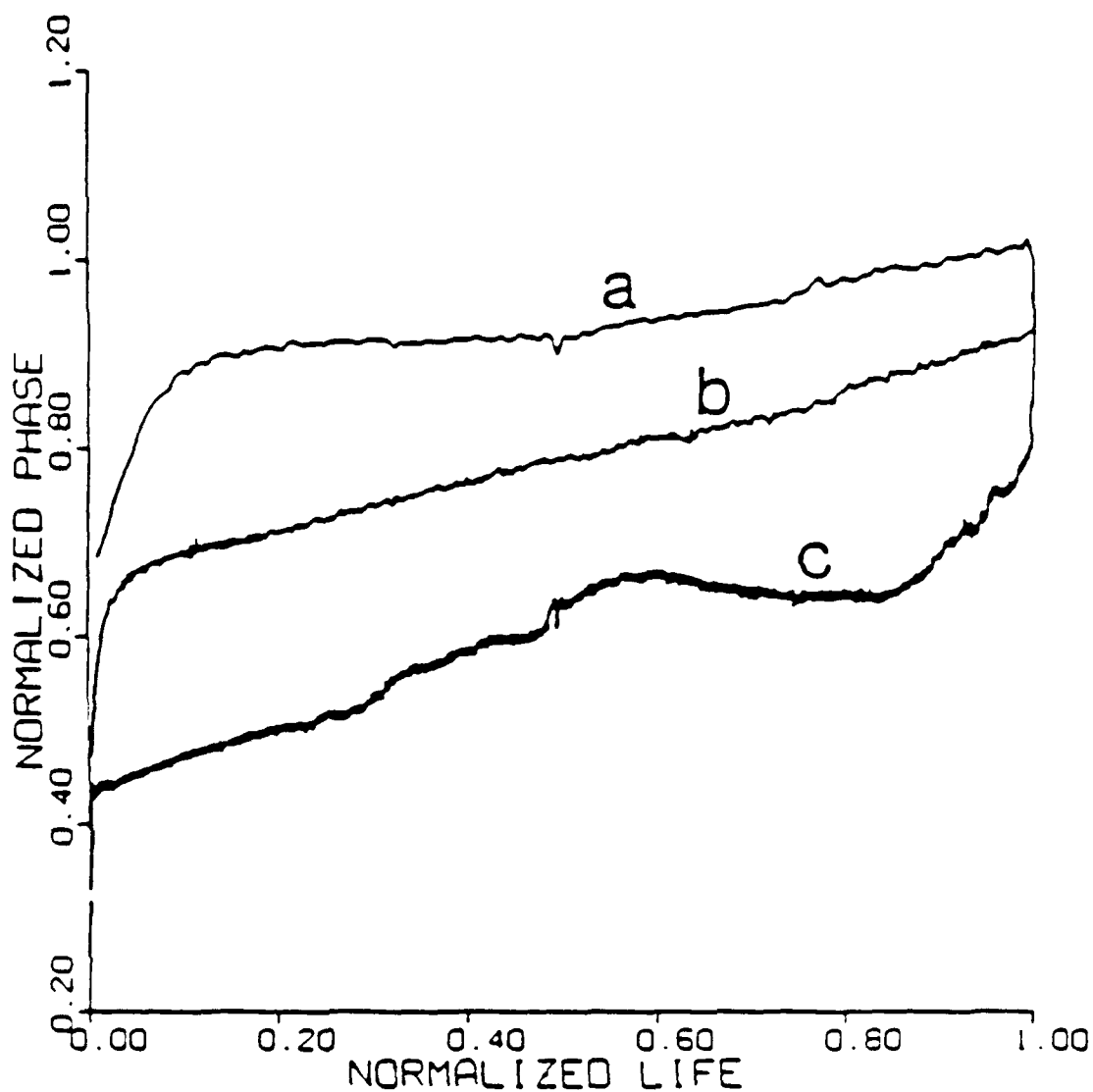
Figure 14. : Normalized phase vs. normalized life of unidirectional laminate at a) 60%, b)65%, and c) 70% σ_u